

博士学位論文

ポリエチレンカーボネート複合型電解質の物性と
イオン伝導特性および二次電池への応用

Characterization and ion-conductive properties of poly(ethylene carbonate)-based composite electrolytes and their application for lithium rechargeable batteries

2019.3

東京農工大学大学院
生物システム応用科学府
生物機能システム科学専攻

李珍光 / Li Zhenguang

Table of Contents

Abstract	1
Chapter 1. Introduction	
1-1 Lithium-ion rechargeable batteries	4
1-2 Current status of solid-state electrolytes for lithium ion batteries	8
1-2-1 Inorganic ceramic-based electrolytes for all-solid-state batteries	10
1-2-2 Organic polymer-based electrolytes for all-solid-state batteries	13
1-3 Solid polymer electrolytes	
1-3-1 Fundamentals of solid polymer electrolytes	16
1-3-2 Ion-transport mechanism of solid polymer electrolytes	20
1-3-3 Polycarbonate-based electrolytes	23
1-4 Concentrated electrolytes	30
1-5 Composite polymer electrolytes	
1-5-1 Ceramic-filled polymer electrolytes	35
1-5-1 Polymer blend electrolytes	38
1-6 Objective of this study	41
References	43
Chapter 2. Effect of silica nanofiber addition on poly(ethylene carbonate)-based composite electrolytes	
2-1 Introduction	59
2-2 Experimental	
2-2-1 Preparation of non-calcined silica nanofiber	62
2-2-2 Materials and electrolyte preparation	63
2-2-3 Characterization	64
2-3 Results and discussion	
2-3-1 Morphology of silica nanofiber filled composite electrolyte	67
2-3-2 Thermal properties	69
2-3-3 Mechanical properties	71
2-3-4 Ion-conductive and electrochemical properties	73
2-3-5 FT-IR spectroscopic study	78

2-4 Conclusion	79
References	81

Chapter 3. Characterization and ion-conductive properties of carbonate-based polymer blend electrolytes

3-1 Introduction	86
3-2 Experimental	
3-2-1 Materials and sample preparation	88
3-2-2 Characterization	89
3-3 Results and discussion	
3-3-1 Physicochemical and thermal properties	92
3-3-2 Ion-conductive properties	100
3-3-3 Electrochemical properties	104
3-3-4 FT-IR spectroscopic study	106
3-4 Conclusion	108
References	109

Chapter 4. Electrochemical characterization and battery performance of concentrated polycarbonate-based composite electrolytes

4-1 Introduction	114
4-2 Experimental	
4-2-1 Materials and electrolyte preparation	116
4-2-2 Coin-cell preparation	117
4-2-3 Characterization	119
4-3 Results and discussion	
4-3-1 Electrochemical stabilities	121
4-3-2 Battery performance of Li/LiFePO ₄ cells	128
4-4 Conclusion	136
References	138

Chapter 5. Summary and future perspectives

List of publications	146
Acknowledgements	147

Abstract

All-solid-state batteries (ASSBs), have taken global attention instead of typical liquid electrolytes. ASSBs have the potential for higher energy densities and safety than conventional lithium-ion batteries. Solid polymer electrolytes (SPEs) are one of electrolyte materials for ASSBs, which consist of polar polymers and metal salts, have greater safety and manufacturing workability. In the past several decades, SPEs have been mainly studied on polyether-based electrolytes such as poly(ethylene oxide) (PEO)-based electrolytes, due to its good ion-conductive behavior and high solubility for many kinds of metal salts. However, those polyether-based SPEs have effectively defects on the electrochemical properties for application towards rechargeable batteries.

In this dissertation, we focused on polycarbonate-based electrolytes such as poly(ethylene carbonate) (PEC). Because of not only its ion-conductive continuously increase with increasing salt concentration, but also the excellent cation (Li^+) transport abilities. These properties have never presented in polyether-based electrolytes. Moreover, PEC-based electrolytes demonstrate a high oxidation stability and a prevention effect of metal corrosion reaction in the highly concentrated electrolytes. Additionally, polycarbonate materials are very worth noting even from an environmentally friendly point of view. PEC can be synthesized from carbon dioxide (CO_2) gas as monomer and biodegradable, low toxicity and so on. However, the ionic conductivity at room temperature and poor thermal and mechanical properties of PEC-based electrolytes are still needed to be improved for application of high performance batteries.

For solving above issues, composite polymer electrolytes (CPEs) of PEC-based

electrolytes have been studied in the present study. PEC and poly(trimethylene carbonate) (PTMC) blend electrolytes were developed and their thermal, ion-conductive and electrochemical properties were investigated. The ionic conductivity of PEC and PTMC blend electrolytes increased with increasing Li salt concentration and PEC content. Moreover, blend electrolytes revealed better thermal properties and stable electrochemical abilities with Li anode than that of PEC and PTMC original electrolytes. The effect of the blended electrolytes also appeared in battery test results. In addition, ion-conductive and mechanical properties of PEC-based electrolytes reinforced by silica nanofiber were analyzed and the fiber size effect on electrolytes was also demonstrated.

According to these findings, it can be suggested that compounding of the electrolyte is an effective method for development of more excellent electrolytes for batteries. We also believe that the present study will contribute to real or practical application of ASSBs with polymer electrolytes in the future.

Chapter 1

Introduction

1-1 Lithium-ion rechargeable batteries

The globally and rapidly increasing demand for energy results in challenges concerning not only the resources but also the conversion and storage of electrical energy. Along with the demand of society and the development of science and technology, the discovery of new energy resources and development of the utilization of renewable energies are greatly boosted. Various types of systems have applied depending on the required capacity and power values, like hydropower plants, wind power plants, and electrochemical energy-storage devices.^[1,2] In particular batteries, many different types of energy-storage devices have researched, for example fuel cells,^[3,4] supercapacitors,^[5,6] and lithium batteries.^[7,8]

Lithium-ion batteries (LIBs), simply known as lithium batteries, also the currently most common battery systems are based on the Li-ion technology. This technology was first proposed by M. S. Whittingham in 1976, and commercialized by SONY in 1990.^[9] In the

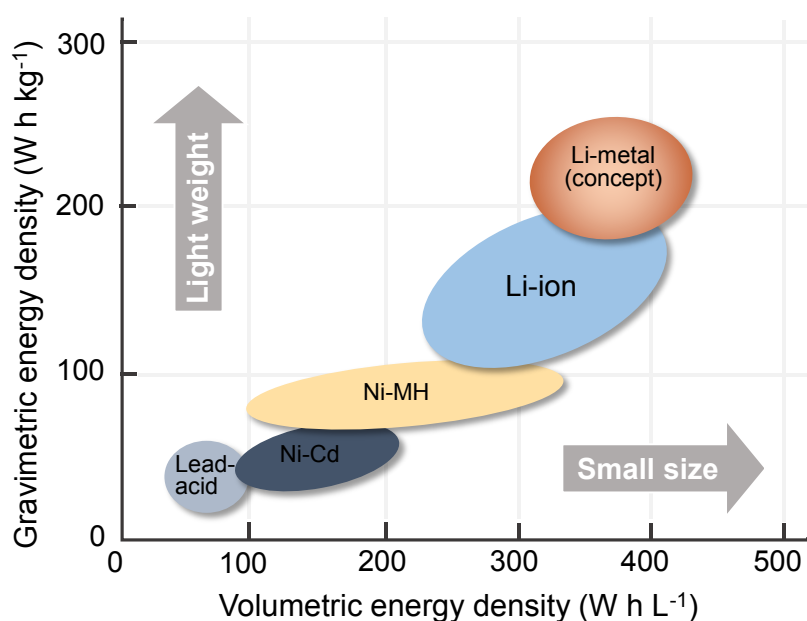


Figure 1-1. Gravimetric and volumetric energy densities of different rechargeable battery systems.^[7]

current era of LIBs, there is an ever-growing demand for even higher densities to power mobile IT devices with increased power consumption and to extend the driving range of electric vehicles.^[10,11] Furthermore, Li-ion technology represents the best investigated, and the most popular battery system today, due to its uniquely high power density (Figure 1-1).

Figure 1-2 shows a typical configuration of LIB. They are mainly consisted of two electrodes, anode and cathode, immersed in a liquid-type electrolyte and separated by a polymer membrane in order to protect cells from short-circuit. Anode and cathode are made of materials that have low and high electrochemical redox potentials, respectively. The difference between these two redox potentials is the electromotive force. In a charged state, the anode contains a high concentration of intercalated lithium while the cathode is depleted of lithium. During the discharge, a lithium ion leaves the anode and migrates through the electrolyte to the cathode while its associated electron is collected by the current collector to be used to power an electric device. The respective equations for the materials are as follows:

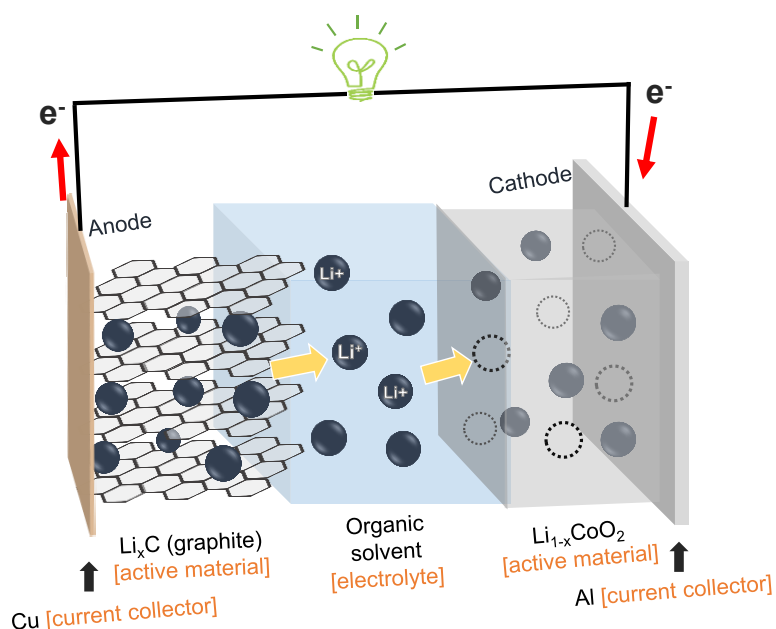
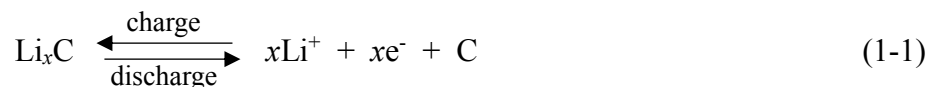
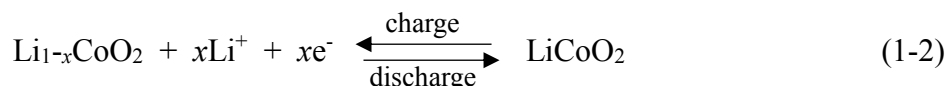


Figure 1-2. Typical configuration of lithium-ion battery (LIB) (during discharge).

Anode:



Cathode:



For the cathode materials, rock salt-type metal oxides which can encapsulate lithium ions in a lattice structure, such as LiCoO_2 , LiMn_2O_4 , and LiFePO_4 are commonly used^[12,13]. While the most used anode is definitely graphite due to its excellent features, such as flat and low working potential vs. lithium, low cost and good cycle life.^[14,15] However, graphite only allows the insertion of one Li-ion with six carbon atoms, with a resulting stoichiometry of LiC_6 and therefore an equivalent reversible capacity of 372 mAh g^{-1} . In addition, the diffusion rate of lithium into carbon materials is between 10^{-12} and $10^{-6} \text{ cm}^2 \text{ s}^{-1}$ (graphite is between 10^{-9} and $10^{-7} \text{ cm}^2 \text{ s}^{-1}$), which results in batteries having a low power density.^[16,17] Therefore, there is an urgent need to replace graphite anodes to materials with higher capacity, energy and power density. Even though lithium metal retains one of the highest capacity (3860 mAh g^{-1}) among anode materials, safety issues hinder the use of lithium as an anode material in secondary batteries. In fact, the short circuit caused by lithium dendrites formation in between lithium anode and cathode is actually the most issue for the lithium metal batteries.^[7,18,19]

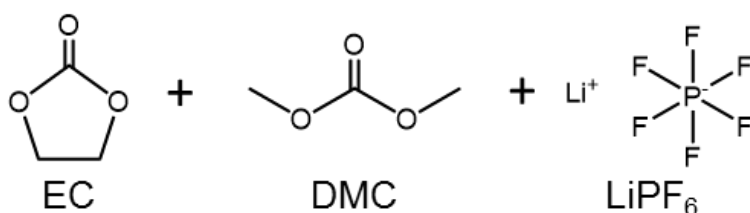


Figure 1-3. Typical composition of organic solution-based electrolyte. ethylene carbonate (EC), dimethyl carbonate (DMC).

On the other hand, electrolytes are playing ion conductors to compensate the current, in between the two electrodes but is an insulator to electrons. The electrolyte of the commercially available lithium ion battery is mainly liquid type. The most common type of liquid electrolyte is shown in Figure 1-3, which is a mixture of carbonate solvents and a lithium salt, such as LiPF_6 . The use of this electrolyte composition is due to a favorable ion-conductive performance and a high electrochemical stability to tolerate the high voltage operation of LIBs. However, this kind of volatile and flammable organic liquid type electrolyte solutions are heavy and pose a safety concerns, including fires or explosions.

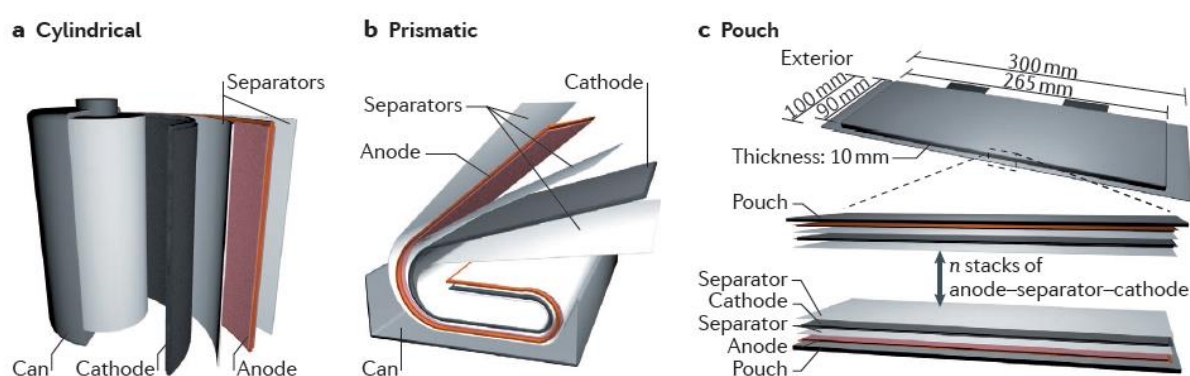


Figure 1-4. Three representative commercial cell structures. (a) cylindrical-type cell, (b) prismatic-type cell, (c) pouch-type cell. The pouch dimensions are denoted, along with the internal configuration for anode-separator-cathode stacks.^[8]

Figure 1-4 shows typical configurations of lithium-ion batteries which are currently available. The use of volatile and flammable organic solution-based electrolytes necessitates secure chassis to avoid fires or explosions. Additionally, there is a safety valve, in case of thermal runaways and resulting gas evolutions. The use of the flammable organic solutions causes not only safety concerns, but also such issues as decrease in energy density and high production cost because of the complexity of the battery structure.

1-2 Current status of solid-state electrolytes for lithium-ion batteries

Recently, all-solid-state batteries (ASSBs) have taken worldwide interest not only in business but also in researches due to their better safety, higher power and energy density, as well as wider operating temperature energy storage as compared to conventional lithium-ion batteries.^[20-22] Normally, conventional LIBs use liquid electrolytes, are based on organic solvents, which are intrinsically volatile and highly flammable. In contrast, solid electrolytes are usually able to withstand high temperatures ($>80^{\circ}\text{C}$). Several challenges related to solidifying batteries still remain to be addressed from fundamental understanding before the technology will be ready for widespread commercialisation.

The key point of ASSBs is the solid electrolyte, and it can be mainly classified into two types, which are inorganic ceramic and organic polymer electrolytes. The difference in electrical, electrochemical and mechanical properties of solid electrolytes is the key to the ASSBs challenge compared to the typical liquid electrolytes. At room temperature, the Li-ion conductivity of a solid electrolyte is typically at least two or three orders of magnitude lower than the Li-ion conductivity of a liquid electrolyte, especially in the case of solid polymers (Figure 1-5). This can result from the solid electrolyte's intrinsic properties or from existing grain boundaries. However, the conductivities of some sulfide-based electrolytes like $\text{Li}_{10}\text{GeP}_2\text{S}_{12}$ (LGPS), $\text{Li}_7\text{P}_3\text{S}_{11}$ and $\text{Li}_6\text{PS}_5\text{X}$ ($\text{X} = \text{Cl}, \text{Br}, \text{I}$) are comparable to or even higher than those of liquid electrolytes.^[23-25] It seems widely accepted and reported that the electrochemical oxidation potentials of solid electrolytes are superior to those of liquid electrolytes. Solid electrolytes may be stable above 5.0 V vs. Li/Li^+ . In the case of liquid electrolytes, it has been shown that decomposition occurs above 4.0 V vs. Li/Li^+ .^[26] In fact, recent results from density functional theory (DFT) computations on the thermodynamic stability of various solid electrolytes hint that above 4.0 V vs. Li/Li^+ most solid electrolytes can

be oxidised and decomposed into different phases.^[27–29]

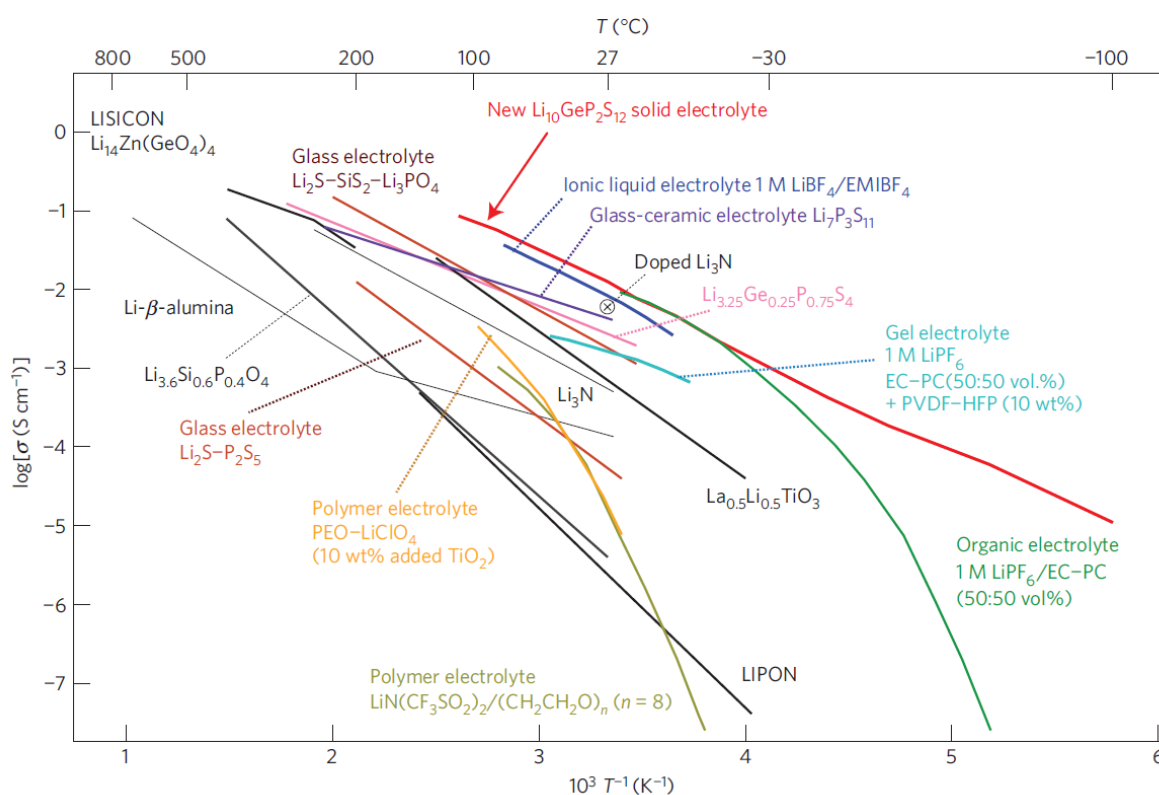


Figure 1-5. Thermal evolution of ionic conductivity of the new $\text{Li}_{10}\text{GeP}_2\text{S}_{12}$ phase, together with those of other lithium solid electrolytes, organic liquid electrolytes, polymer electrolytes, ionic liquids and gel electrolytes. The new $\text{Li}_{10}\text{GeP}_2\text{S}_{12}$ exhibits the highest lithium ionic conductivity (12 mS cm^{-1} at $27 \text{ }^\circ\text{C}$) of the solid lithium conducting membranes of inorganic, polymer or composite systems.^[23]

Relatively speaking, ASSBs are believed to be the future battery system compared to liquid-electrolyte Li batteries, because it is safer, and to have longer cycle life, higher energy density, less requirements on packaging and state-of-charge monitoring circuits.^[30] With respect to this, there is a growing interest in ASSBs R&D. It is expected that ASSBs should be used widely in large electrical power storage systems such as electrical vehicles as well as electronic devices due to their high energy density and safety.

1-2-1 Inorganic ceramic-based electrolytes for all-solid-state batteries

The solid electrolyte was firstly introduced by Bates *et al.* with lithium-phosphorous-oxynitride (LiPON).^[31] They incorporated N₂ to form LiPON, an amorphous analog to the lithium super ionic conductor (LiSICON), by radio frequency magnetron sputtering of lithium silicates, phosphates, or phosphosilicates.^[32] Thin-film batteries with Li anodes and LiPON separators demonstrated thousands of cycles.^[30,33] However, the mechanical stability of bulk-type batteries based on this electrolyte material design seemed to be insufficient. The low conductivity of LiPON at room temperature (2×10^{-6} S cm⁻¹) could also prevent the further development of batteries with thick LiPON membranes.^[32] Thereafter, inorganic ceramic-based electrolytes for solid-state batteries were further expended. For example, lithium ion conducting sulfide glasses such as Li₂S-GeS₂, Li₂SP₂S₅, Li₂S-B₂S₃, and Li₂S-SiS₂ systems were reported to exhibit electrical conductivities higher than 10⁻⁴ S cm⁻¹ at room temperature and wide electrochemical window.^[34,35] Moreover, thio-LiSICON-based electrolytes have conductivity of 3.2×10^{-3} S cm⁻¹ and low activation energy at room-temperature.^[36,37] However, their ionic conductivity still lower than that of liquid-type electrolytes. Table 1-1 summarizes ionic conductivity of some ceramic-based inorganic electrolytes.

Table 1-1. Various ceramic-based inorganic electrolytes and their conductivity.

Electrolytes		Ionic conductivity (S/cm)	Temperature (K)	ref
LISICON- like	Li ₁₀ GeP ₂ S ₁₂	1.20×10^{-2}	300	[23]
	Li _{3.25} Ge _{0.25} P _{0.75} S ₄	2.20×10^{-3}	298	[34]
	Li _{3.4} Si _{0.4} P _{0.6} S ₄	6.40×10^{-4}	300	[38]
perovskite	Li _{0.34} La _{0.51} TiO _{2.94}	1.00×10^{-3}	300	[39]
	Li _{0.06} La _{0.66} Ti _{0.93} Al _{0.06} O ₃	1.68×10^{-6}	300	[40]
NASICON	Li _{1.3} Al _{0.3} Ti _{1.7} (PO ₄) ₃	3.00×10^{-3}	298	[41]
garnet	Li ₇ La ₃ Zr ₂ O ₁₂	2.00×10^{-6}	300	[42]

In 2011, Kanno *et al.*^[23] reported an elemental substitution that the conductivity of Li_3PS_4 crystal could be significantly increased by incorporating phosphorus and germanium into Li_3PS_4 crystal, the resultant $\text{Li}_{3.25}\text{P}_{0.75}\text{Ge}_{0.25}\text{S}_4$ crystal exhibited a high conductivity of $2.2 \times 10^{-3} \text{ S cm}^{-1}$ at room temperature. They also reported that $\text{Li}_{10}\text{GeP}_2\text{S}_{12}$ with a new three-dimensional framework structure, which exhibited an extremely high lithium ionic conductivity of 12 mS cm^{-1} at room temperature. Figure 1-5 shows the thermal evolution of the ionic conductivity of the new $\text{Li}_{10}\text{GeP}_2\text{S}_{12}$ phase in comparison with other electrolytes used in practical batteries. This solid-state electrolyte was claimed to have many advantages in term of fabrication, safety and electrochemical properties.

Figure 1-6 shows the crystal structure of $\text{Li}_{10}\text{GeP}_2\text{S}_{12}$. The framework is composed of $(\text{Ge}_{0.5}\text{P}_{0.5})\text{S}_4$ tetrahedra and LiS_6 octahedra, which are connected to LiS_6 octahedra by a common corner (Figure 1-6b). LiS_4 tetrahedra at the $16h$ and $8f$ sites share a common edge, forming a 1D conducting pathway along the c axis. As observed, the content of germanium in Li-Ge-P-S electrolyte materials tended to be reduced at low potentials.^[43] Moreover, sulfide in the materials easily reacted with the moisture in the atmosphere, producing fatal and harmful H_2S gas. Recently, Sahu *et al.*^[44] reported that the solid electrolyte with a composition of $\text{Li}_{3.833}\text{Sn}_{0.833}\text{As}_{0.166}\text{S}_4$ showed a high ionic conductivity of 1.39 mS cm^{-1} at $25 \text{ }^\circ\text{C}$. Soft acids of As^{5+} and Sn^{4+} were used to form a stable compound against hydrolysis and oxidation. However, extreme manufacturing process and inferior cycle performance induced by the problems on the interface between electrode and electrolyte materials is one of the major drawbacks that needs to be overcome for the successful commercialization of secondary Li batteries.^[23,24,45]

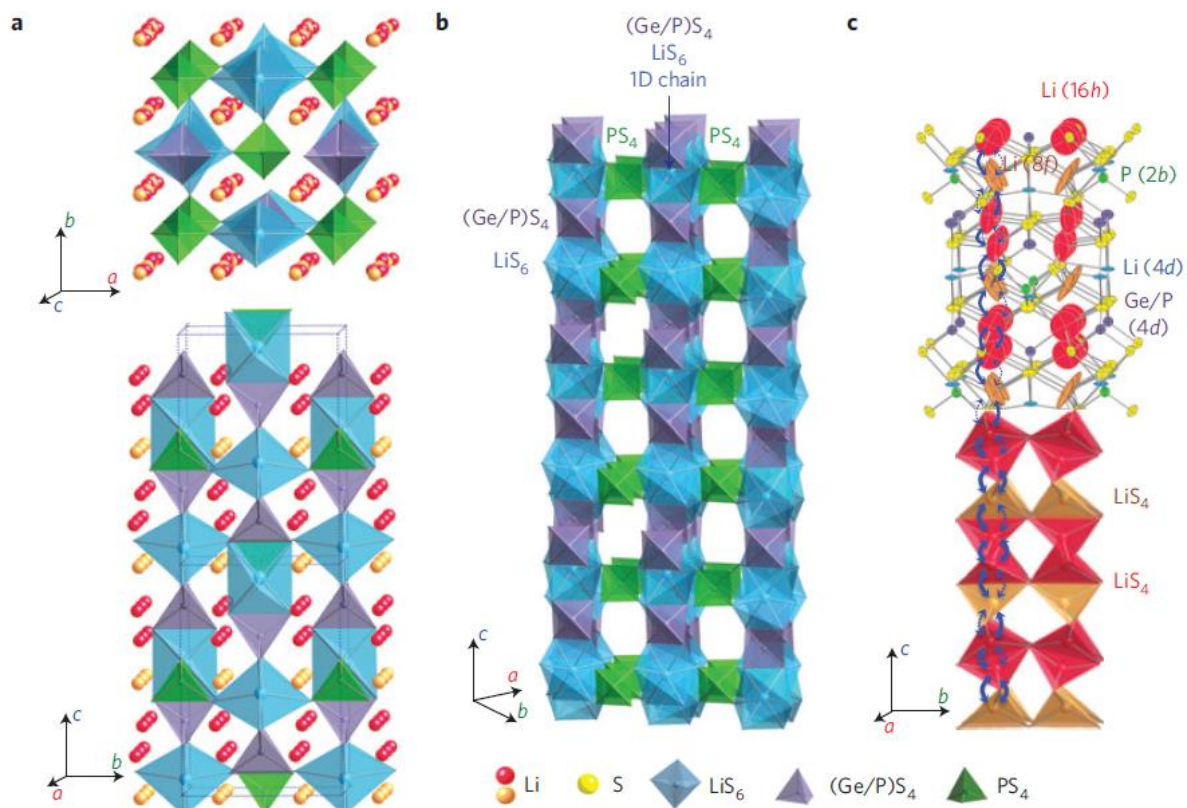


Figure 1-6. Crystal structure of $\text{Li}_{10}\text{GeP}_2\text{S}_{12}$. (a) The framework structure and lithium ions that participate in ionic conduction. (b) Framework structure of $\text{Li}_{10}\text{GeP}_2\text{S}_{12}$. One-dimensional (1D) chains formed by LiS_6 octahedra and $(\text{Ge}_{0.5}\text{P}_{0.5})\text{S}_4$ tetrahedra, which are connected by a common edge. These chains are connected by a common corner with PS_4 tetrahedra. (c) Conduction pathways of lithium ions. Zigzag conduction pathways along the c axis are indicated. Lithium ions in the LiS_4 tetrahedra (16h site) and LiS_4 tetrahedra (8f site) participate in ionic conduction. Thermal ellipsoids are drawn with a 30% probability. The anisotropic character of the thermal vibration of lithium ions in three tetrahedral sites gives rise to 1D conduction pathways.^[23]

1-2-2 Organic polymer-based electrolytes for all-solid-state batteries

Compared to both inorganic solid electrolytes and liquid ones, organic polymer-based solid polymer electrolytes (SPEs), in general, have better flexibility in packaging and higher safety, which have been one kind of the most promising candidate electrolytes for all-solid-state lithium batteries including Li-ion, Li-sulfur and Li-air ones.^[46] In fact, polymers may also act as hosts for ions. The studies of SPEs started from the exploration of polyethylene oxide (PEO) incorporating with lithium salts, and observed that lithium salts could be dissolved by the polymer solvents to form cations and anions in a SPE system.^[47] The ions can move in the space provided by the free volume of the polymer host, and conductivity is thus possible above the glass transition temperature (T_g) of the polymer where the polymer molecules are free to move. The ionic conductivity displays a diffusive liquid-like behavior in the solid electrolyte. Moreover, the number of free Li^+ cations and their moving ability of the chains would significantly affect the Li^+ transportability within SPE; in turn affect the battery's performance. Since lithium ion transportability in SPE at room temperature is lower than that in liquid electrolyte, even lower than that in inorganic solid electrolyte (Figure 1-5). Although SPEs usually show low ionic conductivity at room temperature which is not suitable for practical applications, they have been widely and continuously studied as an ionic conductor for one of potential electrolyte materials of all-solid-state batteries.^[48,49]

Additionally, SPEs have industrially unignorable attractive properties we have mentioned above such as excellent flexibilities in packaging and safeties (Figure 1-7), which are the performances of other types of electrolyte cannot satisfy. Table 1-2 compares basic characteristics of liquid electrolyte, inorganic conductor and SPE. Conductivity of SPE is mostly very low at this point. This is basically due to a strong correlation between ionic conduction and sluggish segmental motion (micro-Brownian motion) of polymer chains. In

contrast, some of the inorganic conductors even surpass that of a conventional liquid electrolyte in ionic conductivity and mechanical strength is very high because the materials are made of hard metal oxides. However, flexibility and processability are limited because of the brittle nature. For similar reason, a good contact between the ionic conductor and electrode is difficult to construct. Narrow electrochemical stability window and poor compatibility with electrode materials also remain challenges.

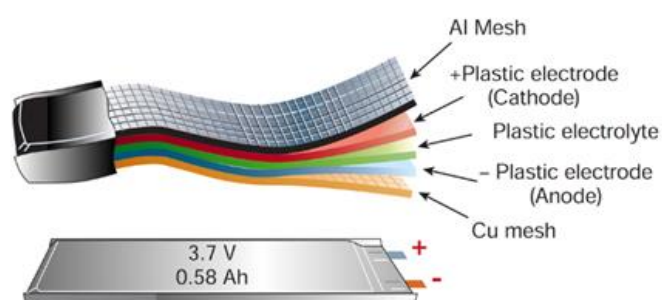


Figure 1-7. Schematic image of conceptual thin and flat polymer-based battery.^[7]

Table 1-2. Comparison of inorganic solid ion-conductor and solid polymer electrolyte (SPE).

Electrolyte	Ionic conductivity	Electrode interface	Electrochemical stability	Mechanical strength	Flexibility/Processability
Liquid-type	Medium	Low	Low	Low	Low
Inorganic-type	High	Low	Low	High	Low
Polymer-type	Low	Medium	Medium	Medium	High

During a long decades, precious metal inorganic materials were commonly used as the cathode active materials, such as LiCoO_2 , LiMn_2O_4 , and LiFePO_4 . The largest natural resources of these metals are located in politically unstable regions, and the substitution with renewable resources is impossible. Recently, organic materials which redox-active polymers as cathode active material has attracted much attention owing to their high theoretical gravimetric capacities and

resource renewability, especially for carbonyl compounds.^[50–52] One of the most advantages of organic carbonyl compound is their high theoretical gravimetric capacities, such as 446 mAh g⁻¹ for quinone.^[53] Unfortunately, organic materials with low molecular weight usually exhibit poor cyclability because of their high solubility in aprotic electrolyte.^[53,54] To overcome this issue, SPEs can be suitable, which enable the fabrication of solid-state batteries with lithium anode and organic cathode with high capacity. J. Chen *et al.*^[55] have reported an all-solid-state organic battery which combined pillar[5] quinone (P5Q) as organic cathode material with SPE and Li metal as anode electrode. As shown in Figure 1-8, this all-solid-state organic battery exhibit a very stable cycle performance and high capacities (keeping in more than 446 mAh g⁻¹) than that of liquid one. This suggest that SPE and organic cathode combined a novel all-solid-state organic battery can be expected for the future electronic storage devices.

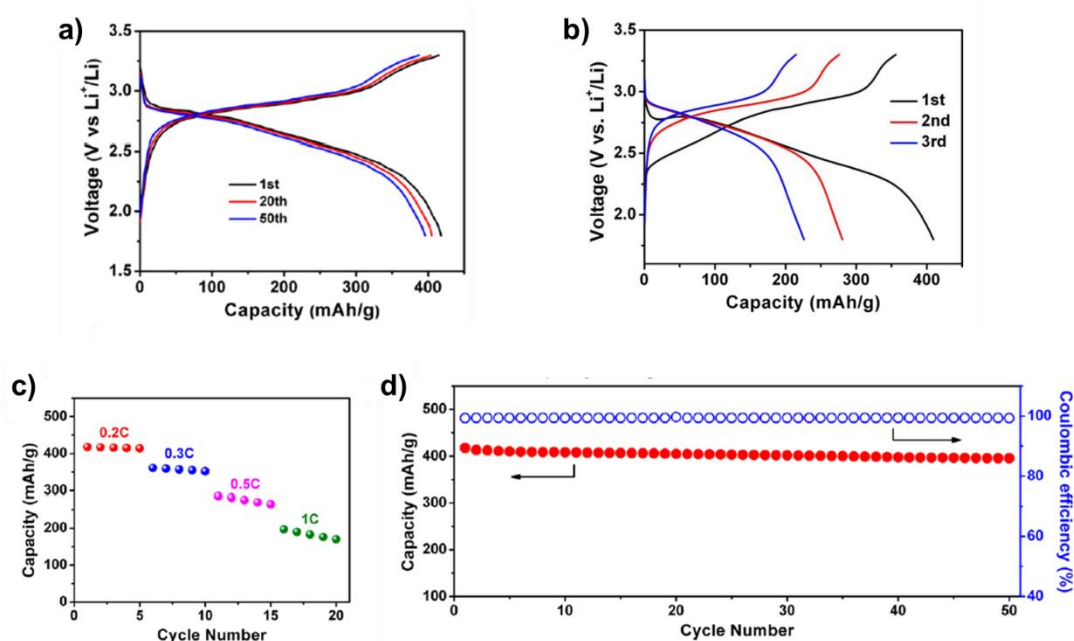


Figure 1-8. Electrochemical performance of the all-solid-state cell with P5Q cathode and PMA/PEG-SiO₂ GPE: typical discharge-charge profiles of (a) with GPE at 0.2C rate, (b) with 1 M LiPF₆ EC:DMC (1:1 in volume); GPE used cell (c) rate capability and (d) the cycling performance between 1.8 and 3.3 V at 0.2C rate.^[55]

1-3 Solid polymer electrolytes

1-3-1 Fundamentals of solid polymer electrolytes

Solid polymer electrolytes (SPEs) are solid ion-conductive materials mainly consisting of polar polymers and metal (lithium) salts. The study of SPE has its roots in early reports of relatively fast ionic conduction in complexes of poly(ethylene oxide) (PEO) and alkali metal salts, such as KSCN and NaSCN by Wright *et al.*^[56,57] in the early 1970s (Figure 1-9). The polymer/salt complex showed an ionic conductivity of the order of 10^{-2} S cm⁻¹ at elevated temperature above the melting point (T_m) of PEO chain, and of 10^{-7} S cm⁻¹ near the ambient temperature. The drop at T_m suggested an ionic conduction in amorphous region. Later, study of this kind of material as conceptual solid electrolyte for lithium rechargeable batteries has become popular, since Armand^[58] first suggested the potential usage. Since then, most studies have been directed to polymer/lithium salt complexes using polyethers like PEO or poly(propylene oxide) (PPO) as the host polymer matrix.

PEO-based electrolytes are the most attractive SPEs owing to their property of excellent solubility for lithium salts. The EO units have a high donor number for Li⁺, and also high chain flexibility for promoting rapid ion transport. Figure 1-10 shows the proposed ion transport mechanism in the PEO matrix, which demonstrates that lithium ions are coordinated by the ether oxygen atoms on a segmental PEO chain in a similar way to their complexation by organic carbonates. With the processes of breaking/forming lithium-oxygen (Li-O) bonds, ion transport occurs by intrachain or interchain hopping in the PEO-based electrolyte.^[59,60] Accompanied by the gradual replacement of the ligands for the solvation of Li⁺, the continuous segmental rearrangement results in a long-range displacement of lithium ions. Polymers which have low glass transition temperature (T_g) are suitable for SPE in general, because the low T_g that reflects more active segmental motion of polymer chains is favorable for a fast ionic transport.

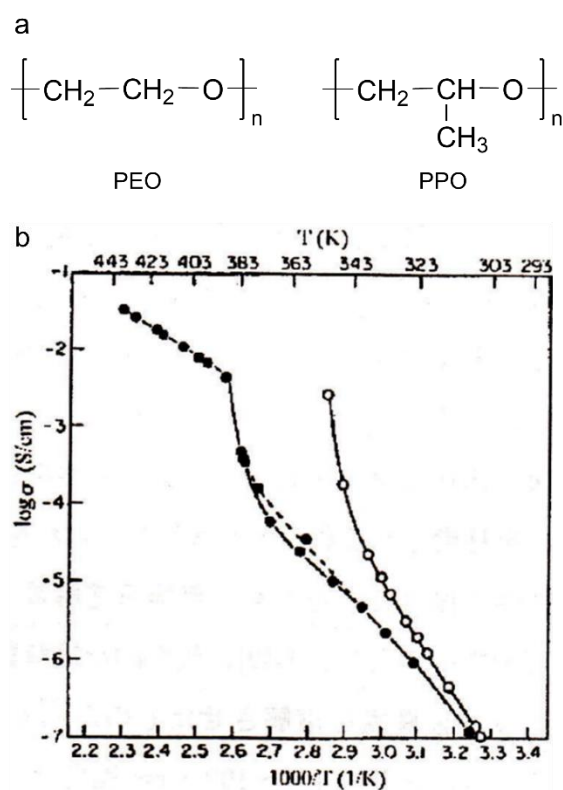


Figure 1-9. (a) Typical SPE polymer hosts. PEO: poly(ethylene oxide); PPO: poly(propylene oxide). (b) Temperature dependence of ionic conductivity for PEO/KSCN (○) and NH₄SCN electrolytes (●). [53]

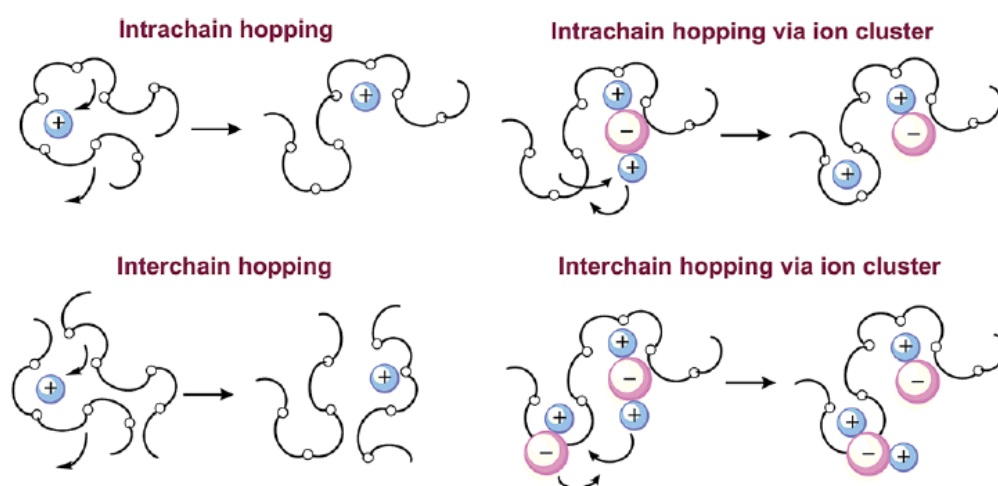


Figure 1-10. Schematic image of the ionic conduction in polyether-based SPE.^[61]

Several ion-conductive characteristics of the polyether electrolytes, which originate from a tight coordination between ether oxygen atoms and lithium ions, have hampered their practical use. Addition of salt slows the segmental motion, and causes the glass transition temperature (T_g) to increase, as a result of a physical cross-linking effect of the ether/Li⁺ coordination. The salt concentration in which the conductivity is high is quite low, and it is impossible to increase the conductivity by simply increasing the salt concentration. Very low lithium transference number (t_+) against the transport of anions, which is due to the selective coordination to Li ions, is also a significant challenge. Highly crystalline nature also hinders the improvement of conductivity, because ionic conduction mainly occurs in an amorphous domain. Additionally, both ether solvents and polyethers are not suitable for lithium batteries operating at a high voltage (> 4 V vs. Li/Li⁺), because ether chain is prone to an oxidation which results from an extraction of lone pairs of oxygen atoms. An alternative material-development strategy is therefore necessary.

Lithium polymer batteries have never reached the stage of large-scale commercial production. The challenging and critical issue with SPE is to improve the ionic conductivity, interfacial contacts between electrodes and electrolytes, and electrochemical stability window. Nonetheless, the ionic conductivity is a key property of the electrolyte for LIBs, and it represents the ion transition character of the electrolyte. The basic requirement of a suitable electrolyte for LIBs is high ionic conductivity. For improvement of conductivity of SPE, numbers of works have been done, Table 1-3 summarizes some of researches about SPEs.

Table 1-3. Conductivities of some solvent-free polymer complexes.

Polymer system	Polymer host	Li salt	Temp (°C)	Conductivity (S/cm)	Ref
<i>Linear</i>	Poly(ethylene oxide)	LiClO ₄	20	1.00×10^{-8}	[62]
	(PEO)	LiTFSI	60	1.30×10^{-4}	[63]
	Poly(oxymethylene-oligo-oxyethylene)	LiClO ₄	25	6.00×10^{-6}	[64]
	(POO)				
	Poly(propylene oxide)	LiClO ₄	20	1.00×10^{-8}	[65]
	(PPO)				
	Poly(dimethyl siloxane)	LiClO ₄	20	1.00×10^{-4}	[66]
	(DMS)				
<i>Branched</i>	(PEO-PPO-PEO)-SC,				
	(SC= siloxane crosslinked)	LiClO ₄	20	1.5×10^{-5}	[67]
	Poly(dimethyl siloxane-co-ethylene oxide)	LiClO ₄	25	2.60×10^{-4}	[66]
	(PDMS-PEO)				
	poly(ethylene oxide-co-2-(2-methoxyethoxy)ethyl glycidyl ether) (PEO-PMEEGE)	LiTFSI	60	1.50×10^{-3}	[68]
	Polyethylene-b-PEO (PE-PEO)	LiClO ₄	25	1.00×10^{-5}	[69]
	PEC-PEG	LiTf	40	1.00×10^{-4}	[70]
<i>Plasticizer added</i>	PEC-PEGDME	LiTFSI		3.60×10^{-4}	[63]
<i>Polymer in-salt</i>	Poly(propylene oxide)	LiClO ₄ -LiBr-	20	2.00×10^{-2}	[71]
	(PPO)	AlCl ₃			

1-3-2 Ion-transport mechanism of solid polymer electrolytes

Like electrolyte solutions, SPEs are also ionic conductors that transport electricity as ions in the electrolytes. However, the ion transport in the SPEs is actually not that easy and simple. For the development solid polymer electrolyte, fundamental understanding of ion-conductive mechanism is essential. It is widely accepted that the ionic conduction in polymer electrolytes occurs cooperatively with micro-Brownian motion of polymer chains, as shown in Figure 1-10. The reason is that the temperature dependence of ionic conductivity σ for solid polymer electrolytes often follows the equations

$$\log\left(\frac{\sigma(T)}{\sigma(T_s)}\right) = \frac{C_1(T - T_s)}{C_2 + (T - T_s)} \quad (1-3)$$

and

$$\sigma = A \exp\left(-\frac{B}{T - T_0}\right) \quad (1-4)$$

which are analogous to Williams-Landel-Ferry (WLF) and Vogel-Tammann-Fulcher (VTF) equation, respectively. These are equations that represent the temperature dependence of the structural relaxation time τ of polymer chains, based on the free volume theory.

Figure 1-11 shows an example WLF plot of ionic conductivity for cross-linked PEO network polymer prepared by dissolving various alkali metal salts.^[72] The temperature dependences of all electrolytes mostly follow the same master curve, where $T_s = T_g + 50$, $C_1 = 4.6$, and $C_2 = 95.6$, which are similar to the universal values for amorphous polymers.

Ionic conductivity of materials can be connected with the mobility of the carrier ions μ by

$$\sigma = \sum \mu_i n_i q_i \quad (1-5)$$

where μ_i , n_i , and q_i are the mobility of the carrier ions, the number density of the carrier ions, and the charge of the ion i , respectively. The mobility μ of the ion can be correlated with diffusion coefficient D by Nernst-Einstein relationship

$$\mu = Dq/kT \quad (1-6)$$

where k is Boltzmann's constant. The correlation between D and viscosity η is given by Stokes-Einstein relationship

$$D = kT/6\pi r\eta \quad (1-7)$$

where r is Stokes radius which represents the hydrodynamic radius of the ion. For rubbery polymer materials, the viscosity η can be defined as a value which is proportional to the inverse of relaxation time τ of the segmental motion.

$$\eta \propto 1/\tau \quad (1-8)$$

The above theories indicate that the temperature dependence of conductivity is largely controlled by the structural relaxation time τ of the polymer chains, and the temperature dependence of ion mobility μ follows the WLF and VTF equation. The above observations indicate that the time scale of the structural relaxation time of polymer chains and mobility of the ions are correlated. This correlation is expected to mostly govern the ionic conduction in an amorphous domain of polyether.

In accordance with the theory, the simplest way to improve the conductivity is as follows.

1. Increase the number of carrier ions.
2. Enhance the segmental motion of polymer chains (without deterioration of mechanical

strength).

3. Reduce the crystallinity if the polymer is semi-crystalline.

So far efforts to improve the ion-conductive performance of SPE have been directed mostly to development of highly dissociating salts, optimization of polyether structure, and exploration of non-polyether structures suitable for SPE use. In the following section efforts which have been made so far to seek improvement of ion-conductive performance will be briefly reviewed.

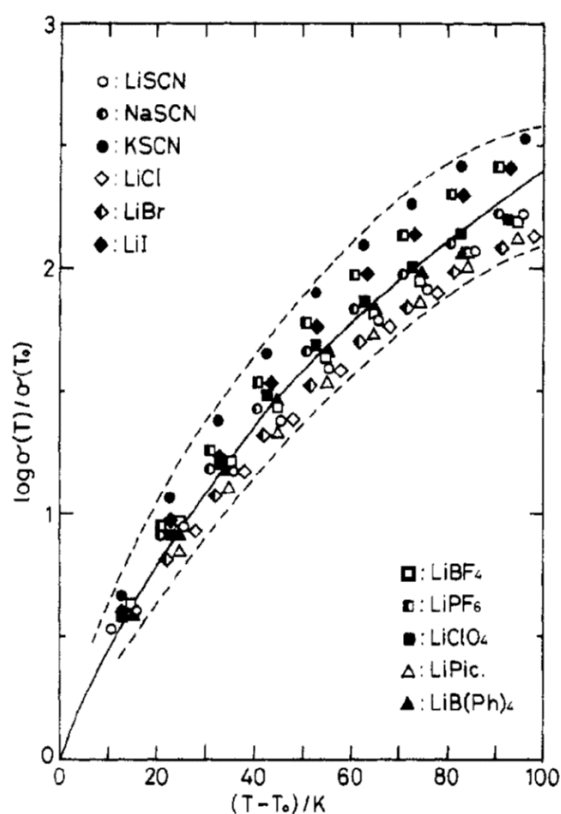


Figure 1-11. WLF plots of ionic conductivity for PEO-alkali metal salt complexes using a reference temperature $T_0 (= T_g + 50)$.^[72]

1-3-3 Polycarbonate-based electrolytes

In the past few decades, SPEs have mainly been studied on polyether-based system due to its good ion-conductive behavior and high solubility for many kinds of metal salts.^[56,73–75] However, the ionic conductivity at room temperature and poor cation (Li^+) transference number of PEO-based electrolytes are still considered to be issue that should be solved (Figure 1-12).^[73,76–78] Thus, a new ion transfer mechanism of polymer is strongly required.

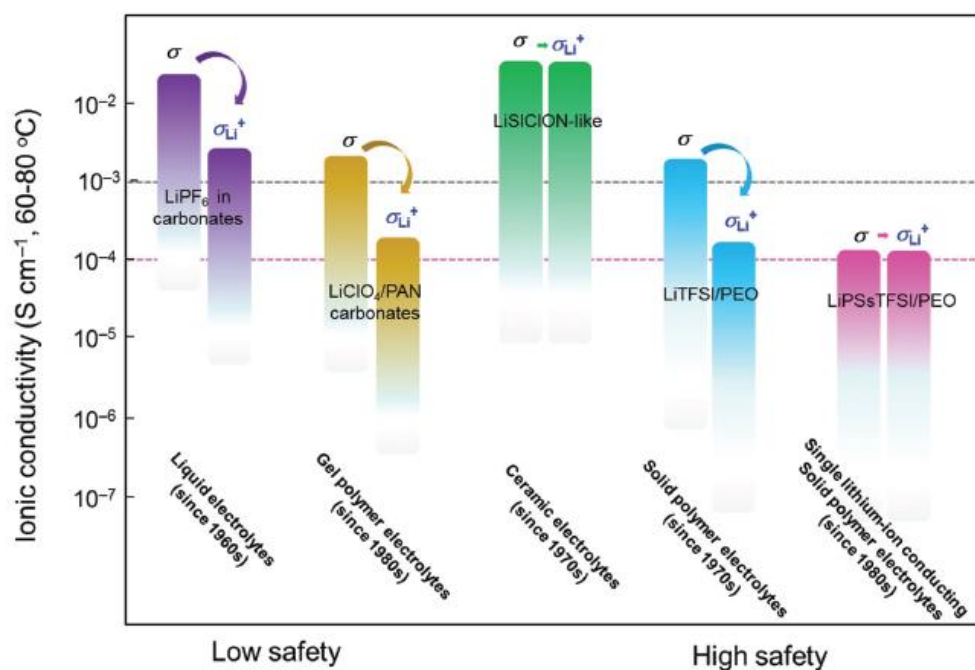
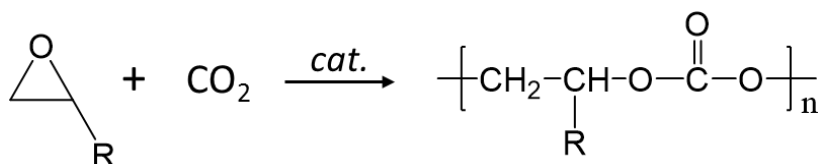


Figure 1-12. Roadmap for the development of Li-ion conducting electrolytes for rechargeable lithium and Li-ion batteries, including liquid electrolytes, gel polymer electrolytes, ceramic electrolytes, solid polymer electrolytes and single lithium-ion conducting solid polymer electrolytes. The requirements of total ionic conductivity (σ) and individual Li^+ conductivity (σ_{Li^+}) for battery operation are shown as gray and pink dashed lines, respectively.^[78]

Recently, some reports of relatively high performances of polycarbonate/ester electrolytes invoke interests. Although carbonate-based organic solutions are predominantly used in commercially available lithium-ion batteries, researches of polycarbonate-based electrolytes

are rare. In the early researches, Smith *et al.*^[79,80] have reported preparation of poly(trimethylene carbonate) (PTMC)-based electrolytes. Electrolytes containing various lithium salts, such as LiCF₃SO₃, LiClO₄, and LiBF₄, showed conductivity of the order of 10⁻⁶ to 10⁻⁴ S cm⁻¹ at elevated temperatures (ca. 70-80 °C). Brandell *et al.*^[81,82] took over the research of PTMC and its derivatives recently. In their report, a PTMC/LiTFSI electrolyte shows a conductivity of the order of 10⁻⁷ S cm⁻¹ at 60 °C.

Tominaga *et al.*^[83-85] have recently studied electrolytes based on poly(ethylene carbonate) (PEC) and achieved impressive results. Poly(alkylene carbonate)s are generated from copolymerization of CO₂ with epoxides (Scheme 1-1). This copolymerization method was first discovered by Inoue and co-workers in the late 1960s,^[86] and has become popular in polymer chemistry^[87] because large portion of polymer chain is derived from CO₂. Despite interesting features (*e.g.* biodegradability) so far no practical application has yet been established. Furthermore, this polycarbonate-based electrolytes demonstrate an unusual ion-conductive behavior.^[85] The PEC system showed a continuous increase in conductivity and decrease in glass transition temperature (*T_g*) with increasing salt concentration (Figure 1-13) and has very high lithium transference number (*t₊*) (Table 1-4). The resulting conductivity of a highly concentrated PEC/LiFSI 80 wt% electrolyte is of the order of 10⁻⁴ S cm⁻¹ at 40 °C, which is comparable to that of PEO electrolytes at elevated temperature.



Scheme 1-1. Synthesis of poly(alkylene carbonate)s by CO₂/epoxide alternating copolymerization.

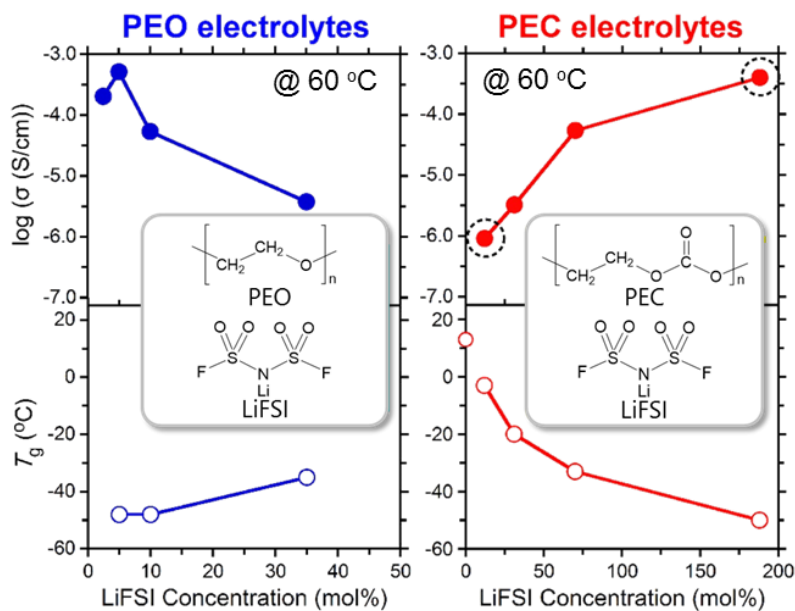


Figure 1-13. Unusual salt concentration dependence of ionic conductivity and glass transition temperature (T_g) of poly(ethylene carbonate) (PEC) electrolytes.^[85]

Table 1-4. High lithium transference number (t_+) of poly(ethylene carbonate) (PEC) electrolytes in comparison with conventional PEO electrolyte.^[85,88]

Electrolyte	t_+
PEC/LiTFSI (100 mol%)	0.71 (80 °C)
PEC/LiTFSI (188 mol%)	0.54 (60 °C)
PEO/LiTFSI (5 mol%)	0.16 (80 °C)

Moreover, the electrochemical stability and aluminum collector corrosion of PEC-based electrolytes are greatly improved upon increase in salt concentration. Tominaga *et al.*^[89] have reported that the anodic oxidation stability and aluminum corrosion reaction were significantly improved with increasing salt concentration, and those properties stable up to more than 5 V at very concentrated region (Figure 1-14). In the highly concentrated PEC-based electrolytes, larger number of the electron ion pairs of the polar groups are stabilized by the coordination to Li^+ , which makes the solvent less prone to oxidation and prevent a dissolution of Al^{3+} (or Al-anion complex). These behaviors are likely to be compatible with high voltage (4–5 V) lithium batteries and similar properties have been reported in several liquid concentrated electrolytes.^[90,91] Therefore, the concentrated polycarbonate-based SPEs can be suggested to one of the potential electrolyte materials for future high energy density all-solid-state lithium batteries.

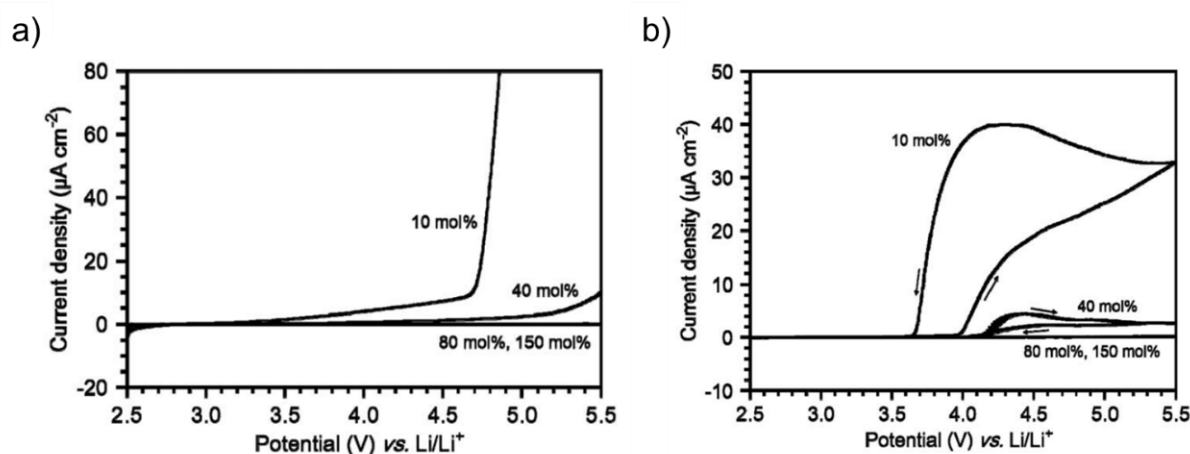


Figure 1-14. (a) linear sweep voltammograms of stainless steel working electrode and (b) cyclic voltammograms (2nd cycle) of Al working electrode using PEC/LiTFSI electrolytes with various salt concentrations at 30 °C and a scan rate of 5 mV s^{-1} .^[89]

High performance at ambient temperature and rate capability of lithium polymer batteries using polycarbonate/ester-based electrolytes, which appears to be better than that of polyether-based

batteries, have been reported recently. For instance, Mindemark *et al.*^[92] reported an ambient temperature operation of LiFePO₄/Li cell using poly(trimethylene carbonate-*co*- ϵ -caprolactone) (poly(TMC-*co*-CL)) (Figure 1-15). Tominaga *et al.*^[93] also demonstrated an operation of LiFePO₄/Li polymer battery using a composite membrane of concentrated PEC/LiFSI electrolyte and polyimide matrix substrate at 30 °C. High compatibility of polycarbonate electrolytes with cathode materials with relatively high operating voltage (> 4 V vs. Li/Li⁺) has been reported by Cui *et al.*^[94] A LiFe_{0.2}Mn_{0.8}PO₄/Li cell using a cellulose-supported polymer electrolyte based on poly(propylene carbonate) (PPC) delivered a specific capacity of around 120 mAh g⁻¹ at 20 °C at a current rate of 0.5 C. A compatibility of an electrolyte comprising poly(vinylene carbonate) (PVCA) polymerized in situ and lithium difluoro(oxalate)borate (LiDFOB) with LiCoO₂ cathode was also confirmed by the same group.^[95] More examples of polymer structures and properties of the carbonate included SPEs are listed in Table 1-5.

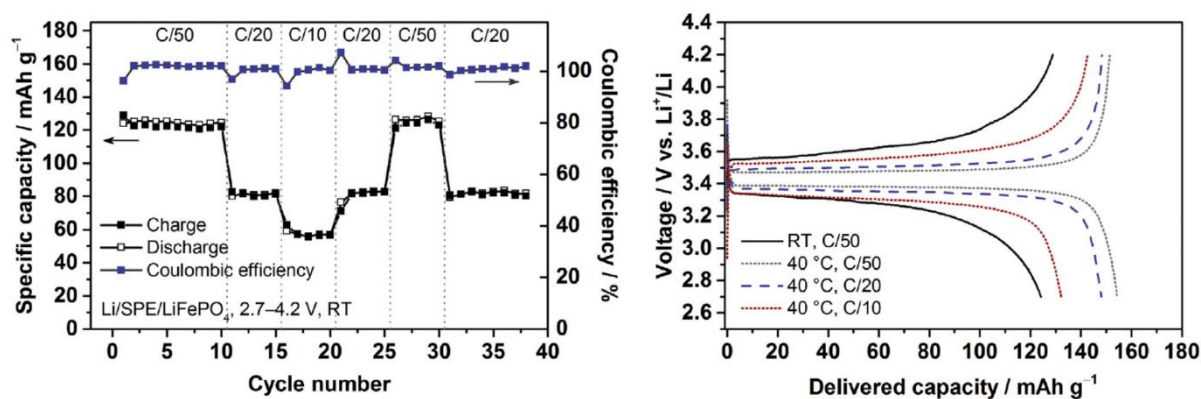
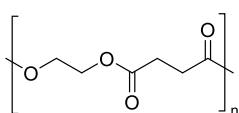
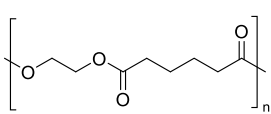
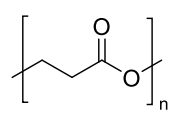
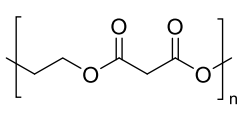
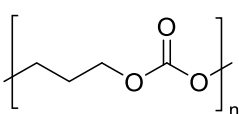
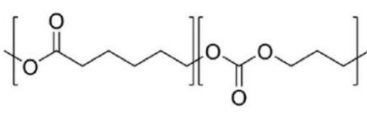
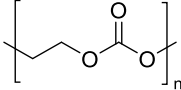


Figure 1-15. Charge/discharge capacities and coulombic efficiencies for a LiFePO₄/SPE/Li cell with the electrolyte based on poly(TMC-*co*-CL) cycled at room temperature (left) and initial charge/discharge voltage curves of the cells cycled at different temperatures and C-rates (right).^[92]

Table 1-5. Examples of carbonate included polymers used in SPEs.

Polymer	salt	T_g	T_m	Conductivity	Ref
 Poly(ethylene succinate)	LiBF ₄	-	-	1.3×10 ⁻⁷ at 41 °C ([Li]/[M]=0.5)	[96]
		-1	-	3.4×10 ⁻⁶ at 65 °C ([Li]/[M]=0.33)	[97]
	LiClO ₄	-7--6	100-101	Ca. 10 ⁻⁵ at 90 °C ([Li]/[M]=0.12)	[98]
 Poly(ethylene adipate)	LiCF ₃ SO ₃	-50	55	Ca. 10 ⁻⁵ at 60 °C ([Li]/[M]=0.25)	[99]
 Poly(β-propiolactone)	LiClO ₄	-21	74-77	Ca. 10 ⁻² at 70 °C ([Li]/[M]=0.1)	[98]
 Poly(ethylene malonate)	LiCF ₃ SO ₃	-15	Amor	4.5×10 ⁻⁵ at 65 °C ([Li]/[M]=1/8)	[100]
	LiCF ₃ SO ₃	-18	Amor	Ca. 10 ⁻⁵ at 85 °C ([Li]/[M]=1/12)	[79]
 Poly(trimethylene carbonate) (PTMC)	LiClO ₄		Amor	Ca. 10 ⁻⁴ at 85 °C ([Li]/[M]=0.5)	[79]
	LiBF ₄	-16	Amor	Ca. 10 ⁻⁶ at 75 °C ([Li]/[M]=0.2)	[101]
	LiTFSI	-15	Amor	Ca. 10 ⁻⁷ at 60 °C ([Li]/[M]=1/8)	[81]
 P(TMC-co-caprolactone)	LiTFSI	-57	Amor	4.1×10 ⁻⁵ at 25 °C (36 wt%)	[92]
	LiTFSI		Amor	4.7×10 ⁻⁴ at 20 °C	[102]

		([Li]/[M]=0.8)		
 Poly(ethylene carbonate) (PEC)	LiTFSI,			
	LiBETI,			
	LiBF ₄ ,	9	Amor	5×10 ⁻⁶ at 30 °C [83]
	LiClO ₄ ,			(80wt% LiTFSI)
	LiCF ₃ SO ₃			

	LiFSI	13–14	Amor	1.4×10 ⁻⁴ at 40 °C [85]

		([Li]/[M]=1.88)		

1-4 Concentrated electrolytes

Superconcentrated (or highly concentrated) solutions are receiving intense attention as a new class of liquid electrolytes (Figure 1-16). Generally, further increasing salt concentration over the conventional 1 mol dm^{-3} standard results in decreased ionic conductivity and increased viscosity, both of which are unfavorable as a battery electrolyte in terms of rate performance. Thus, highly concentrated electrolytes have long been outside the research focus in rechargeable Li-based batteries. However, various unusual functionalities have recently been discovered in the highly concentrated region, which bring about vigorous research worldwide on superconcentrated (highly concentrated) electrolytes. Notably, highly concentrated electrolytes show high stabilities toward both negative and positive electrodes. Those unusual electrochemical stabilities, as well as other unique features, of highly concentrated electrolytes may be a clue to a new electrolyte design strategy with an eye to long-desired breakthroughs in battery technologies.

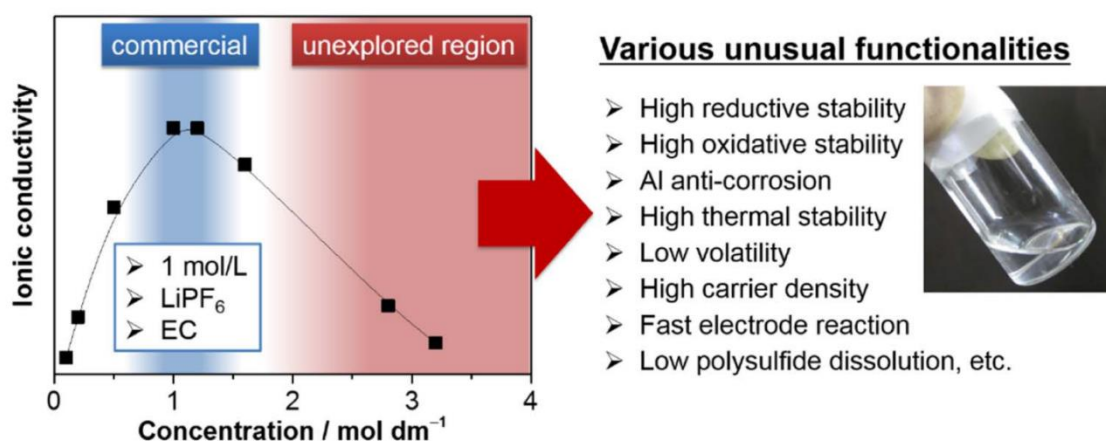
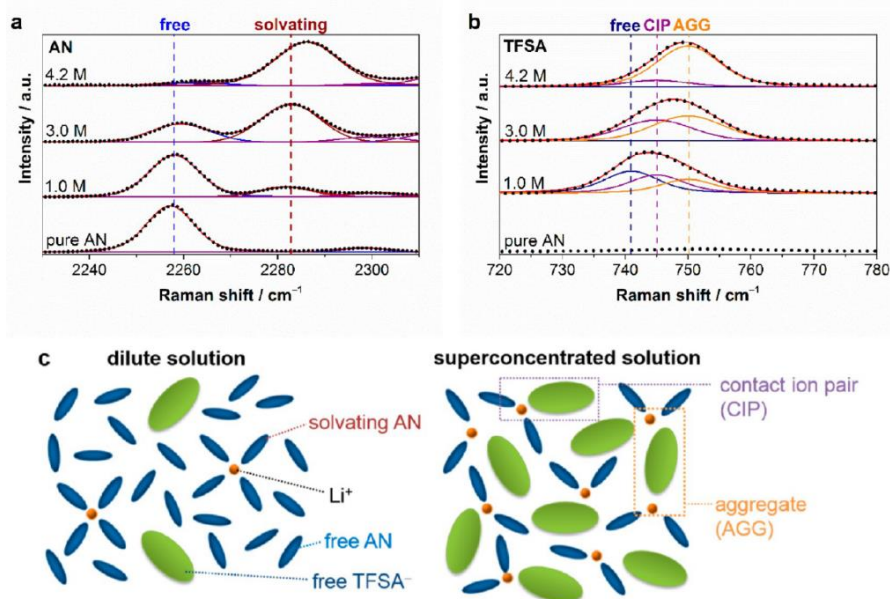


Figure 1-16. Typical ionic conductivity curve of aprotic solvent/lithium salt mixture. Highly concentrated electrolytes have been outside the research mainstream because of decreased ionic conductivity. They have recently received attention because of various unusual functionalities which are beneficial for battery applications.^[103]

A drastic change of interfacial reactions at high concentrations was a major research focus at an early stage. Suppression of solvent co-intercalation into a layered ZrS_2 electrode in a saturated $LiAsF_6$ /propylene carbonate (PC) electrolyte was first reported by McKinnon and Dahn in 1985 prior to the commercialization of Li-ion batteries in 1991.^[104] In 2000's, Ogumi and his co-workers significantly contributed to the development of this research field. They reported in 2003 and 2008 that graphite electrodes drastically change their behavior to reversibly accommodate Li^+ in highly concentrated PC electrolytes, which is impossible in corresponding dilute electrolytes due to exfoliation of graphite layers accompanied with solvent co-intercalation.^[105,106] From 2010, Yamada *et al.*^[90,107–109] extended this approach to various aprotic solvents to report general observation of reversible graphite electrode reactions without ethylene carbonate (EC) solvent. Moreover, they have discovered that the salt-concentrating strategy enable efficient cycling of graphite anode in many solvent species that have been considered unsuitable for LIBs use so far.^[110–113] Interestingly, fast electrode reactions were recently found in particular systems based on lithium LiTFSI (LiTFSI),^[90,108] which defies the conventional notion of inferior kinetics at high concentrations (Figure 1-17). Ogumi *et al.*^[114] also demonstrated in 2008 that the reversibility of Li metal deposition/stripping is significantly improved in highly concentrated PC electrolytes. After this path breaking work, highly reversible cycling of Li metal electrodes were reported by several groups. In 2013, Suo *et al.*^[91] have reported a stable cycling in a concentrated electrolyte of 1,3-dioxolane (DOL):DME (1:1 by vol.) and LiTFSI. In 2015, Qian *et al.*^[115] have also published a faster cycling in a highly concentrated DME/LiFSI electrolyte (Figure 1-18). At a positive electrode side, anti-corrosion of Al current collectors at high concentrations was reported by Matsumoto *et al.*^[116] in 2013 and McOwen *et al.*^[117] in 2014. They explained that dissolution of Al^{3+} (or Al-anion complex) was prevented due to the coordination of the most solvents and Li^+ , at high concentrations. The similar behavior has also confirmed in the concentrated PEC systems (Figure 1-14).



TFSI

Figure 1-17. Raman spectra of acetonitrile (AN)/LiTFSA solutions in (a) 2230–2310 cm^{-1} (C–N stretching mode of AN molecules) and (b) 720–780 cm^{-1} (S–N stretching, C–S stretching, and CF_3 bending mode of TFSA^-). (c) Schematic image of the environment of Li^+ in a conventional dilute solution ($\approx 1 \text{ mol dm}^{-3}$) and a salt-superconcentrated solution (4.2 mol dm^{-3}).^[108]

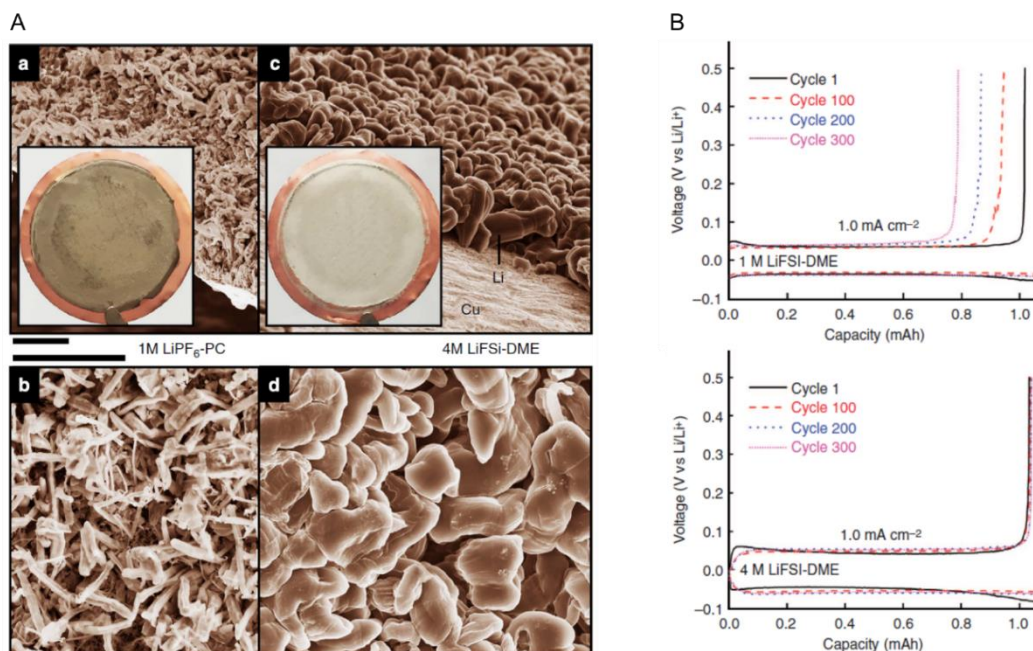


Figure 1-18. (A) SEM images of the morphologies of Li metal after plating on Cu substrates in different electrolytes. (a,b) 1 M PC/LiPF₆; (c,d) 4 M DME/LiFSI. Scale-bar equals 10 μm . (B) Voltage profiles for cells cycled in 1 M DME/LiFSI and in 4 M DME/LiFSI.^[115]

Furthermore, high oxidation stability of highly concentrated electrolytes is suggested from the series of reports. This is presumably due to a plenty of anions which are relatively stable in the proximity of the electrodes. Additionally, the solvent molecules, which are basically more prone to oxidation, are stabilized, because the electron density is reduced by the coordination to Li^+ . This characteristic may enable aqueous lithium batteries with relatively high operating voltage.^[118–120] Aqueous battery has greatly higher safety and can eliminate the manufacturing process in very strict moisture-free condition. This is likely to reduce the manufacturing cost of lithium batteries significantly.^[121] As is widely known, however, water is electrochemically unstable and is easily electrolyzed by low applied potentials, and energy density which is comparable to the current organic solution-based LIBs is difficult to achieve. Suo *et al.*^[118] have discovered that the operational potential window of $\text{H}_2\text{O}/\text{LiTFSI}$ electrolyte is significantly widened when the LiTFSI concentration was increased up to super-high value of 21 M. The super-concentrated (water-in-salt) electrolyte is liquid even if the most portion of the solution consists of the lithium salt. This extension of electrochemical stability window enabled an anode/cathode couple of Mo_6S_8 and LiMn_2O_4 , resulting in a 2.3 V aqueous battery (Figure 1-19). Their Raman and ^{17}O NMR spectroscopy indicated that most TFSI^- coordinate to Li^+ , which leads to sacrificial reduction of TFSI to form an efficient solid electrolyte interface (SEI) on the anode. The reduced number of free solvent also improves the oxidation stability as discussed above. Yamada *et al.*^[120] also reported an aqueous battery using $\text{H}_2\text{O}/\text{LiTFSI}:\text{LiBETI}$ highly concentrated electrolyte (hydrate melt electrolyte). In this report, they achieved a larger salt content and wider electrochemical stability window by mixing two different imide-type salts. So far only a limited number of anode/cathode couples and solvent/lithium salt combinations have been reported, and further exploration is strongly desired.

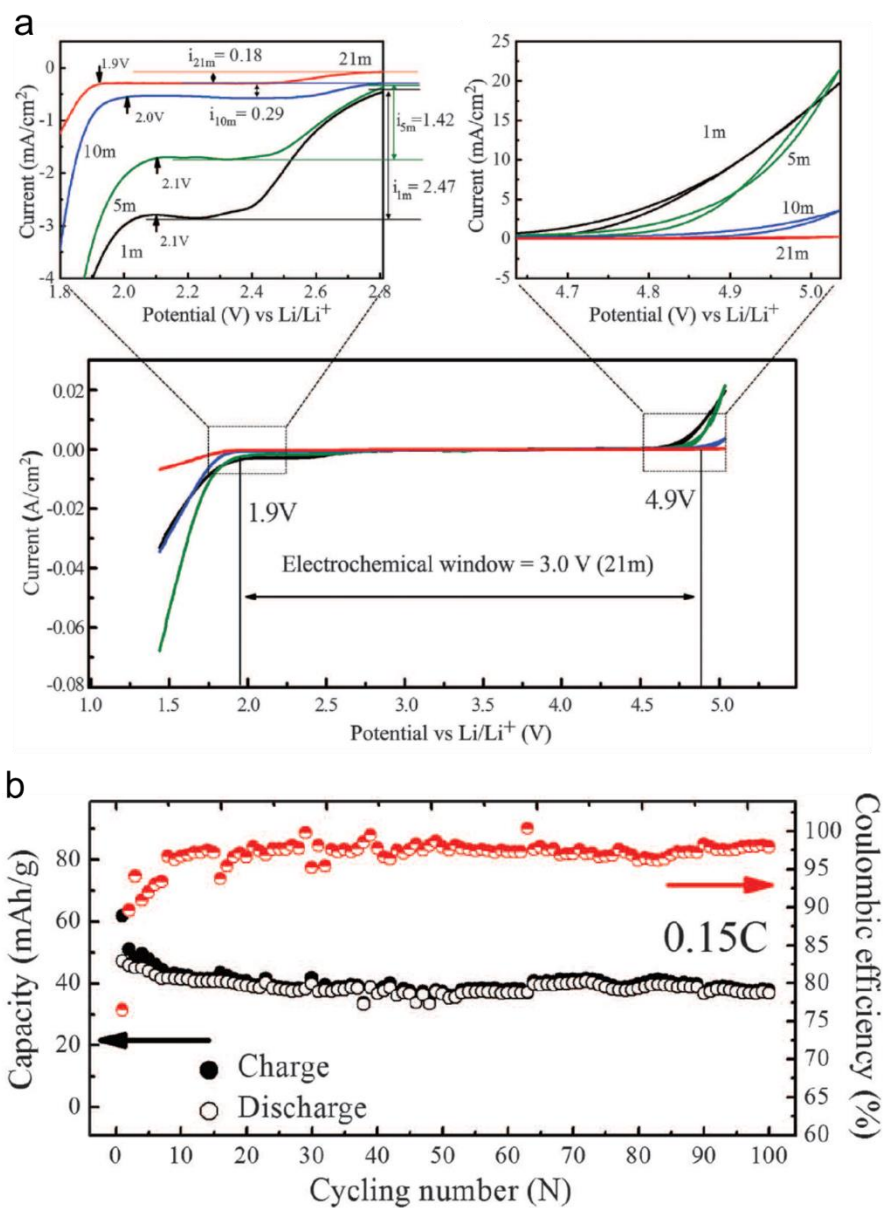


Figure 1-19. (a) Electrochemical stability window measured by using cyclic voltammetry (CV) of stainless steel electrode in $\text{H}_2\text{O}/\text{LiTFSI}$ solutions with different LiTFSI concentrations at a potential scan rate of 10 mV s^{-1} . Magnified figures of the regions near anodic and cathodic extremes are also shown. (b) Cycling stability and Coulombic efficiency of full aqueous lithium-ion cells using Mo_6S_8 and LiMn_2O_4 as anode and cathode materials in 21 M $\text{H}_2\text{O}/\text{LiTFSI}$ solution at a current rate of 0.15 C.^[118]

1-5 Composite polymer electrolytes

1-5-1 Ceramic-filled polymer electrolytes

Since the report by Weston and Steele in 1982,^[122] PEO-based composite polymer electrolytes (CPEs) have been widely studied.^[123–125] The CPEs composing of a filler and polymer matrix could obviously improve the ionic conductivity, mechanical and interfacial properties when compared to the bare polymer electrolytes. In 1998, Scrosati *et al.*^[126] added nanometer-sized ceramic powders (*e.g.*, SiO₂, Al₂O₃, TiO₂, and ZrO₂) into PEO electrolytes, leading to an increase in the ionic conductivity by 1–2 orders of magnitude (Figure 1-20). Subsequently, Bruce^[47] investigated the ionic transport in PEO-based SPE with crystalline phase. They found that the ions could transport in the crystalline state, which opened a new trend for the research of PEO-based SPEs.

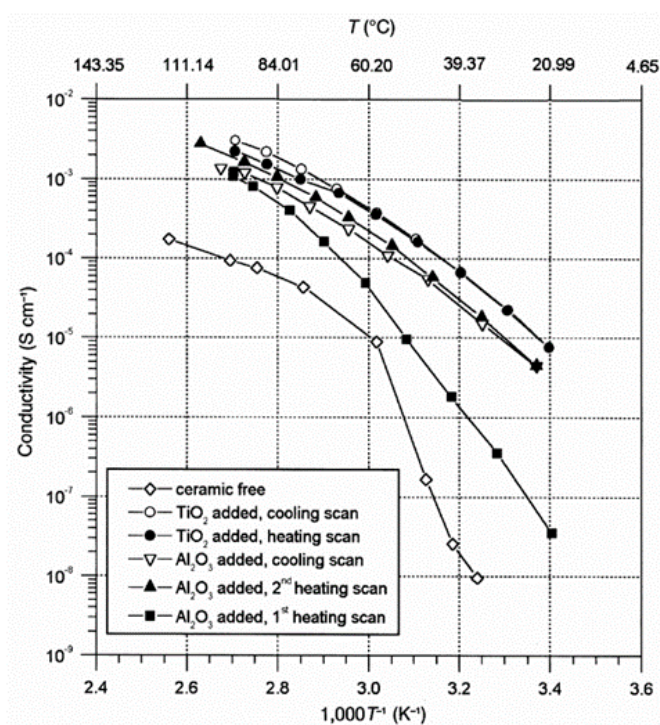


Figure 1-20. Ionic conductivity of composite PEO/LiClO₄ electrolytes containing various particulate ceramics as nano-sized filler.^[126]

Later, Shriver *et al.*^[127] systematically studied the ionic transport mechanism and relaxation coupling of the polymer electrolytes, which provided a theoretical basis for the development of solid polymer electrolytes. In 2001, Scrosati *et al.*^[128] investigated the surface effect of the ceramic filler on P(EO)₂₀ LiSO₃CF₃ polymer electrolyte. The results demonstrated that the role of the filler was not limited to preventing crystallization of the polymer but also promoting specific interactions among the surface groups, the PEO segments and the electrolyte ionic species. Figure 1-21 shows a schematic image of the surface of the ceramic filler in CPEs. Positively charged polar groups on the surface of the ceramic domain, such as OH, interact with anions and polar groups of polymer. These interactions facilitate the dissociation of cations from anions and polymer chains and reduces the crystallinity of the polymer, and in turn increases the cation (Li⁺) conductivity.

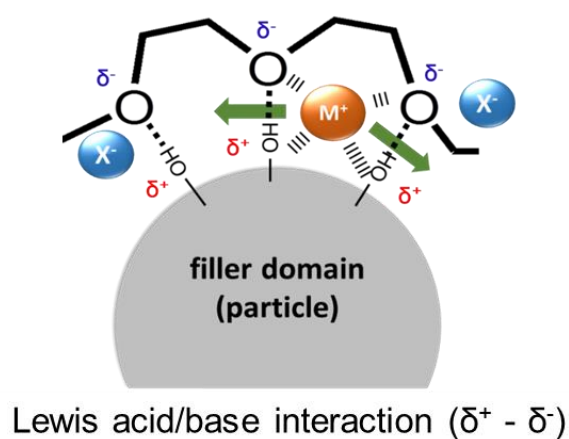


Figure 1-21. Schematic image of Lewis acid/base interaction mechanisms in the CPEs.

In addition, Archer *et al.*^[129] in 2014, reported a cross-linked polyethylene/poly(ethylene oxide) (PE/PEO) SPE with both high ionic conductivity (1.6×10^{-4} S cm⁻¹ at 25 °C) and mechanical property. This cross-linking method effectively could balance the ionic conductivity and mechanically rigid that could be used to suppress dendrite growth. In the previous work, the CPEs were usually synthesized by mechanically blending ceramic particles with polymers.

Recently, Cui *et al.*^[130] prepared a CPE ($4.4 \times 10^{-5} \text{ S cm}^{-1}$ at $30 \text{ }^\circ\text{C}$) by introducing an in-situ hydrolysis method to synthesize ceramic filler directly in solid polymer electrolyte (Figure 1-22), which suppressed the crystallization of PEO and facilitated polymer segmental motion for ionic conduction. Different with the particle ceramic filler, Tominaga *et al.*^[131] have directly filled silica nanofibers (SNFs) to the poly(ethylene oxide-*co*-propylene oxide) (P(EO/PO))-based electrolyte and improved their both ion-conductive and mechanical properties.

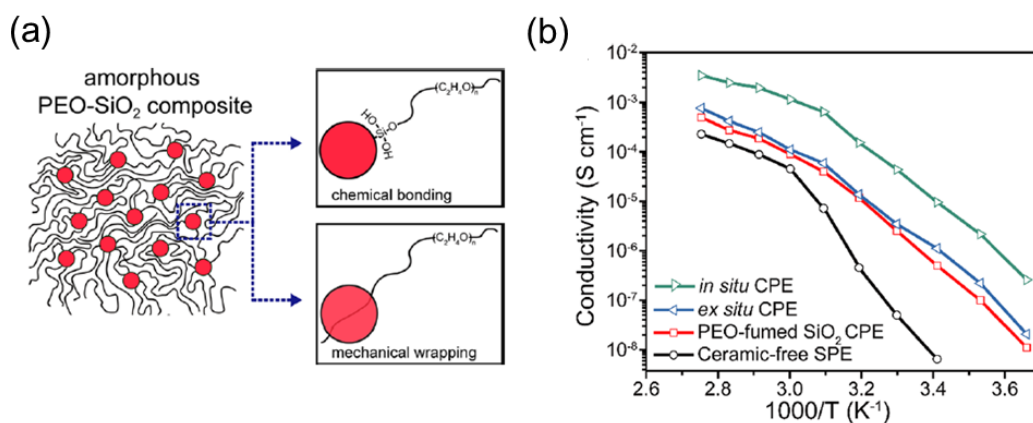


Figure 1-23. (a) Two possible interaction mechanisms including chemical bonding and mechanical wrapping among PEO chains and monodispersed ultrafine SiO₂ (MUSiO₂). (b) Arrhenius plots of ionic conductivity of ceramic-free SPE, PEO-fumed SiO₂ CPE, ex situ CPE, and in situ CPE.^[130]

1-5-2 Polymer blend electrolytes

Among the various approaches, polymer blending is the most feasible technique. Polymer blending is a process of mixing at least two polymers with/without any chemical bonding between them. A polymer blend is therefore a physical mixture of two or more polymers/copolymers. In commercial and industrial applications, polymer blends are viable products due to their unique properties that are superior to those of the component polymers. Blend is also an effective method for polymer electrolytes. Notably, blend-based polymer electrolytes can overcome the serious drawback of preparing electrolytes by nontrivial synthesis methods, thus, blending is considered to be an important method to improve the ionic conductivities and dimensional stability of polymer electrolytes. The main advantages of polymer electrolytes prepared via a blending method are the simplicity of preparation and easy control of physical properties by compositional change.

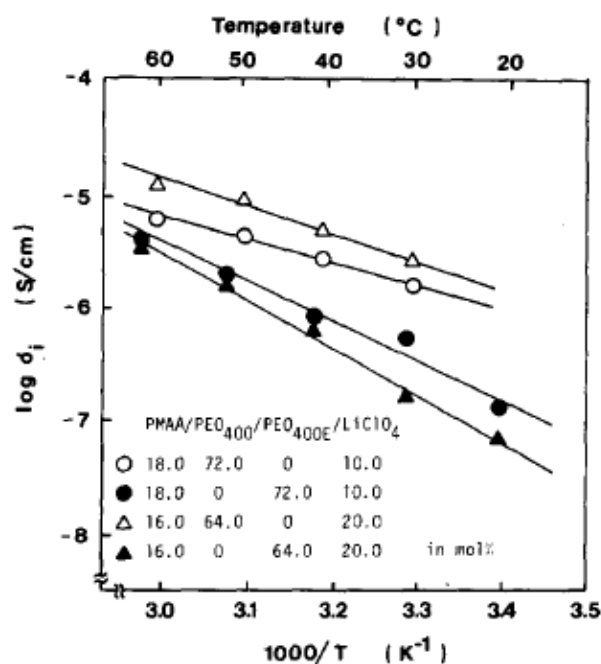


Figure 1-24. Arrhenius plots of lithium ionic conductivity of PMAA-PEO₄₀₀ or -PEO_{400E}/LiClO₄ hybrid films with different amount of LiClO₄.^[132]

In 1983, Tsuchida *et al.*^[132] prepared a solid polymer electrolyte in a hydrogen-bonding type inter-macromolecular complex of PEO-poly(methacrylic acid) (PMAA) matrix. The ionic conductivity increased with increase in the content of PEO with an average molecular weight of 400. A maximum conductivity of $1.3 \times 10^{-5} \text{ S cm}^{-1}$ at 60 °C was obtained. Rocco *et al.*^[133] also prepared a PEO-based electrolyte blended with poly(methyl vinyl ether-maleic acid) (PMVE-Mac). The maximum ionic conductivity of the SPE with 7.5 wt% LiClO₄ reached approximately $10^{-5} \text{ S cm}^{-1}$ at ambient temperature. Because of the intermolecular hydrogen bonds between PEO and PMVE-Mac, the crystallization of PEO was hindered, and the SPE system was associated with a greater blend-free volume, mobility and flexibility than in pure PEO. Later, the authors synthesized a PEO-based electrolyte blended with poly(bisphenol-A-*co*-epichlorohydrin) (PBE) in the presence of LiClO₄.^[134,135] The miscibility of PEO and PBE was attributed to intermolecular hydrogen bonds between the polymers. Fourier transform infrared spectroscopy indicated complexation of the Li⁺ by both PEO and PBE oxygen atoms. The SPE showed a high electrochemical stability window (5.5 V). There are also nonpolyether blend electrolytes have been studied such as using poly(trimethylene carbonate) (PTMC), poly(vinyl alcohol) (PVA), and so on. Table 1-6 summarized various examples of blend electrolytes and their ionic conductivity.

Table 1-6. Various examples of blend electrolytes and their ionic conductivity.

Polymer matrix	Li salt	Temp (°C)	Conductivity (S/cm)	Ref
PEO/PMAA	LiClO ₄	60	1.30×10^{-6}	[132]
PEO/MEEP	LiBF ₄	25	4.00×10^{-6}	[136]
PEO/P2VP	LiClO ₄	25	1.00×10^{-5}	[137]
PEO/PES	LiClO ₄	25	3.00×10^{-5}	[138]
PEO/PET	LiClO ₄	25	2.00×10^{-5}	[139]
PEO/PVDF	LiClO ₄	30	2.62×10^{-5}	[140]
	LiTFSI	30	4.90×10^{-3}	[141]
PEO/PVP	Mg(NO ₃) ₂	25	5.80×10^{-4}	[142]
PEO/PTMC	LiTFSI	25	1.35×10^{-4}	[143]
PEO/PEC	LiBF ₄	25	8.80×10^{-5}	[144]
PVA/PVP	NH ₄ SCN	25	6.85×10^{-4}	[145]

1-6 Objective of the present study

There is increasing worldwide motivation to research and develop all-solid-state batteries in order to achieve better safety, higher power and energy density, as well as wider operating temperature energy storage as compared to conventional lithium-ion batteries (LIBs). However, conventional LIBs normally use liquid electrolytes, are based on organic solvents, which are intrinsically volatile and highly flammable. Due to these reasons, there are many battery safety accidents have happened. Therefore, we suggest solid polymer electrolytes (SPEs) to replace the typical liquid-type electrolytes, because SPEs have better flexibility in packaging and higher safety than that of inorganic ceramic-based electrolytes for all-solid-state batteries. Especially for using poly(ethylene carbonate) (PEC)-based composite polymer electrolytes (CPEs).

SPEs are solid ion-conductive materials, which mainly consist of polar polymer and metal (Li, Na, Mg and so on) salt. As we mentioned in the introduction, SPEs have been mainly studied on polyether-based electrolytes such as poly(ethylene oxide) (PEO)-based electrolytes in the past several decades, due to its good ion-conductive behavior and high solubility for many kinds of metal salts. However, polyether-based SPEs usually reveal poor electrochemical properties, especially very low Li^+ transference number (t_+), because of the strong segmental motion between ether oxygen and Li^+ . This is a fatal defect as an electrolyte material for LIBs. Therefore, an alternative strategy for the material development is required.

Recently, Tominaga's group has introduced polycarbonate-based electrolytes, which exhibit an unusual ion-conductive properties compare with the typical polyether-based electrolytes. In the case of poly(ethylene carbonate) (PEC)-based electrolytes, the ionic conductivity increases and the glass transition temperature (T_g) decreases with increasing salt concentrations. Moreover, this PEC-based electrolytes not only have excellent t_+ (higher than 0.6), but also show a good electrochemical stabilities in the highly concentrated system such as wide electrochemical

window up to 5 V and prevention effect of metal corrosion reaction. Unfortunately, there still are drawbacks even with such excellent electrochemical properties. PEC-based electrolytes exhibit a very poor thermal and mechanical properties result in easy to decompose at high temperature and short circuit during battery test. The ionic conductivity also needed to be further improvement for battery application.

As introduced in the previous section, development of CPE is a good selection for improving both ion-conductive and physical properties of the same time such as filled with inorganic fillers or in addition of other polymers. In the present study, we demonstrate methods to improve both ion-conductive and physical properties, and investigate the battery applications by developing composite electrolytes. The followings are outline of this dissertation.

First, a silica nanofiber (SNF) synthesized by calcination-free process is filled into the PEC-based electrolytes as inorganic filler and their ion-conductive, thermal and mechanical properties are investigated. In addition, the fiber size effects of SNFs in the SPEs are also carried out (Chapter 2). Next, a polycarbonate blend electrolytes based on PEC and poly(trimethylene carbonate) (PTMC) are developed for improving the ionic conductivity and thermal properties of polycarbonate-based electrolytes (Chapter 3). Finally, electrochemical stabilities and battery application by using highly concentrated polycarbonate-based composite electrolytes are revealed (Chapter 4).

References

- [1] D.O. Akinyele, R.K. Rayudu, Review of energy storage technologies for sustainable power networks, *Sustain. Energy Technol. Assessments*. **8** (2014) 74–91.
- [2] S. Hameer, J.L. van Niekerk, A review of large-scale electrical energy storage, *Int. J. ENERGY Res.* **39** (2015) 1179–1195.
- [3] W. Wu, Y. Zhang, D. Ding, T. He, A High-Performing Direct Carbon Fuel Cell with a 3D Architected Anode Operated Below 600 °C, *Adv. Mater.* **30** (2018) 1–6.
- [4] D.J.L. Brett, A. Atkinson, N.P. Brandon, S.J. Skinner, Intermediate temperature solid oxide fuel cells, *Chem. Soc. Rev.* **37** (2008) 1568–1578.
- [5] X.F. Lu, G.R. Li, Y.X. Tong, A review of negative electrode materials for electrochemical supercapacitors, *Sci. China Technol. Sci.* **58** (2015) 1799–1808.
- [6] Y. Zhai, Y. Dou, D. Zhao, P.F. Fulvio, R.T. Mayes, S. Dai, Carbon materials for chemical capacitive energy storage, *Adv. Mater.* **23** (2011) 4828–50.
- [7] J.M. Tarascon, M. Armand, Issues and challenges facing rechargeable lithium batteries, *Nature*. **414** (2001) 359–367.
- [8] J.W. Choi, D. Aurbach, Promise and reality of post-lithium-ion batteries with high energy densities, *Nat. Rev. Mater.* **1** (2016) 1–16.
- [9] M.S. Whittingham, Electrical Energy-Storage and Intercalation Chemistry, *Science (80-.)*. **192** (1976) 1126–1127.
- [10] S. Bauer, Flexible electronics: Sophisticated skin, *Nat. Mater.* **12** (2013) 871–872.
- [11] B. Nykvist, M. Nilsson, Rapidly falling costs of battery packs for electric vehicles, *Nat. Clim. Chang.* **5** (2015) 329–332.
- [12] M.S. Whittingham, Lithium Batteries and Cathode Materials, *Chem. Rev.* **104** (2004).
- [13] C.C. Li, Y.W. Wang, Importance of binder compositions to the dispersion and

- electrochemical properties of water-based LiCoO₂ cathodes, *J. Power Sources*. **227** (2013) 204–210.
- [14] B. Scrosati, J. Garche, Lithium batteries: Status, prospects and future, *J. Power Sources*. **195** (2010) 2419–2430.
- [15] A.D. Roberts, X. Li, H. Zhang, Porous carbon spheres and monoliths: Morphology control, pore size tuning and their applications as Li-ion battery anode materials, *Chem. Soc. Rev.* **43** (2014) 4341–4356.
- [16] N.A. Kaskhedikar, J. Maier, Lithium storage in carbon nanostructures, *Adv. Mater.* **21** (2009) 2664–2680.
- [17] K. Persson, V.A. Sethuraman, L.J. Hardwick, Y. Hinuma, Y.S. Meng, A. Van Der Ven, V. Srinivasan, R. Kostecki, G. Ceder, Lithium diffusion in graphitic carbon, *J. Phys. Chem. Lett.* **1** (2010) 1176–1180.
- [18] F. Orsini, A. du Pasquier, B. Beaudouin, J.M. Tarascon, M. Trentin, N. Langenhuizen, E. de Beer, P. Notten, In situ SEM study of the interfaces in plastic lithium cells, *J. Polym. Sci. Part B Polym. Phys.* **81–82** (1999) 918–921.
- [19] J. Liu, Addressing the grand challenges in energy storage, *Adv. Funct. Mater.* **23** (2013) 924–928.
- [20] Y. Kato, S. Hori, T. Saito, K. Suzuki, M. Hirayama, A. Mitsui, M. Yonemura, H. Iba, R. Kanno, High-power all-solid-state batteries using sulfide superionic conductors, *Nat. Energy*. **1** (2016) 1–7.
- [21] J. Janek, W.G. Zeier, A solid future for battery development, *Nat. Energy*. **1** (2016) 1–4.
- [22] A.L. Robinson, J. Janek, Solid-state batteries enter EV fray, *MRS Bull.* **39** (2014) 1046–1047.
- [23] N. Kamaya, K. Homma, Y. Yamakawa, M. Hirayama, R. Kanno, M. Yonemura, T.

- Kamiyama, Y. Kato, S. Hama, K. Kawamoto, A. Mitsui, A lithium superionic conductor, *Nat. Mater.* **10** (2011) 682–686.
- [24] Y. Seino, T. Ota, K. Takada, A. Hayashi, M. Tatsumisago, A sulphide lithium super ion conductor is superior to liquid ion conductors for use in rechargeable batteries, *Energy Environ. Sci.* **7** (2014) 627–631.
- [25] M.A. Kraft, S.P. Culver, M. Calderon, F. Böcher, T. Krauskopf, A. Senyshyn, C. Dietrich, A. Zevalkink, J. Janek, W.G. Zeier, Influence of Lattice Polarizability on the Ionic Conductivity in the Lithium Superionic Argyrodites Li₆PS₅X (X = Cl, Br, I), *J. Am. Chem. Soc.* **139** (2017) 10909–10918.
- [26] Q. Li, J. Chen, L. Fan, X. Kong, Y. Lu, Progress in electrolytes for rechargeable Li-based batteries and beyond, *Green Energy Environ.* **1** (2016) 18–42.
- [27] Y. Zhu, X. He, Y. Mo, First principles study on electrochemical and chemical stability of solid electrolyte-electrode interfaces in all-solid-state Li-ion batteries, *J. Mater. Chem. A.* **4** (2016) 3253–3266.
- [28] Y. Zhu, X. He, Y. Mo, Origin of Outstanding Stability in the Lithium Solid Electrolyte Materials: Insights from Thermodynamic Analyses Based on First-Principles Calculations, *ACS Appl. Mater. Interfaces.* **7** (2015) 23685–23693.
- [29] W.D. Richards, L.J. Miara, Y. Wang, J.C. Kim, G. Ceder, Interface Stability in Solid-State Batteries, *Chem. Mater.* **28** (2016) 266–273.
- [30] J.B. Bates, N.J. Dudney, B. Neudecker, A. Ueda, C.D. Evans, Thin-film lithium and lithium-ion batteries, *Solid State Ionics.* **135** (2000) 33–45.
- [31] J.B. Bates, O. Rtdge, Glutamate Correlations Between the Anterior Cingulate and Cerebellar Vermis, *Proc. 19th Sci. Meet. Int. Soc. Magn. Reson. Med.* **19** (2011) 2530.
- [32] J.B. Bates, N.J. Dudney, G.R. Gruzalski, R.A. Zuhr, A. Choudhury, C.F. Luck, J.D. Robertson, Fabrication and characterization of amorphous lithium electrolyte thin films

- and rechargeable thin-film batteries, *J. Power Sources*. **43** (1993) 103–110.
- [33] J.B. Bates, N.J. Dudney, D.C. Lubben, G.R. Gruzalski, B.S. Kwak, X. Yu, R.A. Zuhr, Thin-film rechargeable lithium batteries, *J. Power Sources*. **54** (1995) 58–62.
- [34] R. Kanno, M. Murayama, Lithium Ionic Conductor Thio-LISICON The $\text{Li}_2\text{S-GeS}_2\text{-P}_2\text{S}_5$ System, *J. OfThe Electrochem. Soc.* **148** (2001) A742–A746.
- [35] T. Minami, A. Hayashi, M. Tatsumisago, Recent progress of glass and glass-ceramics as solid electrolytes for lithium secondary batteries, *Solid State Ionics*. **177** (2006) 2715–2720.
- [36] R. Kanno, T. Hata, Y. Kawamoto, M. Irie, Synthesis of a new lithium ionic conductor, thio-LISICON-lithium germanium sulfide system, *Solid State Ionics*. **130** (2000) 97–104.
- [37] F. Mizuno, A. Hayashi, K. Tadanaga, M. Tatsumisago, New, Highly Ion-Conductive Crystals Precipitated from $\text{Li}_2\text{S-P}_2\text{S}_5$ Glasses, *Adv. Mater.* **17** (2005) 918–921.
- [38] M. Murayama, R. Kanno, M. Irie, S. Ito, T. Hata, N. Sonoyama, Y. Kawamoto, Synthesis of new lithium ionic conductor thio-LISICON - Lithium silicon sulfides system, *J. Solid State Chem.* **168** (2002) 140–148.
- [39] Y. Inaguma, C. Liqun, M. Itoh, T. Nakamura, T. Uchida, H. Ikuta, M. Wakihara, High ionic conductivity in lithium lanthanum titanate, *Solid State Commun.* **86** (1993) 689–693.
- [40] A. Morata-Orrantia, S. García-Martín, E. Morán, M.Á. Alario-Franco, A New $\text{La}_{2/3}\text{Li}_x\text{Ti}_{1-x}\text{Al}_x\text{O}_3$ Solid Solution: Structure, Microstructure, and Li^+ Conductivity, *Chem. Mater.* **14** (2002) 2871–2875.
- [41] H. Aono, E. Sugimoto, Ionic Conductivity of Solid Electrolytes Based on Lithium Titanium Phosphate, *J. Electrochem. Soc.* **137** (1990) 1023–1027.
- [42] V. Thangadurai, W. Weppner, $\text{Li}_6\text{ALa}_2\text{Ta}_2\text{O}_{12}$ (A=Sr, Ba): Novel garnet-like oxides for

- fast lithium ion conduction, *Adv. Funct. Mater.* **15** (2005) 107–112.
- [43] B.R. Shin, Y.J. Nam, D.Y. Oh, D.H. Kim, J.W. Kim, Y.S. Jung, Comparative Study of TiS₂/Li-In All-Solid-State Lithium Batteries Using Glass-Ceramic Li₃PS₄ and Li₁₀GeP₂S₁₂ Solid Electrolytes, *Electrochim. Acta.* **146** (2014) 395–402.
- [44] G. Sahu, Z. Lin, J. Li, Z. Liu, N. Dudney, C. Liang, Air-stable, high-conduction solid electrolytes of arsenic-substituted Li₄SnS₄, *Energy Environ. Sci.* **7** (2014) 1053–1058.
- [45] T. Ohtomo, A. Hayashi, M. Tatsumisago, Y. Tsuchida, S. Hama, K. Kawamoto, All-solid-state lithium secondary batteries using the 75Li₂S·25P₂S₅ glass and the 70Li₂S·30P₂S₅ glass-ceramic as solid electrolytes, *J. Power Sources.* **233** (2013) 231–235.
- [46] J.G. Kim, B. Son, S. Mukherjee, N. Schuppert, A. Bates, O. Kwon, M.J. Choi, H.Y. Chung, S. Park, A review of lithium and non-lithium based solid state batteries, *J. Power Sources.* **282** (2015) 299–322.
- [47] G.S. MacGlashan, Y.G. Andreev, Structure of the polymer electrolyte poly (ethylene oxide)₆: LiAsF₆, *Nature.* **398** (1999) 792–794.
- [48] B.W.H. Meyer, Polymer Electrolytes for Lithium-Ion Batteries, (1998) 439–448.
- [49] K. Xu, Electrolytes and interphases in Li-ion batteries and beyond, *Chem. Rev.* **114** (2014) 11503–11618.
- [50] Y. Liang, Z. Tao, J. Chen, Organic electrode materials for rechargeable lithium batteries, *Adv. Energy Mater.* **2** (2012) 742–769.
- [51] Z. Song, H. Zhou, Towards sustainable and versatile energy storage devices: An overview of organic electrode materials, *Energy Environ. Sci.* **6** (2013) 2280–2301.
- [52] Y. Liang, P. Zhang, S. Yang, Z. Tao, J. Chen, Fused heteroaromatic organic compounds for high-power electrodes of rechargeable lithium batteries, *Adv. Energy Mater.* **3** (2013) 600–605.
- [53] Y. Liang, P. Zhang, J. Chen, Function-oriented design of conjugated carbonyl

- compound electrodes for high energy lithium batteries, *Chem. Sci.* **4** (2013) 1330–1337.
- [54] H. Chen, M. Armand, G. Demailly, F. Dolhem, P. Poizot, J.M. Tarascon, From biomass to a renewable LiXC₆O₆ organic electrode for sustainable li-ion batteries, *ChemSusChem.* **1** (2008) 348–355.
- [55] Z. Zhu, M. Hong, D. Guo, J. Shi, Z. Tao, J. Chen, All-solid-state lithium organic battery with composite polymer electrolyte and Pillar[5]quinone cathode, *J. Am. Chem. Soc.* (2014).
- [56] D.E. Fenton, J.M. Parker, P. V. Wright, Complexes of alkali metal ions with poly(ethylene oxide), *Polymer (Guildf).* **14** (1973) 589.
- [57] P. V. Wright, Electrical conductivity in ionic complexes of poly(ethylene oxide), *Br. Polym. J.* **7** (1975) 319–327.
- [58] M.B. Armand, J.M. Chabagno, M.J. Duclot, Fast Ion Transport in Solids, North-Holland: Amsterdam, 1979.
- [59] A. Manuel Stephan, K.S. Nahm, Review on composite polymer electrolytes for lithium batteries, *Polymer (Guildf).* **47** (2006) 5952–5964.
- [60] K. Xu, Nonaqueous Liquid Electrolytes for Lithium-Based Rechargeable Batteries, *Chem. Rev.* **104** (2004) 4303–4418.
- [61] Z. Xue, D. He, X. Xie, Poly(ethylene oxide)-based electrolytes for lithium- ion batteries, *J. Mater. Chem. A.* **3** (2015) 19218–19253.
- [62] A.Vallée, S.Besner, J.Prud'Homme, Comparative study of poly(ethylene oxide) electrolytes made with LiN(CF₃SO₂)₂, LiCF₃SO₃ and LiClO₄: Thermal properties and conductivity behaviour, *Electrochim. Acta.* **37** (1992) 1579–1583.
- [63] H. Wang, D. Im, D.J. Lee, M. Matsui, Y. Takeda, O. Yamamoto, N. Imanishi, A composite polymer electrolyte protect layer between lithium and water stable ceramics

- for aqueous lithium-air batteries, *J. Electrochem. Soc.* **160** (2013) A728–A733.
- [64] S. Nagae, H.M. Nekoomanesh, C. Booth, The effect of salt concentration on the properties of poly [oxymethylene-oligo (oxyethylene)]/LiClO₄ polymer electrolytes, *Solid State Ionics.* **53–56** (1992) 1118–1124.
- [65] P. Carlsson, D. Andersson, J. Swenson, R.L. McGreevy, W.S. Howells, L. Börjesson, Structural investigations of polymer electrolyte poly(propylene oxide)-LiClO₄ using diffraction experiments and reverse Monte Carlo simulation, *J. Chem. Phys.* **121** (2004) 12026–12037.
- [66] K. Nagaoka, H. Naruse, I. Shinohara, High Ionic Conductivity in Poly(Dimethyl Siloxane-Co-Ethylene Oxide) Dissolving Lithium Perchlorate., *J. Polym. Sci. Polym. Lett. Ed.* **22** (1984) 659–663.
- [67] K. Ito, Y. Tominaga, H. Ohno, Polyether/salt hybrid (IV). Effect of benzenesulfonate group(s) and PEO molecular weight on the bulk ionic conductivity, *Electrochim. Acta.* **42** (1997) 1561–1570.
- [68] M. Watanabe, T. Endo, A. Nishimoto, K. Miura, M. Yanagida, High ionic conductivity and electrode interface properties of polymer electrolytes based on high molecular weight branched polyether, *J. Power Sources.* **81–82** (1999) 786–789.
- [69] L.A. Guilherme, R.S. Borges, E.M.S. Moraes, G.G. Silva, M.A. Pimenta, A. Marletta, R.A. Silva, Ionic conductivity in polyethylene-b-poly(ethylene oxide)/lithium perchlorate solid polymer electrolytes, *Electrochim. Acta.* **53** (2007) 1503–1511.
- [70] L. Niedzicki, M. Kasprzyk, K. Kuziak, G.Z. Żukowska, M. Armand, M. Bukowska, M. Marcinek, P. Szczeciński, W. Wieczorek, Modern generation of polymer electrolytes based on lithium conductive imidazole salts, *J. Power Sources.* **192** (2009) 612–617.
- [71] C.A. Angell, C. Liu, E. Sanchez, Rubbery solid electrolytes with dominant cationic transport and high ambient conductivity, *Nature.* **362** (1993) 137–139.

- [72] M. Watanabe, M. Itoh, K. Sanui, N. Ogata, Carrier Transport and Generation Processes in Polymer Electrolytes Based on Poly(ethylene oxide) Networks, *Macromolecules*. **20** (1987) 569–573.
- [73] S. Takeoka, H. Ohno, E. Tsuchida, Recent advancement of ion-conductive polymers, *Polym. Adv. Technol.* **4** (1993) 53–73.
- [74] G.B. Appetecchi, F. Croce, L. Persi, F. Ronci, B. Scrosati, Transport and interfacial properties of composite polymer electrolytes, *Electrochim. Acta*. **45** (2000) 1481–1490.
- [75] M.B. Armand, Polymer electrolytes, *Annu. Rev. Mater. Res.* **16** (1986) 245–261.
- [76] S.N. M. Z. A. Munshi, B. B. Owens, Measurement of Li⁺ Ion Transport Number in Poly(ethylene oxide)-LiX complexes, *Polym. J.* **20** (1988) 597–602.
- [77] X. Zhang, P.S. Fedkiw, Ionic Transport and Interfacial Stability of Sulfonate-Modified Fumed Silicas as Nanocomposite Electrolytes, *J. Electrochem. Soc.* **152** (2005) A2413–A2420.
- [78] H. Zhang, C. Li, M. Piszcz, E. Coya, T. Rojo, L.M. Rodriguez-Martinez, M. Armand, Z. Zhou, Single lithium-ion conducting solid polymer electrolytes: Advances and perspectives, *Chem. Soc. Rev.* **46** (2017) 797–815.
- [79] M.J. Smith, Am.M. Silva, S. Cerqueira, J.R. MacCallum, Preparation and characterization of a lithium ion conducting electrolyte based on poly(trimethylene carbonate), *Solid State Ionics*. **140** (2001) 345–351.
- [80] P.C. Barbosa, L.C. Rodrigues, M.M. Silva, M.J. Smith, Characterization of pTMCnLiPF₆ solid polymer electrolytes, *Solid State Ionics*. **193** (2011) 39–42.
- [81] B. Sun, J. Mindemark, K. Edström, D. Brandell, Polycarbonate-based solid polymer electrolytes for Li-ion batteries, *Solid State Ionics*. **262** (2014) 738–742.
- [82] B. Sun, J. Mindemark, K. Edström, D. Brandell, Realization of high performance polycarbonate-based Li polymer batteries, *Electrochem. Commun.* **52** (2015) 71–74.

- [83] Y. Tominaga, V. Nanthana, D. Tohyama, Ionic conduction in poly(ethylene carbonate)-based rubbery electrolytes including lithium salts, *Polym. J.* **44** (2012) 1155–1158.
- [84] Y. Tominaga, Ion-conductive polymer electrolytes based on poly(ethylene carbonate) and its derivatives, *Polym. J.* **49** (2017) 291–299.
- [85] Y. Tominaga, K. Yamazaki, Fast Li-ion conduction in poly(ethylene carbonate)-based electrolytes and composites filled with TiO₂ nanoparticles, *Chem. Commun.* **50** (2014) 4448–4450.
- [86] H. Sugimoto, S. Inoue, Copolymerization of carbon dioxide and epoxide, *J. Polym. Sci. Part A Polym. Chem.* **42** (2004) 5561–5573.
- [87] S. Klaus, M.W. Lehenmeier, C.E. Anderson, B. Rieger, Recent advances in CO₂/epoxide copolymerization-New strategies and cooperative mechanisms, *Coord. Chem. Rev.* **255** (2011) 1460–1479.
- [88] Z. Li, H. Matsumoto, Y. Tominaga, Composite poly(ethylene carbonate) electrolytes with electrospun silica nanofibers, *Polym Adv Technol.* **29** (2018) 820–824.
- [89] K. Kimura, J. Motomatsu, Y. Tominaga, Highly concentrated polycarbonate-based solid polymer electrolytes having extraordinary electrochemical stability, *J. Polym. Sci. Part B Polym. Phys.* **54** (2016) 2442–2447.
- [90] Y. Yamada, M. Yaegashi, T. Abe, A. Yamada, A superconcentrated ether electrolyte for fast-charging Li-ion batteries, *Chem. Commun.* **49** (2013) 11194–11196.
- [91] L. Suo, Y.S. Hu, H. Li, M. Armand, L. Chen, A new class of Solvent-in-Salt electrolyte for high-energy rechargeable metallic lithium batteries, *Nat. Commun.* **4** (2013) 1–9.
- [92] J. Mindemark, B. Sun, E. Törmä, D. Brandell, High-performance solid polymer electrolytes for lithium batteries operational at ambient temperature, *J. Power Sources.* **298** (2015) 166–170.

- [93] K. Kimura, M. Yajima, Y. Tominaga, A highly-concentrated poly(ethylene carbonate)-based electrolyte for all-solid-state Li battery working at room temperature, *Electrochem. Commun.* **66** (2016) 46–48.
- [94] J. Zhang, J. Zhao, L. Yue, Q. Wang, J. Chai, Z. Liu, X. Zhou, H. Li, Y. Guo, G. Cui, L. Chen, Safety-Reinforced Poly(Propylene Carbonate)-Based All-Solid-State Polymer Electrolyte for Ambient-Temperature Solid Polymer Lithium Batteries, *Adv. Energy Mater.* **5** (2015) 1–10.
- [95] J. Chai, Z. Liu, J. Ma, J. Wang, X. Liu, H. Liu, J. Zhang, G. Cui, L. Chen, In Situ Generation of Poly (Vinylene Carbonate) Based Solid Electrolyte with Interfacial Stability for LiCoO₂Lithium Batteries, *Adv. Sci.* **4** (2017) 1–9.
- [96] D.F. Shrivera, B.L. Papkea, M.A. Ratnera, R. Dupona, T. Wongb, M. Brodwin, Structure and ion transport in polymer-salt complexes, *Solid State Commun.* **5** (1981) 83–88.
- [97] R. Dupon, B.L. Papke, M.A. Ratner, D.F. Shriver, Ion Transport in the Polymer Electrolytes Formed Between Poly(ethylene succinate) and Lithium Tetrafluoroborate, *J. Electrochem. Soc.* **131** (1984) 586.
- [98] M. Watanabe, M. Togo, K. Sanui, N. Ogata, T. Kobayashi, Z. Ohtakilb, Ionic Conductivity of Polymer Complexes Formed by Poly(β -Propiolactone) and Lithium Perchlorate, *Macromolecules.* **17** (1984) 2908–2912.
- [99] R.D. Armstrong, M.D. Clarke, Lithium ion conducting polymeric electrolytes based on poly(ethylene adipate), *Electrochim. Acta.* **29** (1984) 1443–1446.
- [100] Y.C. Lee, M.A. Ratner, D.F. Shriver, Ionic conductivity in the poly(ethylene malonate)/lithium triflate system, *Solid State Ionics.* **138** (2001) 273–276.
- [101] Y.-Z.M. Xiao-Yuan Yu, Min Xiao, Shuang-Jin Wang, Qi-Qiang Zhao, Fabrication and characterization of PEO/PPC polymer electrolyte for lithium-ion battery, *J. Appl.*

- Polym. Sci.* **115** (2010) 2718–2722 456.
- [102] T. Okumura, S. Nishimura, Lithium ion conductive properties of aliphatic polycarbonate, *Solid State Ionics*. **267** (2014) 68–73.
- [103] Y. Yamada, A. Yamada, Superconcentrated Electrolytes to Create New Interfacial Chemistry in Non-aqueous and Aqueous Rechargeable Batteries, *Chem. Lett.* **46** (2017) 1056–1064.
- [104] W.R. Mckinnon, J.R. Dahn, How to Reduce the Cointercalation of Propylene Carbonate in Li_xZrS and Other Layered Compounds, *J. Electrochem. Soc.* **132** (1985) 364–366.
- [105] S.-K. Jeong, M. Inaba, Y. Iriyama, T. Abe, Z. Ogumi, Electrochemical Intercalation of Lithium Ion within Graphite from Propylene Carbonate Solutions, *Electrochem. Solid-State Lett.* **6** (2003) A13–A15.
- [106] S.K. Jeong, M. Inaba, Y. Iriyama, T. Abe, Z. Ogumi, Interfacial reactions between graphite electrodes and propylene carbonate-based solutions: Electrolyte-concentration dependence of electrochemical lithium intercalation reaction, *J. Power Sources*. **175** (2008) 540–546.
- [107] Y. Yamada, Y. Takazawa, K. Miyazaki, T. Abe, Electrochemical lithium intercalation into graphite in dimethyl sulfoxide-based electrolytes: Effect of solvation structure of lithium ion, *J. Phys. Chem. C*. **114** (2010) 11680–11685.
- [108] Y. Yamada, K. Furukawa, K. Sodeyama, K. Kikuchi, M. Yaegashi, Y. Tateyama, Y. Atsuo, Unusual Stability of Acetonitrile-Based Superconcentrated Electrolytes for Fast-Charging Lithium-Ion Batteries, *J. Am. Chem. Soc.* **136** (2014) 5039–5046.
- [109] Y. Yamada, K. Usui, C.H. Chiang, K. Kikuchi, K. Furukawa, A. Yamada, General observation of lithium intercalation into graphite in ethylene-carbonate-free superconcentrated electrolytes, *ACS Appl. Mater. Interfaces*. **6** (2014) 10892–10899.

- [110] Y. Yamada, Y. Iriyama, T. Abe, Z. Ogumi, Kinetics of lithium ion transfer at the interface between graphite and liquid electrolytes: effects of solvent and surface film, *Langmuir*. **25** (2009) 12766–12770.
- [111] K. Sodeyama, Y. Yamada, K. Aikawa, A. Yamada, Y. Tateyama, Sacrificial Anion Reduction Mechanism for Electrochemical Stability Improvement in Highly Concentrated Li-Salt Electrolyte, *J. Phys. Chem. C*. **118** (2014) 14091–14097.
- [112] Y. Yamada, C.H. Chiang, K. Sodeyama, J. Wang, Y. Tateyama, A. Yamada, Corrosion Prevention Mechanism of Aluminum Metal in Superconcentrated Electrolytes, *ChemElectroChem*. **2** (2015) 1687–1694.
- [113] J. Wang, Y. Yamada, K. Sodeyama, C.H. Chiang, Y. Tateyama, A. Yamada, Superconcentrated electrolytes for a high-voltage lithium-ion battery, *Nat. Commun.* **7** (2016) 12032.
- [114] S.K. Jeong, H.Y. Seo, D.H. Kim, H.K. Han, J.G. Kim, Y.B. Lee, Y. Iriyama, T. Abe, Z. Ogumi, Suppression of dendritic lithium formation by using concentrated electrolyte solutions, *Electrochem. Commun.* **10** (2008) 635–638.
- [115] J. Qian, W.A. Henderson, W. Xu, P. Bhattacharya, M. Engelhard, O. Borodin, J.-G. Zhang, High rate and stable cycling of lithium metal anode, *Nat. Commun.* **6** (2015) 6362.
- [116] K. Matsumoto, K. Inoue, K. Nakahara, R. Yuge, T. Noguchi, K. Utsugi, Suppression of aluminum corrosion by using high concentration LiTFSI electrolyte, *J. Power Sources*. **231** (2013) 234–238.
- [117] D.W. McOwen, D.M. Seo, O. Borodin, J. Vatamanu, P.D. Boyle, W.A. Henderson, Concentrated electrolytes: Decrypting electrolyte properties and reassessing Al corrosion mechanisms, *Energy Environ. Sci.* **7** (2014) 416–426.
- [118] L. Suo, O. Borodin, T. Gao, M. Olguin, J. Ho, X. Fan, C. Luo, C. Wang, K. Xu, "

- Water - in - salt " electrolyte enables high - voltage aqueous lithium - ion chemistries, *Science* (80-.). **350** (2015) 938–943.
- [119] L. Suo, O. Borodin, W. Sun, X. Fan, C. Yang, F. Wang, T. Gao, Z. Ma, M. Schroeder, A. von Cresce, S.M. Russell, M. Armand, A. Angell, K. Xu, C. Wang, Advanced High-Voltage Aqueous Lithium-Ion Battery Enabled by “Water-in-Bisalt” Electrolyte, *Angew. Chemie Int. Ed.* **55** (2016) 7136–7141.
- [120] Y. Yamada, K. Usui, K. Sodeyama, S. Ko, Y. Tateyama, A. Yamada, Hydrate-melt electrolytes for high-energy-density aqueous batteries, *Nat. Energy.* **1** (2016) 1–9.
- [121] H. Kim, J. Hong, K.-Y. Park, H. Kim, S.-W. Kim, K. Kang, Aqueous Rechargeable Li and Na Ion Batteries, *Chem. Rev.* **114** (2014) 11788–11827.
- [122] J.E. Weston, B.C.H. Steele, Effects of inert fillers on the mechanical and electrochemical properties of lithium salt-poly(ethylene oxide) polymer electrolytes, *Solid State Ionics.* **7** (1982) 75–79.
- [123] M. Armand, Polymer solid electrolytes - an overview, *Solid State Ionics.* **9–10** (1983) 745–754.
- [124] F. Capuano, Composite Polymer Electrolytes, *J. Electrochem. Soc.* **138** (1991) 1918.
- [125] M.C. Borghini, M. Maslmgostino, S. Passerini, B. Scrosati, Electrochemical Properties of Polyethylene Oxide- Li[(CF₃SO₂)₂N]-Gamma-LiAlO₂ Composite Polymer Electrolytes, *J. Electrochem. Soc.* **142** (1995) 2118–2121.
- [126] F. Croce, G.B. Appetecchi, B. Scrosati, L. Persi, Nanocomposite polymer electrolytes for lithium batteries, *Nature.* **394** (1998) 456–458.
- [127] M.A. Ratner, P. Johansson, D.F. Shriver, Polymer Electrolytes: Ionic Transport Mechanisms and Relaxation Coupling, *MRS Bull.* **25** (2000) 31–37.
- [128] F. Croce, L.L. Persi, B. Scrosati, F. Serraino-Fiory, E. Plichta, M.A. Hendrickson, Role of the ceramic fillers in enhancing the transport properties of composite polymer

- electrolytes, *Electrochim. Acta.* **46** (2001) 2457–2461.
- [129] Q. Zheng, L. Ma, R. Khurana, L.A. Archer, G.W. Coates, Structure-property study of cross-linked hydrocarbon/poly(ethylene oxide) electrolytes with superior conductivity and dendrite resistance, *Chem. Sci.* **7** (2016) 6832–6838.
- [130] D. Lin, W. Liu, Y. Liu, H.R. Lee, P.C. Hsu, K. Liu, Y. Cui, High Ionic Conductivity of Composite Solid Polymer Electrolyte via in Situ Synthesis of Monodispersed SiO₂ Nanospheres in Poly(ethylene oxide), *Nano Lett.* **16** (2016) 459–465.
- [131] S. Ishibe, K. Anzai, J. Nakamura, Y. Konosu, M. Ashizawa, H. Matsumoto, Y. Tominaga, Ion-conductive and mechanical properties of polyether/silica thin fiber composite electrolytes, *React. Funct. Polym.* **81** (2014) 40–44.
- [132] E. Tsuchida, H. Ohno, K. Tsunemi, N. Kobayashi, Lithium ionic conduction in poly (methacrylic acid)-poly (ethylene oxide) complex containing lithium perchlorate, *Solid State Ionics.* **11** (1983) 227–233.
- [133] A.M. Rocco, C.P. Da Fonseca, R.P. Pereira, A polymeric solid electrolyte based on a binary blend of poly(ethylene oxide), poly(methyl vinyl ether-maleic acid) and LiClO₄, *Polymer (Guildf).* **43** (2002) 3601–3609.
- [134] A.M. Rocco, D.P. Moreira, R.P. Pereira, Specific interactions in blends of poly(ethylene oxide) and poly(bisphenol A-co-epichlorohydrin): FTIR and thermal study, *Eur. Polym. J.* **39** (2003) 1925–1934.
- [135] A.M. Rocco, C.P. Fonseca, F.A.M. Loureiro, R.P. Pereira, A polymeric solid electrolyte based on a poly(ethylene oxide)/poly(bisphenol A-co-epichlorohydrin) blend with LiClO₄, *Solid State Ionics.* **166** (2004) 115–126.
- [136] K.M. Abraham, M. Alamgir, R.R. K. Polyphosphazene-Poly (Olefin Oxide) Mixed Polymer Electrolytes, *J. Electrochem. Soc.* **136** (1989) 3576–3582.
- [137] G. bin Zhou, I.M. Khan, J. Smid, Solvent-Free Cation-Conducting Polysiloxane

- Electrolytes with Pendant Oligo(oxyethylene) and Sulfonate Groups, *Macromolecules*. **26** (1993) 2202–2208.
- [138] D. Kim, J. Park, H. Rhee, Conductivity and thermal studies of solid polymer electrolytes prepared by blending poly(ethylene oxide), poly(oligo[oxyethylene]oxy sebacoyl) and lithium perchlorate, *Solid State Ionics*. **83** (1996) 49–56.
- [139] J.S. Oh, S.H. Kim, Y. Kang, D.W. Kim, Electrochemical characterization of blend polymer electrolytes based on poly(oligo[oxyethylene]oxyterephthaloyl) for rechargeable lithium metal polymer batteries, *J. Power Sources*. **163** (2006) 229–233.
- [140] M. Jacob, Effect of PEO addition on the electrolytic and thermal properties of PVDF-LiClO₄ polymer electrolytes, *Solid State Ionics*. **104** (1997) 267–276.
- [141] Y. Gan, Q. Qin, S. Chen, Y. Wang, D. Dong, K. Xie, Y. Wu, Composite cathode La_{0.4}Sr_{0.4}TiO_{3- δ} -Ce_{0.8}Sm_{0.2}O_{2- δ} impregnated with Ni for high-temperature steam electrolysis, *J. Power Sources*. **245** (2014) 245–255.
- [142] K.M. Anilkumar, B. Jinisha, M. Manoj, S. Jayalekshmi, Poly(ethylene oxide) (PEO) – Poly(vinyl pyrrolidone) (PVP) blend polymer based solid electrolyte membranes for developing solid state magnesium ion cells, *Eur. Polym. J.* **89** (2017) 249–262.
- [143] L.C. Rodrigues, M.M. Silva, M.J. Smith, Synthesis and characterization of amorphous poly(ethylene oxide)/poly(trimethylene carbonate) polymer blend electrolytes, *Electrochim. Acta*. **86** (2012) 339–345.
- [144] W. Whang, C. Lu, Effects of polymer matrix and salt concentration on the ionic conductivity of plasticized polymer electrolytes, *J. Appl. Polym. Sci.* **56** (1995) 1635–1643.
- [145] M. Premalatha, N. Vijaya, S. Selvasekarapandian, S. Selvalakshmi, Characterization of blend polymer PVA-PVP complexed with ammonium thiocyanate, *Ionics (Kiel)*. **22** (2016) 1299–1310.

Chapter 2

Effect of silica nanofiber addition on poly(ethylene carbonate)-based composite electrolytes

2-1 Introduction

Fabrication of nanostructured materials is increasingly important in many scientific fields,^[1] including electrochemistry and battery research,^[2,3] because of their unique properties. Electrospinning is a versatile method for fabricating thin polymer fibers having diameter of nano- to submicron-size.^[4-6] Since the first reports of certain electrospun metal oxides, such as α -Al₂O₃ (Figure 2-1a),^[7] TiO₂ (Figure 2-1b),^[8] and SiO₂,^[9] a number of ceramic nanofibers have been electrospun along with more common polymer fibers.^[10] Generally, as-electrospun ceramic fibers are composed of the intended ceramic, and also carrier polymers, such as polyvinylpyrrolidinone, which are added to adjust the viscosity of the sol-gel precursors, and in turn necessitates calcination. Tominaga *et al.*^[11] have reported previously that addition of calcination-free silica nanofiber (SNF) to amorphous polyether electrolytes can improve their ion-conductive and mechanical properties at room temperature (Figure 2-2). Unfortunately, the conductivity is still limited, and it is extremely difficult to enhance the lithium (cation) transference number (t_+) for polymer electrolytes. The migration of ions in polyether arises from the segmental motion of polymer chains in the amorphous region,^[12] and a strong coordination structure between polyether chains and cations impairs the conductivity.

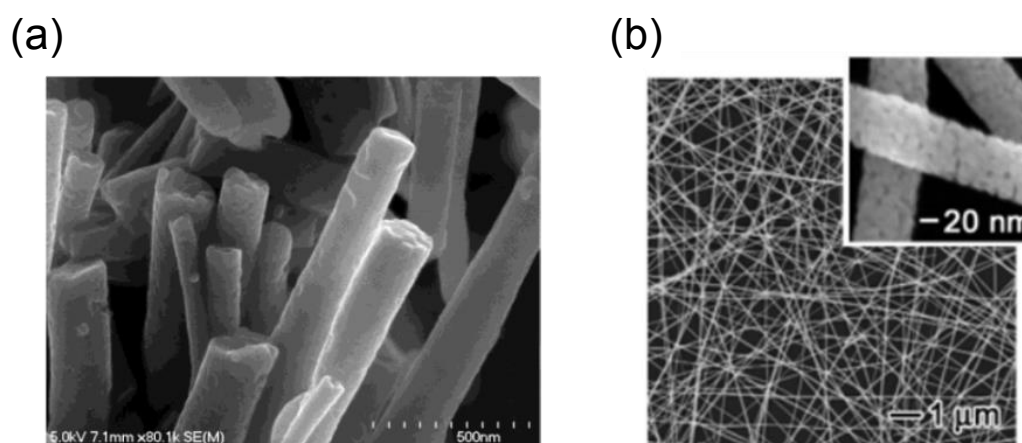


Figure 2-1. SEM images of electrospun (b) α -Al₂O₃^[18] and (c) TiO₂^[19] nanofibers.

Tominaga's group has been focused on a novel candidate using ethylene carbonate-based polymers for electrolytes,^[13–17] after CO₂/epoxide copolymers having glycidylether side groups were first reported in 2010.^[14] Recently, Tominaga *et al.*^[15] determined that simple poly(ethylene carbonate) (PEC)-Li salt mixtures give rise to very different ion-conductive behaviors from typical polyether-based electrolytes. In the case of PEC-LiFSI electrolytes, the conductivity increases and the glass-transition temperature (T_g) decreases with increasing Li salt concentration.^[15,16] Furthermore, high t_{Li^+} values, greater than 0.5, and good electrochemical stability, are among the advantages of polycarbonate-based electrolytes.^[16,18]

This chapter focuses on SNF as a filler for PEC-based composite electrolytes. In the last three decades it has been found that the addition of inorganic fillers can improve electrochemical and mechanical properties of SPEs, because they have high aspect ratios and large surface areas. In addition, the functional groups on the surface can give rise to a high dispersion state of fibers

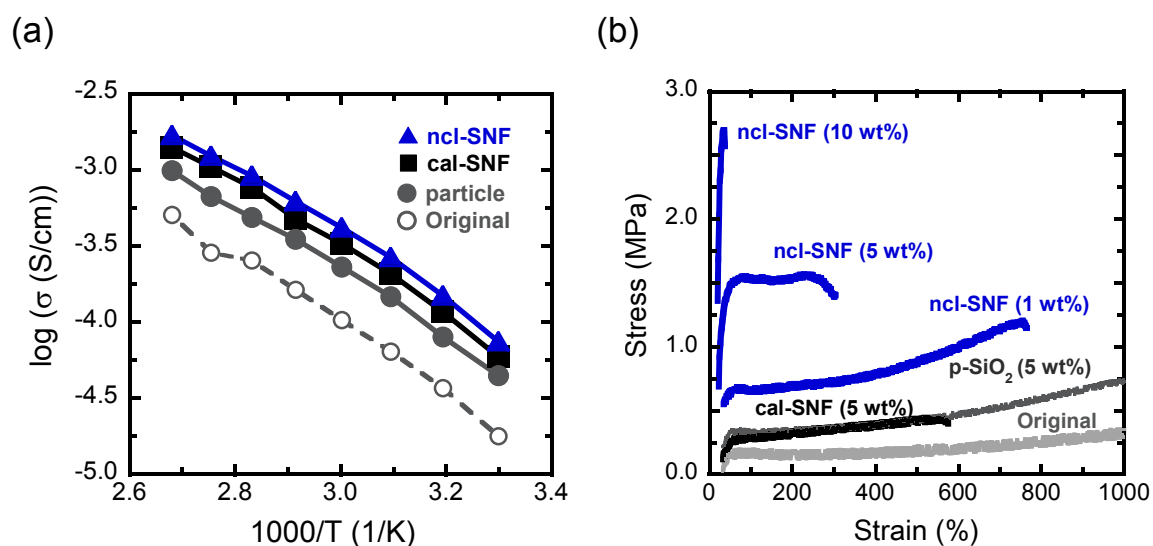


Figure 2-2. (a) Temperature dependence of ionic conductivity for poly(ethylene oxide-*co*-propylene oxide) (P(EO/PO))/LiTFSI 5 mol% electrolyte and 5 wt% composite electrolytes (ncl-SNF: non-calcined silica nanofiber, cal-SNF: calcined silica nanofiber, particle: SiO₂, original: without filler). (b) Stress-strain curves of P(EO/PO)/LiTFSI 5 mol% electrolyte and composite electrolytes.^[11]

in SPE and from efficient ion-conductive paths.^[19,20] In this chapter, poly(ethylene carbonate) (PEC), lithium bis(trifluoromethanesulfonyl) imide (LiTFSI), and SNFs were used for preparing composite polymer electrolytes to improve the electrochemical properties and mechanical strength. Three different average diameters of SNFs (300, 700, and 1000 nm) were used, and we determined the physicochemical effects of the addition on ion-conductive properties.

2-2 Experimental

2-2-1 Preparation of silica nanofibers

A sample of γ -Aminopropyl triethyl silicate (Dow Corning Toray, Japan) and Tetraethylorthosilicate (TEOS) oligomer (Colcoat-40) (Colcoat, Japan) were obtained from the commercial. Boric acid, citric acid, sodium chloride (NaCl), and methanol (MeOH) were purchased from Wako, Japan. These materials were directly used for synthesis without any purification. Silica-based sol for using electrospinning was obtained from boric acid, γ -aminopropyl triethyl silicate and TEOS oligomer with the following composition: boric acid / γ -aminopropyl triethylsilicate / TEOS oligomer = 1 / 4 / 8 in weight ratios. The TEOS oligomer was added dropwise to being made the boric acid and γ -aminopropyl triethylsilicate mixture under stirring and ultrasonication. Then, the reaction mixture was sealed up and left for 2 days, before the addition of saturated citric acid aqueous solution. The sol was stirred in air for 30 min before electrospinning.^[21] The electrospinning device was the same as that used in a previous study^[22]. The spinning solution was contained in a syringe with a stainless steel nozzle. The nozzle was connected to a high-voltage regulated DC power supply (HAR-100P0.3,

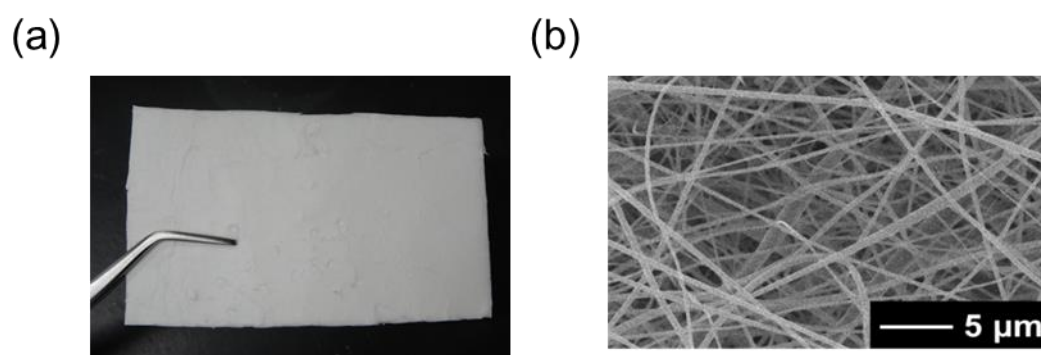


Figure 2-3. (a) Photograph and (b) SEM image of non-woven cloth of the silica nanofiber (SNF₇₀₀).^[11]

Matsusada Precision, Japan). A constant rate of volume flow rate was maintained via a syringe-type infusion pump (MCIPIII, Minato Concept, Japan). An aluminum plate was used as a counter-electrode. The distance between the nozzle tip and the counter-electrode was 10-20 cm, the applied voltage was 30 kV, and the flow rate was 20 $\mu\text{L}/\text{min}$. Electrospinning was carried out at 25 $^{\circ}\text{C}$ and at relative humidity of less than 40%, then the silica nanofiber (SNF) was prepared without calcination process. The photograph and SEM image of the SNF were shown in Figure 2-3. Three different SNFs with average diameter of 300, 700 and 1000 nm (SNF₃₀₀, SNF₇₀₀, and SNF₁₀₀₀) were prepared for this study.

2-2-2 Materials and electrolyte preparation

A commercial poly(ethylene carbonate) (PEC, QPAC[®]25, Empower Materials, USA, $M_w=238,000$) was precipitated from acetonitrile into methanol for rising, and was dried under vacuum at 60 $^{\circ}\text{C}$ for 2 days prior to use. Lithium bis(trifluoromethanesulfonyl) imide (LiTFSI, battery grade, Kanto Chemical Co., Japan) was used as received. The chemical structures of PEC and LiTFSI are shown in Figure 2-4. Three different diameter size SNFs were cut into small pieces, dispersed in ethanol and then filtered and removed all solvent for using. All materials were stored in a glovebox filled with dry Ar gas. The PEC-based composite

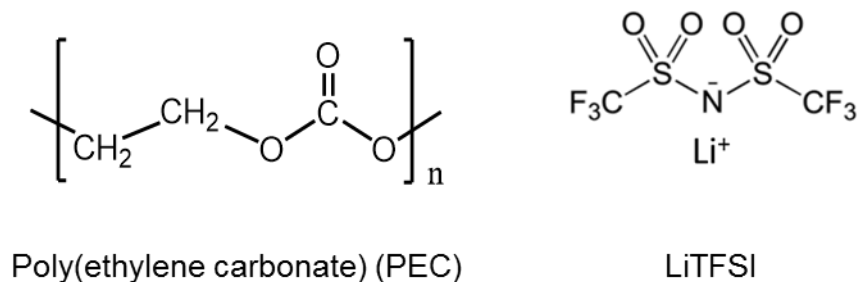


Figure 2-4. Chemical structures of poly(ethylene carbonate) (PEC) and LiTFSI.

electrolytes were prepared using a simple casting method. PEC, LiTFSI, and SNFs were mixed in acetonitrile (99 %, Kanto Chemical Co., Japan) at room temperature for 24 hours. Then, the composite solvents were casted onto Teflon[®] dishes, and dried under vacuum at 60 °C for 48 hours. The relative concentration of LiTFSI to PEC mixture, which corresponds to the molar ratio of ethylene carbonate (EC) unit to Li⁺ ion ($[EC]/[Li^+] = a \times 100 \text{ mol\%}$). SNFs were added in a mass ratio of the total electrolyte amount from 1-10 wt%.

2-2-3 Characterizations

Morphological and physicochemical characterizations

The morphology of the cross section of composite electrolytes was observed using a scanning electron microscope (SEM, JCM-5700, JEOL, Japan) operated at 10 kV. Prior to the SEM measurement, all samples were etched and sputtered by Au using an ion coater (Eiko Engineering, Co., Ltd.) on the surface. Differential scanning calorimetry (DSC) and thermogravimetric analysis (TGA) were performed by using DSC7020 (Hitachi High-Tech Co., Japan) and TG/DTA7200 (Hitachi High-Tech Co., Japan) for measurements of the thermal properties and thermal degradation of the electrolyte films. All samples of DSC and TGA were made in a dry Ar-filled globe box using Al pans and measured under dry N₂. The second heating of DSC was from -100 °C to 100 °C at a scan rate of 10 °C min⁻¹. The TGA samples were heated from room temperature to 500 °C at a scan rate of 10 °C min⁻¹. Tensile tests for electrolytes were performed by using a small-sized tensile tester OZ502 system (Sentec Co., Japan). Test samples were cut in of width 5 mm and length 10 mm. Sample preparation and test processes were all carried out in a dry N₂ filled glove box and measured at an elongation rate of 10 mm min⁻¹ at room temperature.

Ion-conductive and electrochemical measurements

Ionic conductivity of the electrolytes were determined by electrochemical impedance spectroscopy (EIS) with a potentiostat/galvanostat SP-150 (Bio-Logic Instrument co., France). The conductivity cells consisted of two stainless steel blocking electrodes which sandwiched the 9 mm diameter of electrolyte. A perforated Teflon[®] film was used as spacer to fix the distance between the two electrodes and the active area between electrolyte and electrode. All cells were measured from 100 to 30 °C in the frequency range of 100 Hz to 1 MHz. The ionic conductivity (σ) was given by the following Eq. (2-1);

$$\sigma = l/AR \quad (2-1)$$

where l is the distance between the two electrodes, A is the active area between electrolyte and electrode, and R is the bulk resistance of the electrolyte. The thickness and the area of the circle-shaped hole of the spacer used were assigned as l and A , respectively.

Lithium transference number (t_+) of the electrolytes were evaluated according to a Bruce-Vincent-Evans method^[23] combining EIS and chronoamperometry for symmetric Li/Li cells by using a VersaSTAT4 (Princeton Applied Research). The t_+ was estimated by the following Eq. (2-2);

$$t_{\text{Li}^+} = \frac{I_{\text{SS}}(\Delta V - R_0 I_0)}{I_0(\Delta V - R_{\text{SS}} I_{\text{SS}})} \quad (2-2)$$

where ΔV (10 mV in this study) is the DC voltage applied to the cell, I_0 and I_{SS} are the initial current and steady-state current, and R_0 and R_{SS} are the Li/electrolyte interphase resistances before and after the polarization. Oxidative electrochemical stabilities of the electrolytes were evaluated by linear sweep voltammetry (LSV) by using a VersaSTAT4 at 80 °C and a scan rate of 0.5 mV s⁻¹. Two electrode cells were assembled using stainless steel plates as working

electrodes and the Li metals attached to the stainless steel plate as both counter and reference electrodes. All processed of sample preparations and measurements were done in the strictly controlled glovebox filled with dry Ar gas.

FT-IR spectroscopy

FT-IR spectroscopy used to identify the interaction between the components of mixtures and analyse the complexity and chemical interaction. The electrolyte samples cut by a small piece and used for the measurement. FT-IR spectra were acquired in an attenuated total reflection (ATR) unit (ZnSe lens) with a FT-IR spectrometer (FT/IR-4100, JASCO Co.). The spectra were recorded from 400 to 4000 cm^{-1} with a resolution of 4 cm^{-1} under dry N_2 gas at room temperature.

2-3 Results and discussion

2-3-1 Morphology of silica nanofiber filled composite electrolytes

Figure 2-5 shows photographs of original PEC-LiTFSI 100 mol% electrolyte and SNF₇₀₀ 5 wt% filled composite electrolyte. All electrolyte samples were obtained as highly homogeneous and free-standing films. The SNF filled electrolytes became opaque due to the addition of fiber, but the composite films gained flexibility. Figure 2-6 shows cross-section SEM images of the original PEC electrolyte and the SNF composites. Based on the SEM images, we confirm that SNFs with different diameter exhibit good dispersion in the PEC/LiTFSI electrolytes. In previous study^[11] the characteristics of the non-calcined silica nanofiber (SNF) were investigated using ²⁹Si cross-polarization/magic angle spinning (CP/MAS) and ¹¹B MAS NMR, X-ray photoelectron spectroscopy (XPS), and X-ray diffraction (XRD). The SNF contains the elements Si, O, and B, and has many polar functional groups on its surface, *i.e.*, silanol (Si-OH) and γ -aminopropyl (Si-(CH₂)₃-NH₂). In accordance with the XRD study, the SNF is composed of an amorphous silica. It is probable that the calcination-free procedure allows the fiber to retain the surface groups and the non-crystalline state. These polar functional groups may play important role in the dispersion of SNFs. Indeed, the SNF system had superior dispersibility than the other composites with particle SiO₂ and calcined SNF.^[11] Similar studies have been done previously. Izutsu and Gojny have reported that amino groups on the carbon nanotubes surface improved the dispersibility in the polymer matrix.^[24,25] Therefore, the calcination-free process for fiber preparation can increase the functional groups on the fiber surface and led to compatibility with polymer electrolytes.

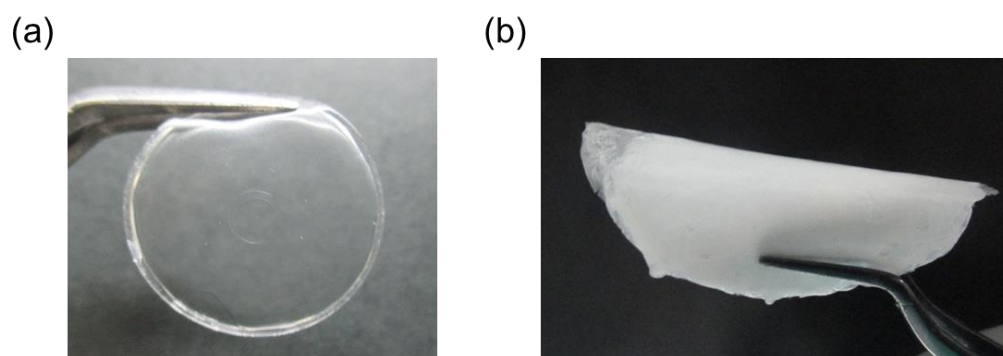


Figure 2-5. Photograph of (a) original PEC-LiTFSI 100 mol% electrolyte and (b) PEC-LiTFSI 100 mol% with SNF₇₀₀ 5 wt% composite electrolyte.

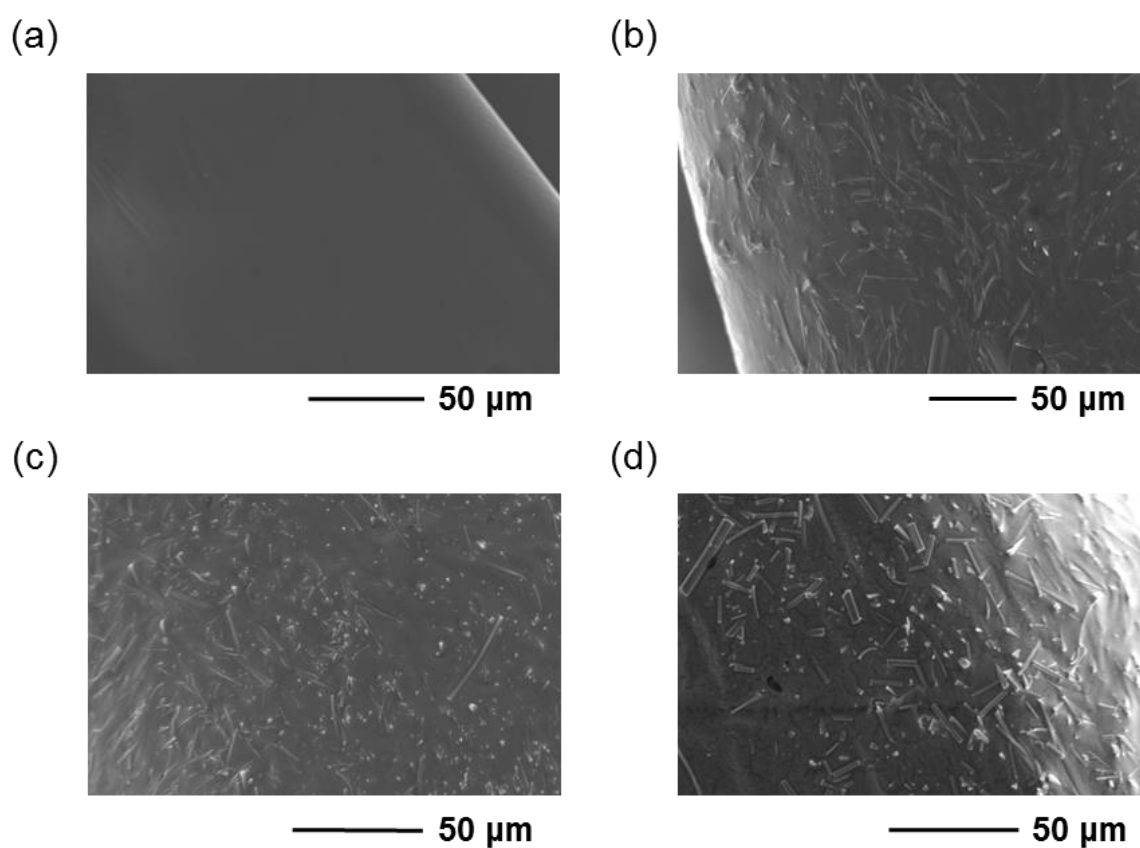


Figure 2-6. Cross-section SEM images of (a) PEC/LiTFSI 100 mol% (b) PEC/LiTFSI 100 mol% + SNF₃₀₀, (c) PEC/LiTFSI 100 mol% + SNF₇₀₀, (d) PEC/LiTFSI 100 mol% + SNF₁₀₀₀ composite electrolytes (SNF content: 5 wt%).

2-3-2 Thermal properties

The thermal degradation behavior of the SNF composite electrolytes measured by TGA is shown Figure 2-7. Table 2-1 sets out values of the weight-loss temperature (T_{d5}). The first valley is derived from the decomposition of PEC and the second valley shows decomposition of salt. The value of T_{d5} for PEC/LiTFSI 100 mol% was the lowest observed, at 167 °C. However, it is clearly observed that the addition of SNF delays the decomposition of PEC, which means the thermal stability for all composite electrolytes were improved. This is in good agreement with the observation reported previously in a similar study on polymer electrolytes filled with clay.^[26] It is obvious that the value of T_{d5} increases with decreasing diameter of the SNFs. For the PEC-LiTFSI 100 mol%-SNF₃₀₀ composite electrolyte, T_{d5} is above 200 °C, with an increase of approximately 40 °C over the value for the original PEC-LiTFSI electrolyte. The SNF have many Si-OH and γ -aminopropyl groups on the surface, and these polar groups can interact with polymer chains and ions that may improvement in segmental motion of polymer chains which is the effect of Lewis acid-base interactions. Additionally, the thinner fiber have more number of fibers in the unit area which means the thinner fiber have bigger specific surface area and more polar groups on the surface, lead to more interactions with polymers. This may be the reason of improving the values of T_{d5} of composite electrolytes filled with the thinner SNFs and in turn to increase the ionic conductivity.

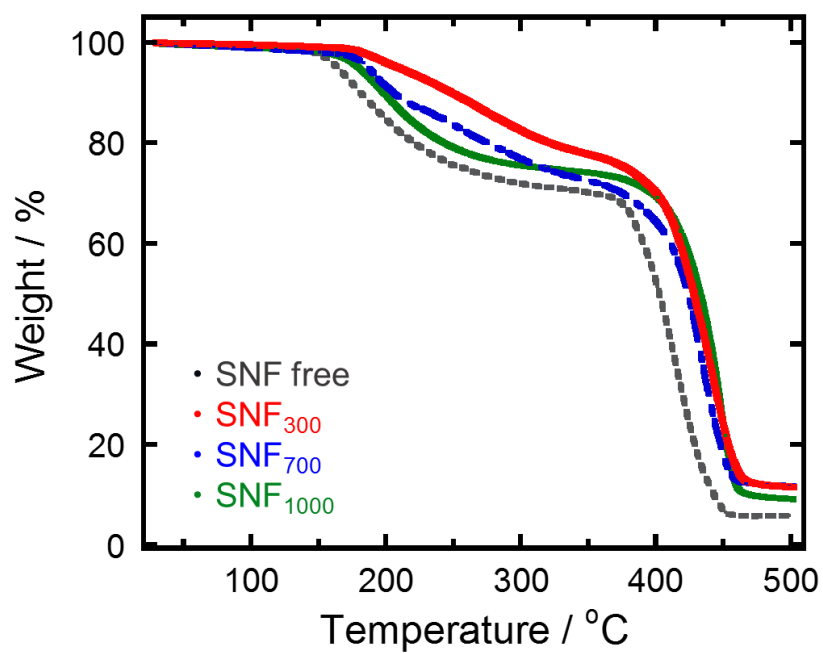


Figure 2-7. TGA curves of the original PEC-LiTFSI 100 mol% electrolyte and composite electrolyte (SNF content: 5 wt%).

Table 2-1. Thermal properties PEC-LiTFSI 100 mol% and the SNF composite electrolytes.

Sample	T_{d5} / °C
PEC/LiTFSI 100 mol%	167
PEC/LiTFSI 100 mol% + SNF ₃₀₀ 5 wt%	205
PEC/LiTFSI 100 mol% + SNF ₇₀₀ 5 wt%	184
PEC/LiTFSI 100 mol% + SNF ₁₀₀₀ 5 wt%	180

2-3-3 Mechanical properties

To obtain both excellent ion-conductive and mechanical properties for SPEs, many studies have been made, mainly on PEO systems.^[27,28] It is difficult to achieve both aims simultaneously.^[26] Figure 2-8 compares the stress-strain curves for the PEC/LiTFSI electrolyte and the SNFs composites. The tensile test data are summarized in Table 2-2. All maximum stress and Young's modulus values were improved significantly with the addition of SNFs to the PEC/LiTFSI original electrolyte and the maximum stresses are increased with addition of thinner. Even for the SNF electrolytes the specimen can extend by more than 200 % from the original length. Addition of SNF to the electrolyte is similar to its effect on fiber-reinforced plastics (FRP). Our previous study determined that polyether electrolytes filled with calcination-free SNF have better mechanical properties, because of moderate interactions between functional groups such as Si-OH and γ -aminopropyl on the fiber surface, and polar groups of the polymers.^[11] This polyether system has good ion-conductive and mechanical properties when thinner SNF was used. Furthermore, maximum stress at around 7 MPa in the SNF₃₀₀ composite is almost the same as the value for a typical separator. We expect that these composite membranes will prove useful for electrolytes for solid-state batteries.

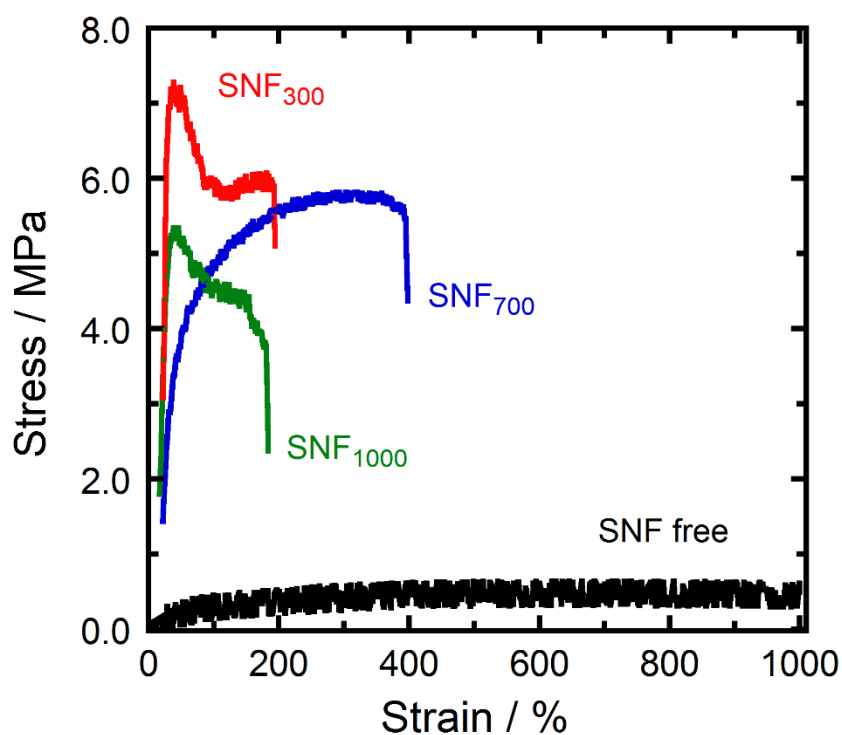


Figure 2-8. Stress-strain curves of PEC-LiTFSI 100 mol% and SNF composite electrolytes at room temperature (SNF content: 5 wt%).

Table 2-2. Mechanical properties of PEC/LiTFSI 100 mol% and the SNF composite electrolytes.

Sample	Maximum stress/ MPa	Strain at Break	Young's Modulus / MPa
PEC/LiTFSI 100 mol%	0.86	15.5	0.08
PEC/LiTFSI 100 mol% + SNF ₃₀₀ 5 wt%	7.28	0.4	4.03
PEC/LiTFSI 100 mol% + SNF ₇₀₀ 5 wt%	5.82	3.2	2.97
PEC/LiTFSI 100 mol% + SNF ₁₀₀₀ 5 wt%	5.34	0.5	4.04

2-3-4 Ion-conductive and electrochemical properties

Figure 2-9 shows the temperature dependence of ionic conductivity for original PEC-LiTFSI 100 mol% electrolyte and the SNF composites filled with different diameter displayed in the form of Arrhenius plot. For the improvement in the 5 wt% addition of SNFs to PEC-LiTFSI electrolyte was suitable except for SNF₁₀₀₀. The conductivity increased with decreasing the diameter of SNFs. The highest conductivity values were as high as the order of 10^{-4} S cm⁻² at 60 °C and 10^{-6} S cm⁻² at 30 °C for a PEC-LiTFSI 100 mol%-SNF₃₀₀ composite electrolyte. The increase in the ionic mobility in the composite is typically due to the Lewis acid-base interaction between polar groups on the filler surface and polymer chains and anions,^[25] and probably ion-conductive paths were improved. We may assume that thinner fiber has a large number of surface groups if the dispersion state is the same. There should have be more interactions between the surface and ions or PEC chains, improving conductivity was improved, in thinner SNFs filled composite electrolytes. This means that the SNFs, acting as inorganic fillers, improve the conductivity of PEC-based electrolytes as well as the PEO system.^[19,20] Addition of inorganic fillers to the PEO-based electrolytes is well known to promote salt dissociation and reduce T_g , giving rise to very good conductivity and electrochemical stability.^[19,29,30]

Figure 2-10 shows polarization curves recorded by chronoamperometries and Nyquist impedance plots of symmetric Li/Li cells for t_+ measurement of the PEC-LiTFSI 100 mol% original electrolyte and the SNF composite electrolytes. It has been known that PEC-based electrolytes have high t_+ values in high concentrated samples.^[16] The results in this study are summarized in Table 2-3, in accordance with Eq. 2-1. The result shown in the table shows that the t_+ of original PEC-LiTFSI 100 mol% electrolyte is estimated to be as high as 0.71. That is a value rarely achieved by typical polyether-based electrolytes, *e.g.* PEO-based ones, where the t_+ values commonly average around 0.1 to 0.2. Certain single-ion conductors can be

exceptions,^[31] but these systems only have low conductivities in general. The PEC-LiTFSI 100 mol%-SNF₃₀₀ composite electrolyte showed a higher t_+ in the value of 0.77 and other composite electrolytes were decreased (0.58 and 0.57). This unusually high lithium-ion transport property of PEC electrolytes is well accorded with the previous reports of our group. The fast Li-transport property was also demonstrated by solid-state pulse-field-gradient (pfg)-NMR.^[16] This property is attributed to a loose coordination structure and a high salt concentration. More discussions will be talked in the FT-IR measurement analysis later. We assume that the improvement in both conductivity and t_+ promoted by the addition of the SNF can be explained by the Lewis acid-base interactions between the polar functional groups on the filler surface and TFSI anions. The interactions are expected to promote lowering of the ionic coupling, based on the model described by Scrosati and co-workers for PEO-ceramic filler (*e.g.* SiO₂, Al₂O₃, TiO₂, and ZrO₂) composite electrolytes.^[32]

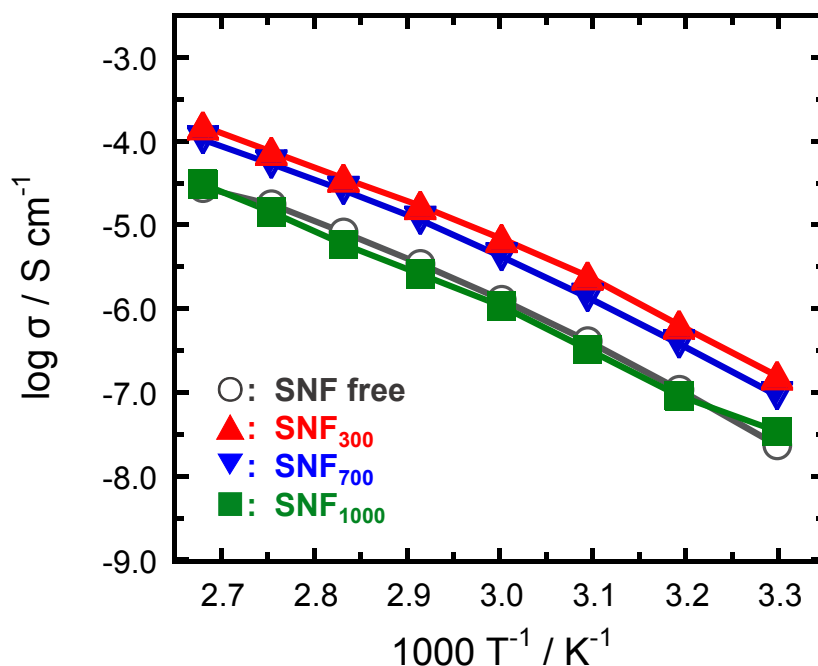


Figure 2-9. Temperature dependence of the ionic conductivity for PEC-LiTFSI 100 mol% original electrolyte and the SNF composite electrolytes (SNF content: 5 wt%).

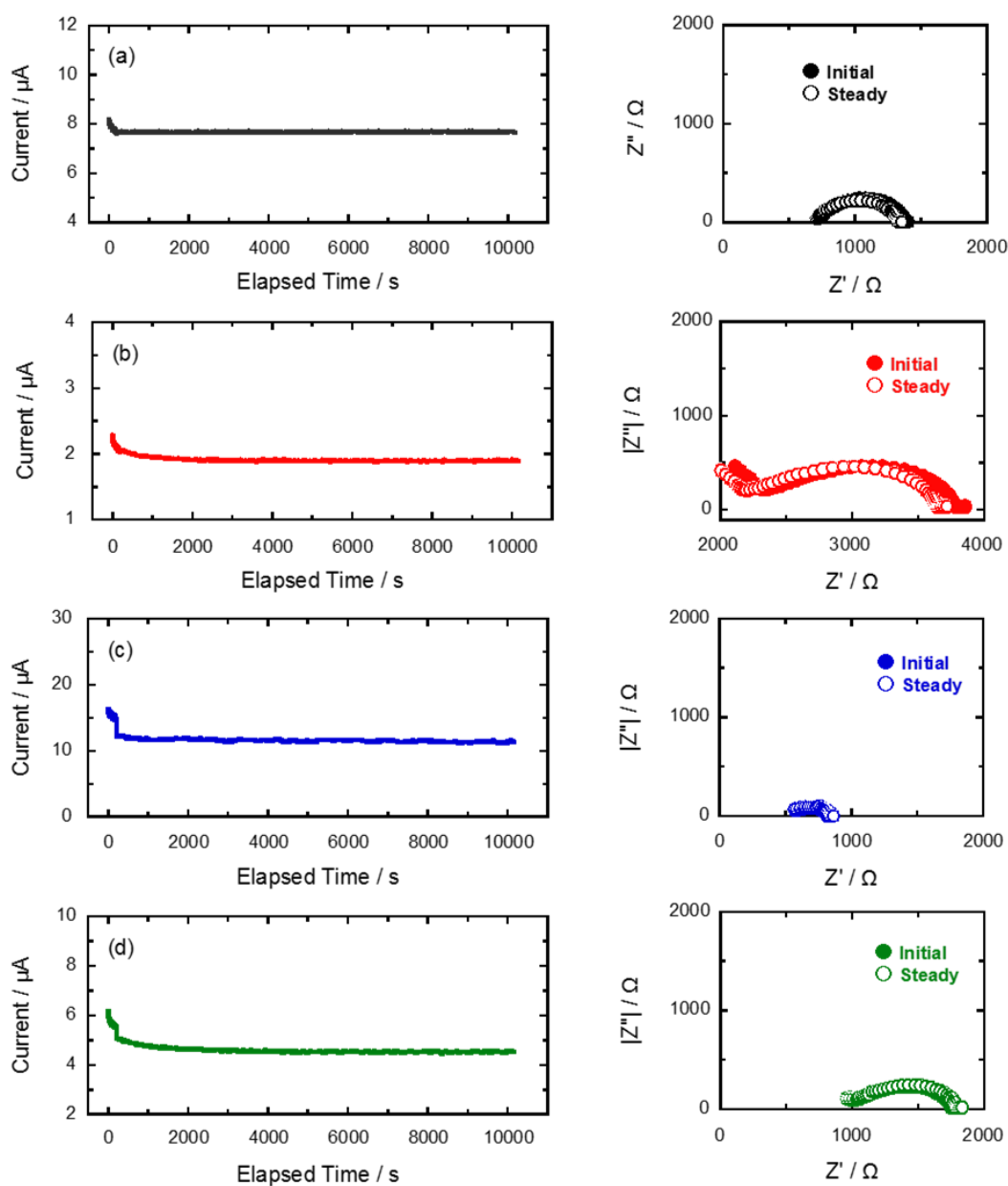


Figure 2-10. DC polarizations and AC impedance measurements of symmetric Li/Li cells with (a) PEC-LiTFSI 100 mol% (b) PEC-LiTFSI 100 mol%-SNF₃₀₀, (c) PEC-LiTFSI 100 mol%-SNF₇₀₀, (d) PEC/LiTFSI 100 mol%-SNF₁₀₀₀ composite electrolytes at 60 °C (SNF content: 5 wt%).

Table 2-3. Values of initial and steady state currents (I_0 , I_{SS}), and interfacial resistances (R_0 , R_{SS}) of symmetric Li/Li cells with the PEC-based electrolytes. Li transference number (t_+) is estimated according to Eq. 2-2.

Sample	$I_0 / \mu\text{A}$	$I_{SS} / \mu\text{A}$	R_0 / Ω	R_{SS} / Ω	t_+
(a) PEC-LiTFSI 100mol%	8.15	7.06	680.5	640.7	0.71
(b) PEC-LiTFSI 100mol%-SNF ₃₀₀ 5 wt%	2.28	1.89	1390	1380	0.77
(c) PEC-LiTFSI 100mol%-SNF ₇₀₀ 5 wt%	16.0	11.4	287.2	294.5	0.58
(d) PEC-LiTFSI 100mol%-SNF ₁₀₀₀ 5 wt%	6.16	4.50	855.7	920.5	0.59

For high-voltage operations in future Li battery systems, a wide electrochemical window is an important electrolyte property. Figure 2-11 shows linear sweep voltammetry (LSV) of stainless steel working electrode in Li cells for original PEC-LiTFSI 100 mol% electrolyte and the SNF composite electrolytes at 80 °C measured by using the electrolytes investigated in this study. Stable currents were observed in all samples. The electrochemical stability at the anodic potential was improved by the addition of SNFs to the SNF-free electrolyte. Croce *et al.*^[33] have reported that the addition of inorganic fillers such as ZrO₂ to the PEO-based electrolytes improves their electrochemical stability. In addition, it has also been published by the author's group that the oxidation potential of TFSI anion itself is high and a large amount of anions on the proximity of the electrode probably inhibits the oxidative decomposition of PEC. The oxidation potential of solvent (PEC in this case) is expected to rise because a larger number of the electron ion pairs the polar groups are stabilized by the coordination to Li⁺.^[34,35] The fiber size effect was also observed in oxidation stability and the PEC-LiTFSI composite electrolyte with SNF₃₀₀ was electrochemically stable up to 4.7 V vs. Li/Li⁺. This indicates that the composite electrolyte should be useful in high-voltage battery materials.

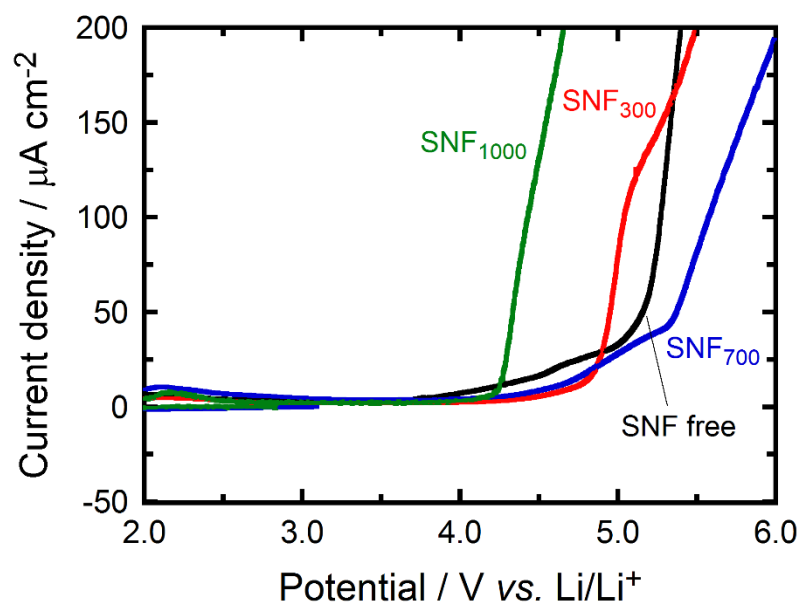


Figure 2-11. LSV measurement of PEC/LiTFSI 100 mol% and the SNF composite electrolytes (SNF content: 5 wt%).

2-3-5 FT-IR spectroscopy

To study the dissociation state of Li ions in polycarbonate electrolytes, FT-IR measurements for polycarbonate-based electrolytes are essential. It has been known that the peak for stretching vibrational mode for free C=O and the interacting band (C=O \cdots Li $^+$) appear at approximately 1740 cm $^{-1}$ and at 1720 cm $^{-1}$ respectively.^[36] In addition, the author's group has been published that the C=O \cdots Li $^+$ interaction peak shift to lower wavenumbers in the low salt concentration regions due to the interaction between C=O and Li $^+$. However, the C=O \cdots Li $^+$ interaction peak shift to higher wavenumbers in the high concentration region which is close to the original position of the free C=O in the neat PEC. This is because ionic aggregation is easier to occur in the highly concentrated electrolyte systems.^[35,36] Figure 2-12 shows FT-IR spectra of original PEC-LiTFSI 100 mol% electrolyte and the SNF composite electrolytes. The C=O \cdots Li $^+$ interaction peak appears clearly at 1725 cm $^{-1}$ for the SNF-free electrolyte. Compare to the original electrolyte, the band shifted slightly to higher wavenumbers with the thinner SNF added, which shows similar behavior with increase salt concentration in the PEC-based electrolytes.^[36] This result indicate that the free C=O groups were increased with the addition of SNFs, which also can be considered that the interaction of C=O and Li $^+$ is weakened by the addition of SNFs. Interestingly, the C=O \cdots Li $^+$ interaction peak gradually shift to higher wavenumbers for adding thinner SNFs, which is due to the stronger Lewis acid-base interactions with thinner SNF. Therefore, the number of free Li $^+$ increased in the composites, and the value of t_+ consequently increased.

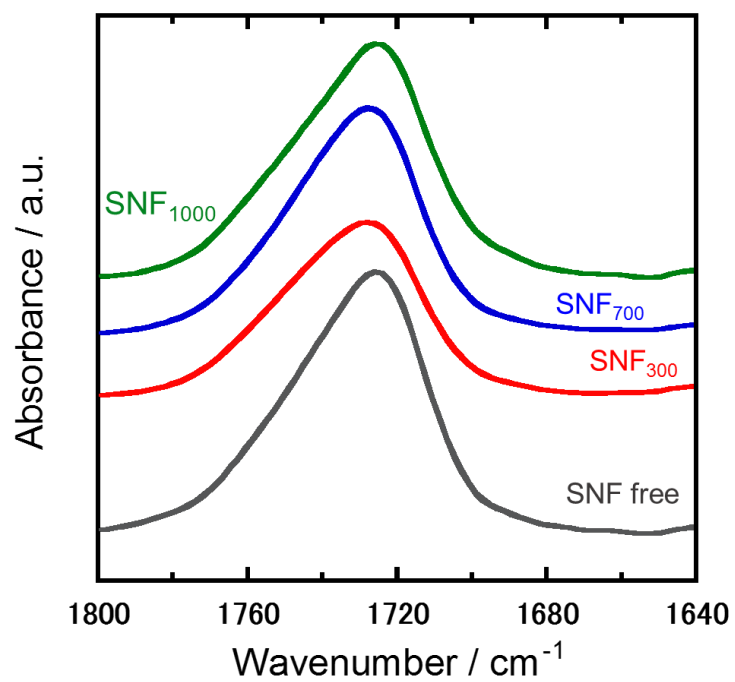


Figure 2-12. FTIR spectra of original PEC-LiTFSI 100 mol% electrolyte and SNF composite electrolytes (SNF content: 5 wt% in the C=O stretching vibration mode).

2-4 Conclusions

In this chapter, the silica nanofibers (SNFs) were synthesized by an electrospinning without calcination process. Because of the calcination-free procedure allows the fiber to retain many polar functional groups on its surface, *i.e.*, silanol (Si-OH) and γ -aminopropyl (Si-(CH₂)₃-NH₂). Hence, further performance improvement of electrolyte is expected as compared with conventional SNF filling. However, it is in general difficult to achieve both ionic conductivity and mechanical strength of polymer electrolytes simultaneously.

A ternary electrolyte systems were prepared which are including PEC, LiTFSI, and SNF (SNF₃₀₀, SNF₇₀₀ and SNF₁₀₀₀), and their electrochemical and mechanical properties were studied in this chapter. The homogeneous and self-standing electrolyte membranes were successfully obtained with a good flexibility. Moreover, it was confirmed by SEM that the three different diameters of SNF were uniformly dispersed in the PEC-based electrolytes. For the ion-conductive properties, the ionic conductivity and Li transference number (t_+) of composite electrolytes were improved by just addition 5 wt% of SNF compared with the original PEC-based electrolyte. Especially, the composite electrolyte with SNF₃₀₀ achieved a maximum ionic conductivity of order of 10^{-4} S cm⁻¹, the highest t_+ value of 0.77 at 60 °C and an excellent oxidation stability up to 4.7 V vs. Li/Li⁺ at 80 °C. Furthermore, the maximum stress and Young's modulus for the electrolyte increased significantly with the addition of SNF₃₀₀. The 5 % weight-loss temperature for the composite was approximately 40 °C higher than that for the SNF-free electrolyte. Interestingly, the thinner the SNF exhibited the better filler filling effect. In conclusion, the addition of thin SNF is an effective method to improve both ion-conductive and mechanical properties of PEC electrolytes.

References

- [1] B.Y. Xia, P. Yang, Y. Sun, Y. Wu, B. Mayers, B. Gates, Y. Yin, F. Kim, H. Yan, One-dimensional nanostructures synthesis, characterization, and application, *Adv. Mater.* **15** (2003) 353–389.
- [2] P.G. Bruce, B. Scrosati, J.-M. Tarascon, Nanomaterials for rechargeable lithium batteries, *Angew. Chemie - Int. Ed.* **47** (2008) 2930–2946.
- [3] A.S. Aricò, P. Bruce, B. Scrosati, J.-M. Tarascon, W. van Schalkwijk, Nanostructured materials for advanced energy conversion and storage devices, *Nat. Mater.* **4** (2005) 366–377.
- [4] A. Greiner, J.H. Wendorff, Electrospinning: A fascinating method for the preparation of ultrathin fibers, *Angew. Chemie - Int. Ed.* **46** (2007) 5670–5703.
- [5] D.H. Reneker, A.L. Yarin, Electrospinning jets and polymer nanofibers, *Polymer (Guildf)*. **49** (2008) 2387–2425.
- [6] P. Raghavan, D.H. Lim, J.H. Ahn, C. Nah, D.C. Sherrington, H.S. Ryu, H.J. Ahn, Electrospun polymer nanofibers: The booming cutting edge technology, *React. Funct. Polym.* **72** (2012) 915–930.
- [7] G. Larsen, R. Velarde-Ortiz, K. Minchow, A. Barrero, I.G. Loscertales, A method for making inorganic and hybrid (organic/inorganic) fibers and vesicles with diameters in the submicrometer and micrometer range via sol-gel chemistry and electrically forced liquid jets, *J. Am. Chem. Soc.* **125** (2003) 1154–1155.
- [8] D. Li, Y. Xia, Fabrication of Titania Nanofibers by Electrospinning, *Nano Lett.* **3** (2003) 555–560.
- [9] S.-S. Choi, S.G. Lee, S.S. Im, S.H. Kim, Y.L. Joo, Silica Nanofibers from Electrospinning/Sol-Gel Process, *J. Mater. Sci. Lett.* **22** (2003) 891–893.
- [10] D. Li, J.T. McCann, Y. Xia, M. Marquez, Electrospinning: A simple and versatile technique for producing ceramic nanofibers and nanotubes, *J. Am. Ceram. Soc.* **89** (2006) 1861–1869.

- [11] S. Ishibe, K. Anzai, J. Nakamura, Y. Konosu, M. Ashizawa, H. Matsumoto, Y. Tominaga, Ion-conductive and mechanical properties of polyether/silica thin fiber composite electrolytes, *React. Funct. Polym.* **81** (2014) 40–44.
- [12] X. Wei, D.F. Shriver, Highly Conductive Polymer Electrolytes Containing Rigid Polymers, *Chem. Mater.* **10** (1998) 2307–2308.
- [13] M. Nakamura, Y. Tominaga, Utilization of carbon dioxide for polymer electrolytes [II]: Synthesis of alternating copolymers with glycidyl ethers as novel ion-conductive polymers, *Electrochim. Acta.* **57** (2011) 36–39.
- [14] Y. Tominaga, T. Shimomura, M. Nakamura, Alternating copolymers of carbon dioxide with glycidyl ethers for novel ion-conductive polymer electrolytes, *Polymer (Guildf)*. **51** (2010) 4295–4298.
- [15] Y. Tominaga, V. Nanthana, D. Tohyama, Ionic conduction in poly(ethylene carbonate)-based rubbery electrolytes including lithium salts, *Polym. J.* **44** (2012) 1155–1158.
- [16] Y. Tominaga, K. Yamazaki, Fast Li-ion conduction in poly(ethylene carbonate)-based electrolytes and composites filled with TiO₂ nanoparticles, *Chem. Commun.* **50** (2014) 4448–4450.
- [17] T. Okumura, S. Nishimura, Lithium ion conductive properties of aliphatic polycarbonate, *Solid State Ionics.* **267** (2014) 68–73.
- [18] K. Kimura, M. Yajima, Y. Tominaga, A highly-concentrated poly(ethylene carbonate)-based electrolyte for all-solid-state Li battery working at room temperature, *Electrochem. Commun.* **66** (2016) 46–48.
- [19] F. Capuano, Composite Polymer Electrolytes, *J. Electrochem. Soc.* **138** (1991) 1918.
- [20] F. Croce, G.B. Appetecchi, B. Scrosati, L. Persi, Nanocomposite polymer electrolytes for lithium batteries, *Nature.* **394** (1998) 456–458.
- [21] H. Matsumoto, A. Tanioka, M. Minagawa, Y. Xie, S. Tamura, JP 4943355, 2012.
- [22] H. Matsumoto, Y. Wakamatsu, M. Minagawa, A. Tanioka, Preparation of ion-exchange fiber

- fabrics by electrospray deposition, *J. Colloid Interface Sci.* **293** (2006) 143–150.
- [23] J. Evans, C.A. Vincent, P.G. Bruce, Electrochemical measurement of transference numbers in polymer electrolytes, *Polymer (Guildf)*. **28** (1987) 2324–2328.
- [24] F.H. Gojny, M.H.G. Wichmann, B. Fiedler, K. Schulte, Influence of different carbon nanotubes on the mechanical properties of epoxy matrix composites - A comparative study, *Compos. Sci. Technol.* **65** (2005) 2300–2313.
- [25] H. Izutsu, F. Mizukami, T. Sashida, K. Maeda, Y. Kiyozumi, Y. Akiyama, Effect of malic acid on structure of silicon alkoxide derived silica, *J. Non. Cryst. Solids*. **212** (1997) 40–48.
- [26] D. Ratna, S. Divekar, S. Patchaiappan, A.B. Samui, B.C. Chakraborty, Poly(ethylene oxide)/clay nanocomposites for solid polymer electrolyte applications, *Polym. Int.* **56** (2007) 900–904.
- [27] L.Z. Fan, J. Maier, Composite effects in poly(ethylene oxide)–succinonitrile based all-solid electrolytes, *Electrochem. Commun.* **8** (2006) 1753–1756.
- [28] H.J. Walls, J. Zhou, J.A. Yerian, P.S. Fedkiw, S.A. Khan, M.K. Stowe, G.L. Baker, Fumed silica-based composite polymer electrolytes : synthesis , rheology , and electrochemistry, *J. Power Sources*. **89** (2000) 156–162.
- [29] F. Croce, F. Bonino, S. Panero, B. Scrosati, Properties of mixed polymer and crystalline ionic conductors, *Philos. Mag. B Phys. Condens. Matter; Stat. Mech. Electron. Opt. Magn. Prop.* **59** (1989) 161–168.
- [30] B. Scrosati, F. Croce, Composite polymer ionics: advanced electrolyte materials for thin - film batteries, *Polym. Adv. Technol.* **4** (1993) 198–204.
- [31] R. Bouchet, S. Maria, R. Meziane, A. Aboulaich, L. Lienafa, J.-P. Bonnet, T.N.T. Phan, D. Bertin, D. Gignes, D. Devaux, R. Denoyel, M. Armand, Single-ion BAB triblock copolymers as highly efficient electrolytes for lithium-metal batteries, *Nat. Mater.* **12** (2013) 452–457.
- [32] B. Scrosati, F. Croce, S. Panero, Progress in lithium polymer battery R&D, *J. Power Sources*. **100** (2001) 93–100.

- [33] F. Croce, S. Sacchetti, B. Scrosati, Advanced, high-performance composite polymer electrolytes for lithium batteries, *J. Power Sources*. **161** (2006) 560–564.
- [34] K. Kimura, J. Motomatsu, Y. Tominaga, Correlation between Solvation Structure and Ion-Conductive Behavior of Concentrated Poly(ethylene carbonate)-Based Electrolytes, *J. Phys. Chem. C*. **120** (2016) 12385–12391.
- [35] K. Kimura, J. Motomatsu, Y. Tominaga, Highly concentrated polycarbonate-based solid polymer electrolytes having extraordinary electrochemical stability, *J. Polym. Sci. Part B Polym. Phys.* **54** (2016) 2442–2447.
- [36] J. Motomatsu, H. Kodama, T. Furukawa, Y. Tominaga, Dielectric relaxation behavior of a poly(ethylene carbonate)-lithium bis-(trifluoromethanesulfonyl) imide electrolyte, *Macromol. Chem. Phys.* **216** (2015) 1660–1665.

Chapter 3

Characterization and ion-conductive properties of carbonate-based polymer blend electrolytes

3-1 Introduction

Solid polymer electrolytes (SPEs) are of great interest for their possible deployment in next-generation secondary batteries.^[1-3] In the past several decades, many studies of SPE with single polymer host have been done by using such as poly(vinyl alcohol), poly(acrylonitrile), and poly(urea-sulfonyl imide).^[4-7] However, their Li^+ transference properties are very poor compared to liquid electrolytes, primarily because of the ion-transport mechanism in complex-formed polymer electrolytes,^[8-10] and the ionic conductivities also need to be further improved.

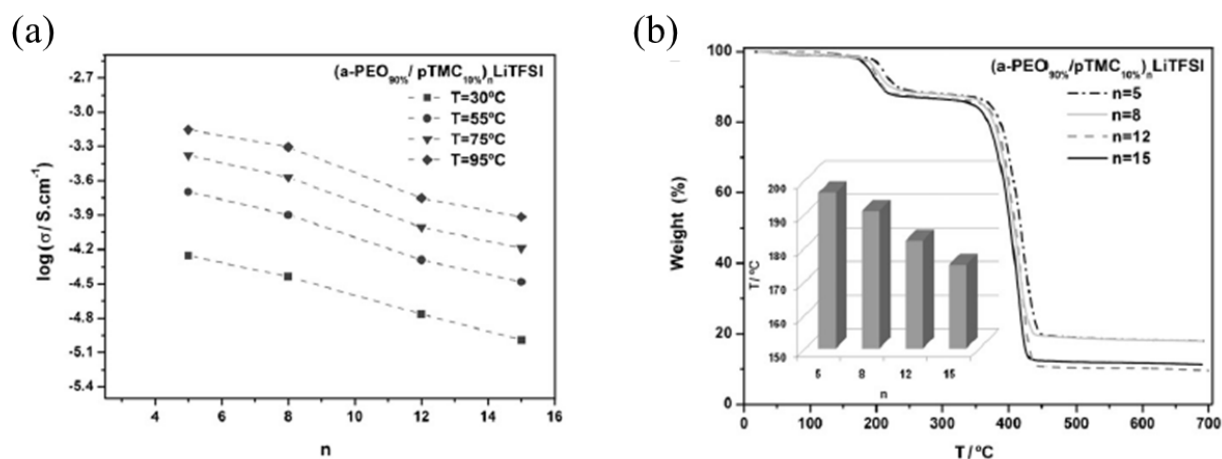


Figure 3-1. Salt concentration dependence of (a) the ionic conductivity and (b) TGA curves for (a-PEO₉₀%/p-PTMC₁₀%)_nLiTFSI blend electrolytes.^[11]

Therefore, a blend polymer electrolyte was proposed. Polymer blending is a feasible and cost-effective technique for developing SPEs having excellent properties. It may be possible to use blend systems to prepare SPEs, based on previous successes.^[12-14] Notably, blend-based polymer electrolytes can overcome the serious drawback of preparing electrolytes by nontrivial synthesis methods, thus, blending is considered to be an important method to improve the ionic conductivities and dimensional stability of polymer electrolytes. The main advantages of polymer electrolytes prepared via a blending method are the simplicity of preparation and easy

control of physical properties by compositional change. Previously, there are some studies reported about PEO combined with polycarbonates, such as PEC, PPC and PTMC.^[11,15,16] In the case of PEO-PTMC-LiTFSI, the ion-conductive and thermal properties were improved by the blending and increasing salt concentrations (Figure 3-1). However, further improvement of the electrochemical properties are still necessary.

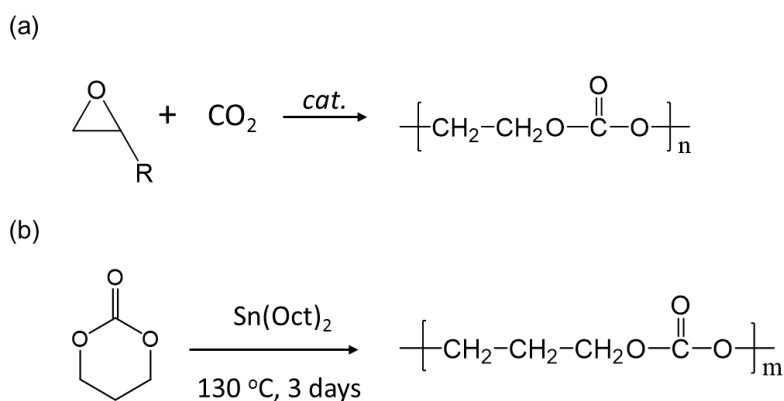


Figure 3-2. Synthesis of (a) PEC by CO₂/epoxide alternating copolymerization and (b) PTMC by radical ring-opening.

As mentioned in the previous chapter, polycarbonates have recently been studied as a new class of host polymer which has very different ion-conductive properties from typical poly(ethylene oxide) (PEO)-based electrolytes. In the case of poly(ethylene carbonate) (PEC), the conductivity and Li⁺ transference number (t_+) increases with increasing lithium salt concentration.^[17] Unfortunately, PEC-based electrolytes have low thermal stability and weak mechanical properties.^[18] In contrast, poly(trimethylene carbonate) (PTMC)-based electrolytes have good electrochemical properties and thermal stability.^[19,20] The conductivity and t_+ of PTMC-based electrolyte are nevertheless lower than for PEC-based electrolytes. The objective of the present study is to combine PEC with PTMC so as to prepare polycarbonate-based electrolytes having superior ion-conductive properties, thermal stability and mechanical properties.

3-2 Experimental

3-2-1 Materials and electrolyte preparation

Poly(ethylene carbonate) (PEC, Empower Materials, $M_n=1.0\times 10^5$, $M_w/M_n=2.7$ from SEC) was precipitated from acetonitrile into methanol, and was dried under vacuum at 60 °C for 24 h prior to use. Poly(trimethylene carbonate) (PTMC) was synthesized by a simple ring-opening polymerization. Trimethylene carbonate (TMC) and $\text{Sn}(\text{Oct})_2$ solution were used as monomer and polymerization catalyst. The synthesis was performed in a stain-less still reactor and placed in a 130 °C oven for 3 days. The detailed polymerization processes have described in a previous paper.^[19] PTMC was provided by Prof. Daniel Brandell's group from Uppsala University, Sweden. The chemical structures of PEC, PTMC, LiTFSI, and LiFSI are shown in Figure 3-3. Lithium bis(trifluoromethanesulfonyl)imide ($\text{Li}[\text{N}(\text{SO}_2\text{CF}_3)_2]$, LiTFSI, battery grade, Purolyte, Ferro Corporation) and Lithium bis(fluorosulfonyl)imide ($\text{Li}[\text{N}(\text{SO}_2\text{F})_2]$, LiFSI, battery grade, Kishida Chemical) were used as received. Polymer mixtures and self-standing electrolytes were prepared by a casting method, as follows. PEC, PTMC and Li salts were mixed in acetonitrile (electrochemical grade) and stirred overnight. The resulting solution were dried in a vacuum

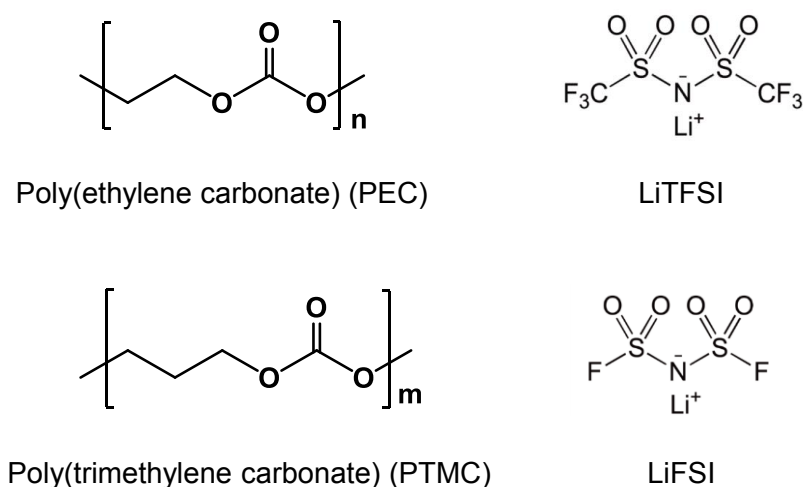


Figure 3-3. Chemical structures of PEC, PTMC, LiTFSI, and LiFSI.

oven at 60 °C for 72 hours in order to eliminate all residual solvents. The Li salt concentrations of electrolytes were set by the monomer range of Li⁺ and carbonyl group (C=O) units in the polymers ($([Li^+]/[C=O]) \times 100 = a \text{ mol\%}$). The LiTFSI concentrations were set in 10, 50 and 100 mol% and the LiFSI concentrations were flexibly set from 5 to 150 mol%. Furthermore, the ratio of PEC and PTMC blend was decided in their molar rate of C=O units and distinguished as PEC_xPTMC_y, (x = 9~1 and y = 1~9).

3-2-2 Characterization

Thermal characterization

For using LiTFSI electrolyte systems and polymer mixtures, differential scanning calorimetry (DSC) and thermogravimetric analysis (TGA) were carried out using TA Instruments DSC Q2000 and Hitachi High-Tech TG/DTA7200 for measurements of the thermal properties and thermal degradation of the blend electrolytes. DSC samples were hermetically sealed in Al pans under argon. After rapidly heating and cooling, the second heating of DSC was from -80 °C to 90 °C at a scan rate of 10 °C min⁻¹. The TGA samples were heated from room temperature to 500 °C at a scan rate of 10 °C min⁻¹. For using LiFSI electrolyte systems, differential scanning calorimetry (DSC) was performed by using DSC7020 (Hitachi High-Tech). The sample preparation and basic measurement operation are same with above mentioned, but the measurement temperature range was changed as from -100 °C to 100 °C. All measurements carried out under dry N₂.

Ion-conductive measurements

Electrochemical impedance spectroscopy (EIS) was carried out for the ionic conductivities of all electrolytes. For the LiTFSI used electrolytes, the EIS measured by using a system equipped

with a potentiostat/galvanostat SI 1260 Impedance/Gain-Phase Analyzer (Schlumberger) at a frequency range of 1 Hz-10 MHz and an amplitude of 10 mV. Blend electrolytes were cut out as 12 mm diameter of circle and sandwiched between stainless steel blocking electrodes and sealed in Swagelok-type cells. The cells were heated to 80 °C and kept at 2 hours before measurement to ensure good interfacial contacts between electrolyte and electrode. The sample was then allowed to cool down and measurements were done from 80 °C to 30 °C with an interval of 10 °C, and at 25 °C as well. For the LiFSI used electrolytes, the EIS measured by using a potentiostat/galvanostat SP-150 (Bio-Logic Instrument). The conductivity cell consisted with two stainless steel (SS) blocking electrodes was used for the 9 mm diameter of electrolyte. The perforated Teflon[®] film was used as spacer. Before starting the measurement, the cells were kept at 70 °C for about 2 h to ensure good electrode/electrolyte contact. The EIS measurement was performed every 10 °C from 100 to 25 °C with signal amplitude of 10 mV in the frequency range 100 mHz to 1 MHz. The cell assembly was carried out in an Ar-filled glovebox. The ionic conductivity (σ) was calculated by the Eq. (2-1), which we have introduced in the chapter 2.

Electrochemical measurements

DC polarization and AC impedance measurements were carried out using an Impedance Analyzer 1280C (Solartron) for symmetric Li|SPE|Li cells at 50 °C to estimate values of Li⁺ transference number (t_+) was measured using potentiostatic polarization.^[21] The electrolyte sample was sandwiched between two SS plates to which a Li foil was attached as a non-blocking electrode to prepare measurement cells. EIS was carried out before and after the chronoamperometry by applying an alternate voltage signal with amplitude of 10 mV in frequency range from 100 mHz to 7 MHz. Chronoamperometry was performed by applying to the cells a voltage of 10 mV for 480 min. The symmetric cells were assembled and thermally

equilibrated for 12 hours at 50 °C in order to improve the interface before measurements. All processed of sample preparations and measurements were done in the strictly controlled glovebox filled with dry Ar gas. The value of t_+ was estimated by the Eq. (2-2), which we have introduced in the chapter 2. Since, the Li electrode is non-blocking with respect to Li ions but blocking with anions, the current flowing through the cell decreases with time from the initial value (I_0) and reaches the steady state current (I_{ss}). In other words, both the anion and the cation move at the initial stage of the DC polarization, unlike the anion where the cation is always supplied, but the anion does not contribute further to the current value once it moved. Therefore, only the contribution of the cation in the steady state current. At this time, if there is no change in interfacial resistance, the Li ion transport rate can simply be obtained by the ratio of I_{ss} and I_0 . However, when there is a change in the interface resistance, the current value also fluctuates. Accordingly, the formula may eliminate the influence of the interface resistance.

FT-IR spectroscopy

FT-IR spectra were acquired in an attenuated total reflection (ATR) unit (ZnSe lens) with a FT-IR spectrometer (FT/IR-4100, JASCO Co.). The spectra were recorded from 400 to 4000 cm^{-1} with a resolution of 4 cm^{-1} under dry N_2 gas at room temperature.

3-3 Results and discussion

3-3-1 Physicochemical and thermal properties

The chemical structures of PEC and PTMC were shown in Figure 3-3. They have a very similar chemical structures, and both have the same carbonate unit (O-C(=O)-O) in the main chain. Flexible and transparent self-standing membranes were obtained for all PEC and PTMC mixtures and their blend electrolytes. The polymer mixture becomes softer and sticky after addition of high amount of Li salts. Figure 3-4 shows photographs of PEC₆PTMC₄ mixture and PEC₆PTMC₄-LiTFSI 100 mol% electrolyte. A small phase separation, based on the appearance of the PEC and PTMC mixture has thus been confirmed (Figure 3-4a). This phenomenon reminds us that neat PEC and PTMC are basically incompatible, even though they have very similar chemical structures. In contrast, the Li salt added PEC₆PTMC₄-LiTFSI 100 mol% electrolyte is showing a homogenous and clear membrane, without any phase separation found (Figure 3-4b). The addition of Li salts may be improved the compatibility in between the both polycarbonates.

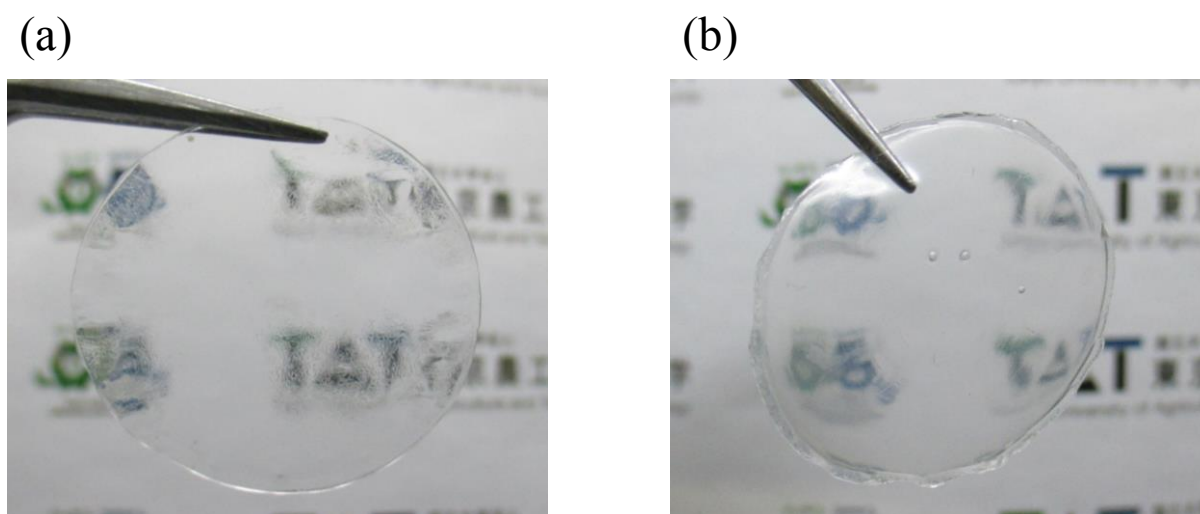


Figure 3-4. Photographs of (a) PEC₆PTMC₄ mixture and (b) PEC₆PTMC₄-LiTFSI 100 mol% electrolyte.

The differential scanning calorimetry (DSC) curves of the second heating runs for neat PEC and PTMC, and for PEC-PTMC mixtures, are shown in Figure 3-5a. On the DSC traces of the neat PEC and PTMC polymers, a single glass transition is clearly observed for each polymer without any further transition above this temperature, which implies that PEC and PTMC are both amorphous polymers. The glass transition temperatures (T_g) for neat PEC and PTMC appear around 10 °C and -15 °C, respectively. This is a quite interesting behavior that they are showing completely different glass transition properties, even they have very similar chemical structures and only a difference in presence/absence of one methyl group. Moreover, there are two transitions that appeared which are at values around -18 °C for PTMC and 20 °C for PEC for all PEC and PTMC mixtures (Figure 3-5a). These results also demonstrate that the polymers cannot be compatibilized and that phase separation has occurred as shown in the Figure 3-4a.

On the other hand, the Li salt added blend electrolytes are exhibiting a different thermal properties compared with PEC and PTMC mixtures. Figure 3-5b shows DSC curves at the second heating scan for PEC, PTMC and PEC₆PTMC₄ with addition of the LiTFSI, the values of T_g are also summarized in Table 3-1. The values of T_g for single PEC and PTMC electrolytes with 100 mol% LiTFSI are lower than that of PEC neat polymer, but higher for PTMC. As seen in the polymer mixture without the LiTFSI (0 mol%), the glass transitions deriving from PEC and PTMC are clearly visible separately. Interestingly, addition of LiTFSI to the blend gives rise to changes in the glass transition temperature. These PEC- and PTMC-derived glass transitions become weaker relative to the corresponding single polymer systems. Moreover, T_g for PTMC converge to the T_g of PEC with further addition of LiTFSI, where 100 mol% LiTFSI was added into the PEC₆PTMC₄ mixture, the two glass transitions from PTMC and PEC disappeared and merged into a single curve. The similar behavior has also been observed from other blend compositions (Figure 3-6). These results demonstrate that the addition of Li salt can

lead PEC and PTMC to be compatible, and the dissolved ions act as physical cross-linkers between the two carbonate polymers.

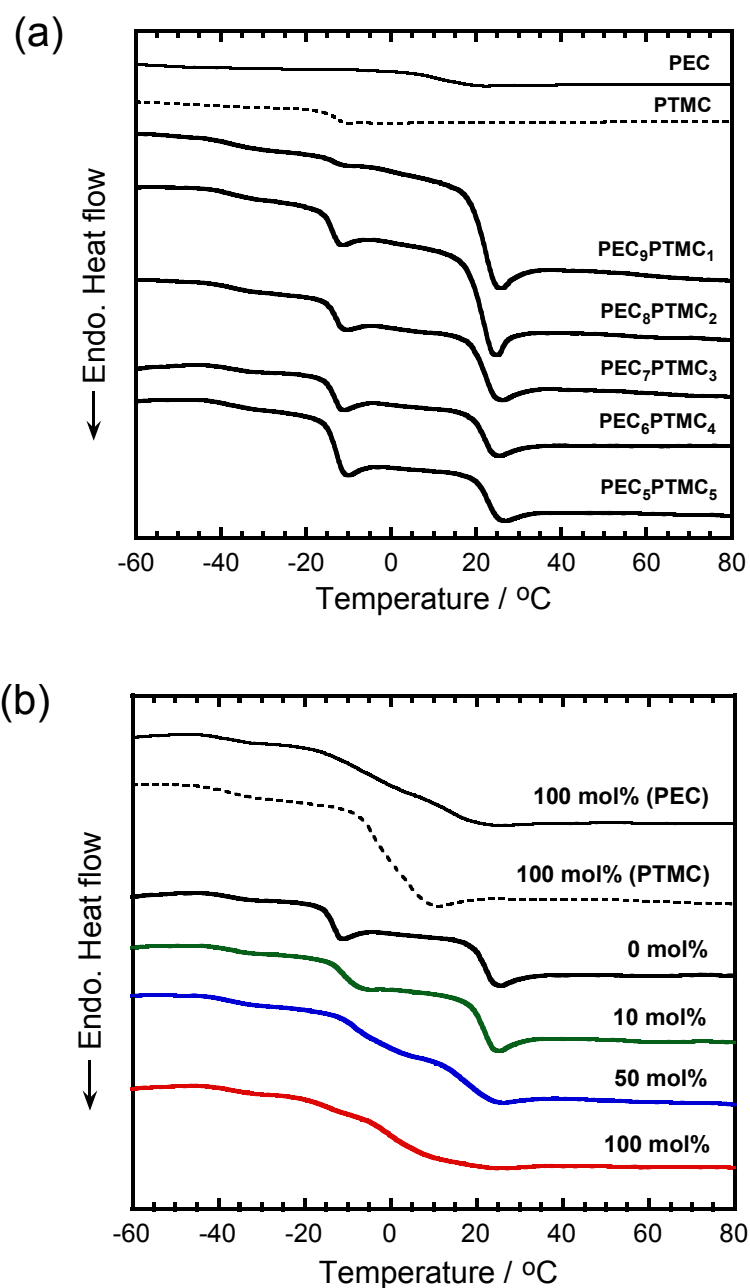
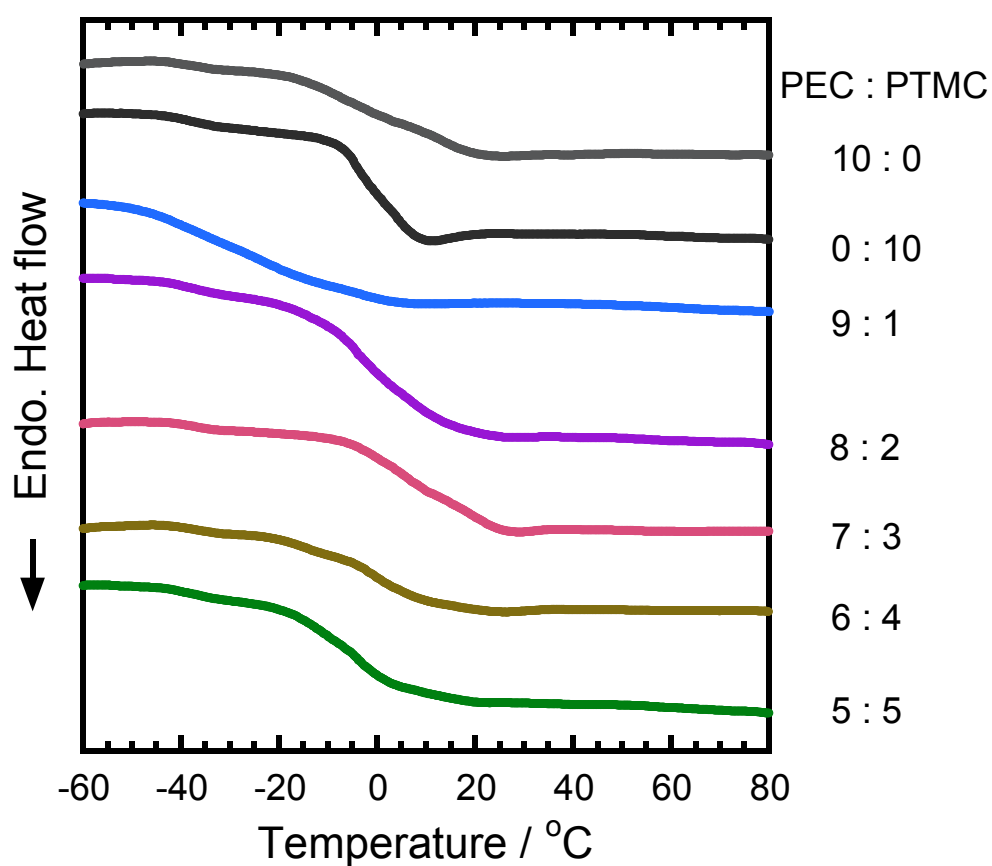


Figure 3-5. DSC traces of (a) neat PEC, PTMC and PEC_xPTMC_y mixtures, and (b) their electrolytes (PEC-LiTFSI 100 mol%, PTMC-LiTFSI 100 mol% and PEC₆PTMC₄-LiTFSI *n* mol%).

Table 3-1. DSC results for PEC, PTMC and PEC₆PTMC₄ electrolytes with LiTFSI.

Sample	T_g (°C)	
	PEC derived	PTMC derived
PEC-LiTFSI 100 mol%	-8	-
PTMC-LiTFSI 100 mol%	-	-4
PEC ₆ PTMC ₄ -LiTFSI 0 mol%	-13	22
PEC ₆ PTMC ₄ -LiTFSI 10 mol%	-10	22
PEC ₆ PTMC ₄ -LiTFSI 50 mol%	-8	16
PEC ₆ PTMC ₄ -LiTFSI 100 mol%	-6	

**Figure 3-6.** DSC traces of PEC_xPTMC_y-LiTFSI 100 mol% electrolytes.

Furthermore, the LiFSI with PEC, PTMC, and their blend electrolytes were also carried out in this study. Because of LiFSI has been intensively investigated as next-generation conducting salt for Li batteries due to its high ionic conductivity, good chemical stability, and capability of forming stable SEI films on various electrodes.^[22-24] The dependence on salt concentration of T_g for PEC- and PTMC-based electrolytes is shown in Figure 3-7. The ionic conduction and glass transition behavior of the PEC-LiFSI electrolytes have been confirmed by our previous research,^[17] and the same results were also obtained in this study (Figure 3-7a). In the case of the PTMC-LiFSI electrolytes, the changes in the T_g value for PTMC electrolytes is different from the PEC system in the low salt concentration range. The values of T_g for PEC electrolytes basically continues to decrease with increasing salt concentration after the addition of LiFSI, but the PTMC system increases T_g with increasing concentration at lower salt concentrations below 30 mol% (Figure 3-7b). This behavior of the PTMC system has been reported previously^[19]. Furthermore, the T_g of the PTMC system decreased with further increasing the salt concentration. This is a similar behavior to that observed in the concentrated PEC system (Figure 3-7a) in that the T_g decreases by the existence of many aggregated ions without stable solvation between polymer chains and Li ions, increasing the conductivity.^[25] In addition, Figure 3-8 shows DSC curves at the second heating scan for $\text{PEC}_x\text{PTMC}_y$ with addition of the LiFSI 150 mol%. Same with the $\text{PEC}_x\text{PTMC}_y\text{-LiTFSI}$ systems, only one glass transition curve was obtained for very concentrated blend electrolytes. According to the results, this can be considered that PEC and PTMC are also compatible within the LiFSI.

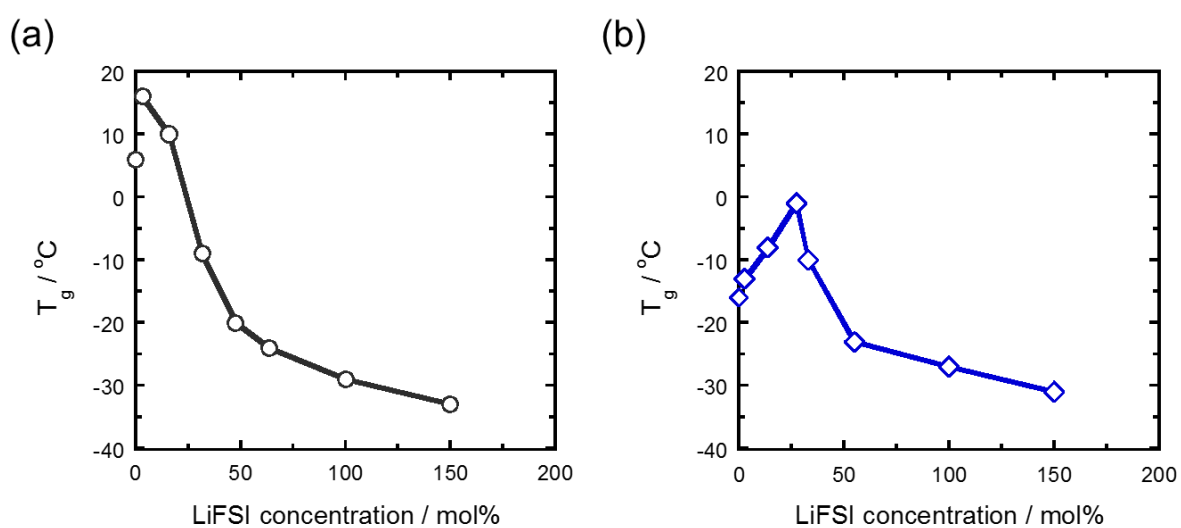


Figure 3-7. Dependence on salt concentration of glass transition temperature (T_g) for (a) PEC-LiFSI and (b) PTMC-LiFSI electrolytes.

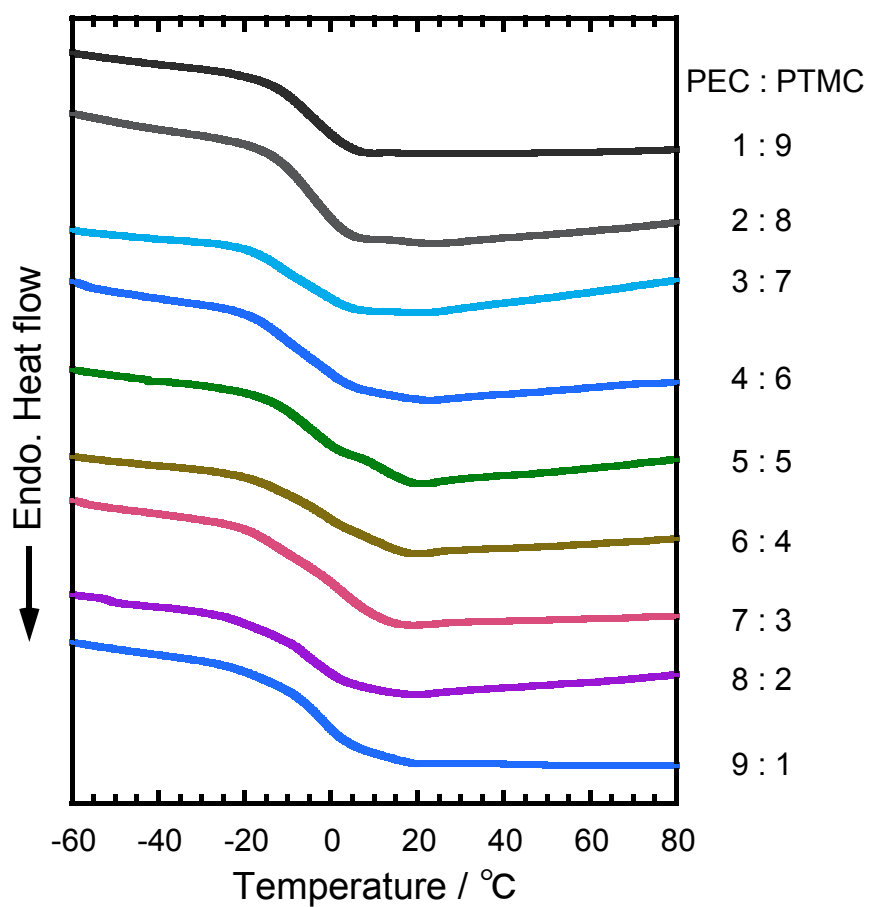


Figure 3-8. DSC curves of PEC_xPTMC_y-LiFSI 150 mol% electrolytes.

Furthermore, the thermal stability of these electrolytes were determined by thermogravimetry, and the results are shown in Figure 9. The values of 5 wt% weight-loss temperatures are also summarized in Table 3-2. The onset temperatures for degradation of PEC-LiTFSI 100 mol% and PTMC-LiTFSI 100 mol% are approximately 150 °C and 200 °C, respectively. The first and second-stage degradation reactions occurring at around 150-300 °C and 300-400 °C are due to the thermal degradation of the polymer and Li salts, respectively. Based on the thermogravimetric analysis (TGA) curves, it was observed that the value of T_{d5} for PEC₆PTMC₄-LiTFSI electrolytes increased slightly with increasing salt concentration. Normally, the value of T_{d5} decreased with increasing salt concentration for polycarbonate based SPEs,^[19] because polymers become softer and lost their original strong polymer interstructure. However, in the case of this study, may be due to the increase in compatibility of PEC and PTMC with the addition of LiTFSI, which improves the coordination between the two polymers. Moreover, the addition of PTMC improves the T_{d5} value of blend electrolytes relative to that of the PEC-based electrolytes (Figure 3-10 and Table 3-2).

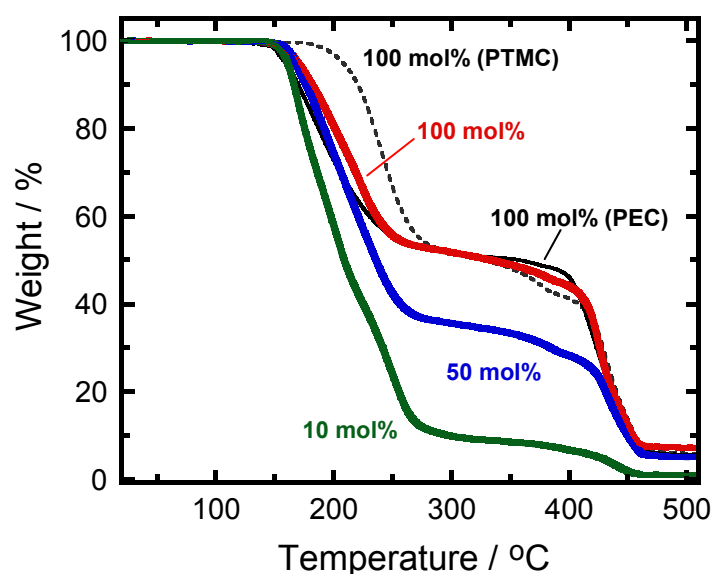


Figure 3-9. TGA curves of PEC-LiTFSI 100 mol%, PTMC-LiTFSI 100 mol% and PEC₆PTMC₄-LiTFSI electrolytes with different salt concentrations.

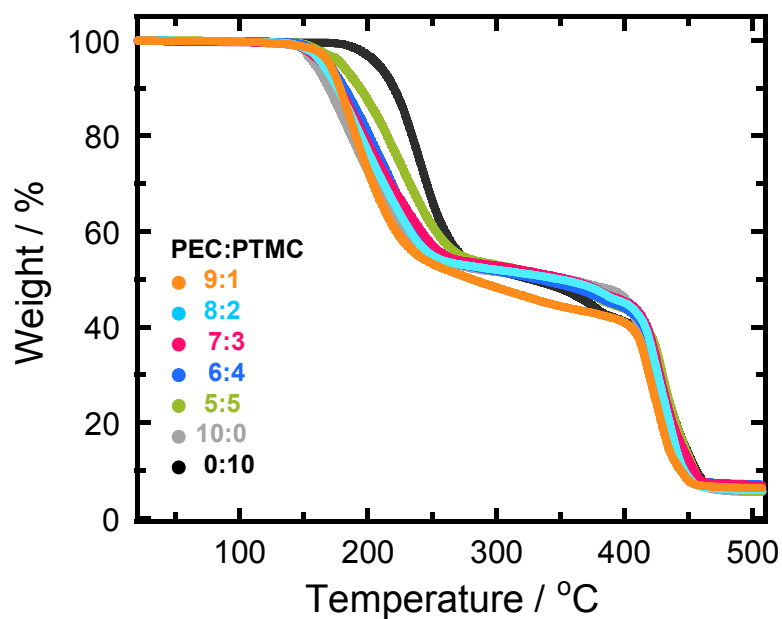


Figure 3-10. TGA curves of $\text{PEC}_x\text{PTMC}_y\text{-LiTFSI}$ 100 mol% electrolytes.

Table 3-2. TGA results of the weight-loss temperatures (T_{d5}) for PEC, PTMC and $\text{PEC}_6\text{PTMC}_4$ electrolytes with LiTFSI.

Sample	T_{d5} (°C)
PEC-LiTFSI 100 mol%	159
PTMC-LiTFSI 100 mol%	207
$\text{PEC}_6\text{PTMC}_4\text{-LiTFSI}$ 10 mol%	160
$\text{PEC}_6\text{PTMC}_4\text{-LiTFSI}$ 50 mol%	167
$\text{PEC}_6\text{PTMC}_4\text{-LiTFSI}$ 100 mol%	169
$\text{PEC}_9\text{PTMC}_1\text{-LiTFSI}$ 100 mol%	164
$\text{PEC}_8\text{PTMC}_2\text{-LiTFSI}$ 100 mol%	165
$\text{PEC}_7\text{PTMC}_3\text{-LiTFSI}$ 100 mol%	164
$\text{PEC}_5\text{PTMC}_5\text{-LiTFSI}$ 100 mol%	179

3-3-2 Ion-conductive properties

The ionic conductivity was measured for all PEC and PTMC blend electrolytes with various LiTFSI concentrations. All electrolytes showed reasonable variations of conductivity that were smooth and essentially non-linear curves with respect to $1/T$. This behavior can be seen in the typical amorphous polymer electrolyte system. Figure 3-11a shows the temperature dependence of the ionic conductivity for $\text{PEC}_x\text{PTMC}_y\text{-LiTFSI}$ 100 mol% electrolytes. The conductivity increases with increasing PEC content until the value reaches a maximum and then decreases, which is matching with the previous study.^[16] The $\text{PEC}_6\text{PTMC}_4\text{-LiTFSI}$ 100 mol% electrolyte displayed the highest conductivity of all blend electrolytes, the order of conductivity as high as $10^{-6} \text{ S}\cdot\text{cm}^{-1}$ at 50°C . For this sample the ionic conductivity is higher than for other blend electrolytes at all temperatures (Figure 3-11a). Furthermore, these blend electrolytes reveal slightly higher conductivities than those of original PEC- and PTMC-based electrolytes. This is probably due to the good combination of the two polymers and LiTFSI.^[11,16] The temperature dependence of the conductivity for the $\text{PEC}_6\text{PTMC}_4\text{-LiTFSI}$ electrolytes in different salt concentrations are shown in Figure 3-11b. The conductivity of the $\text{PEC}_6\text{PTMC}_4\text{-LiTFSI}$ electrolyte increases with increasing LiTFSI concentration. The concentration increases to 100 mol%, the conductivity reaches approximately $10^{-4} \text{ S}\cdot\text{cm}^{-1}$ at 80°C , which is more than one order of magnitude greater than the 10 mol% LiTFSI added electrolyte. The PEC and PTMC mixtures become compatible and the existence of interactions between host matrix and Li^+ upon adding LiTFSI can explain the increase in conductivity. This matches the fact that the conductivity was improved by the addition of Li salts into the PEO/PTMC blend system.^[11]

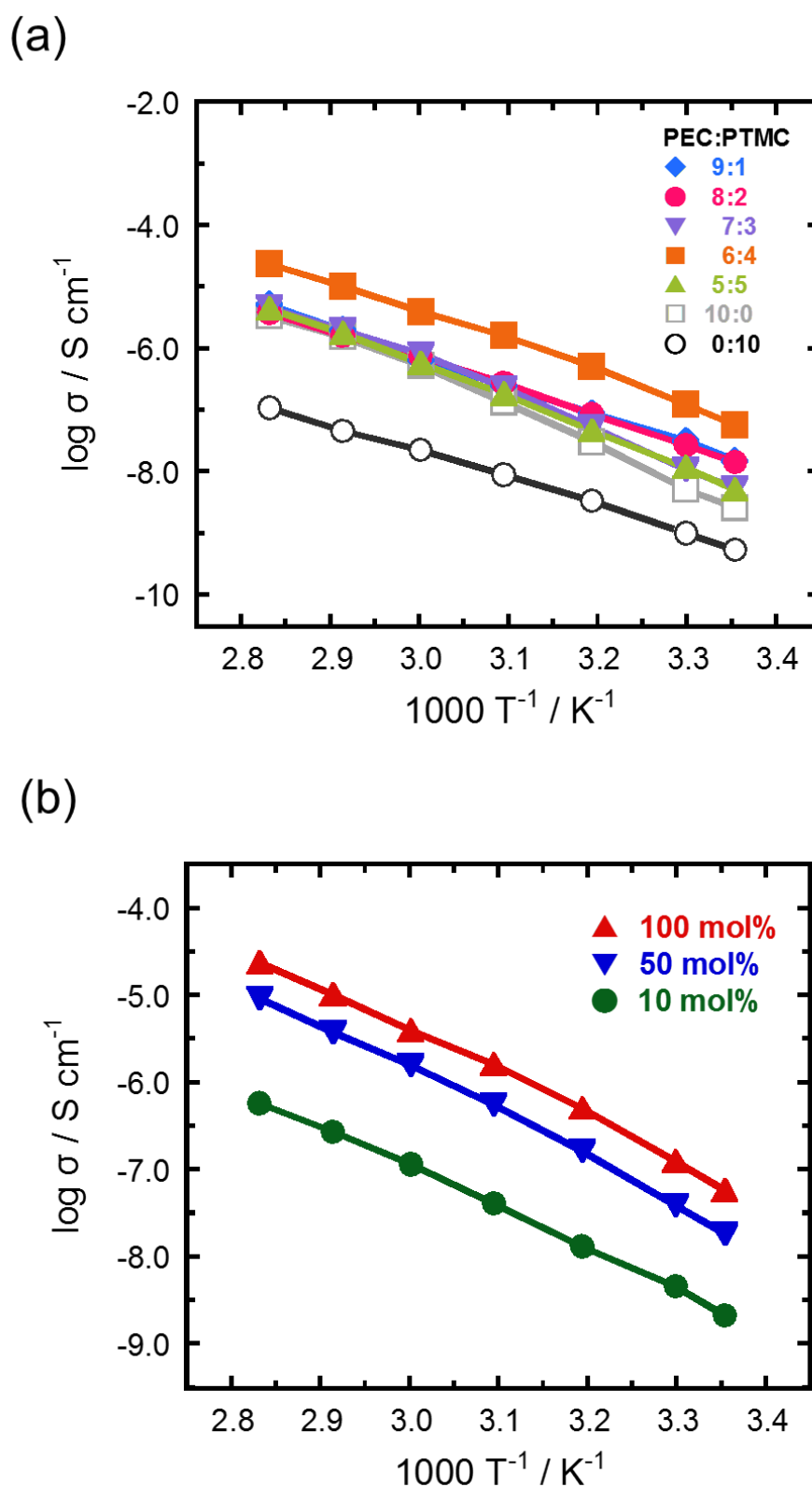


Figure 3-11. Temperature dependence of the ionic conductivity for (a) $\text{PEC}_6\text{PTMC}_4\text{-LiTFSI}$ electrolytes with various salt concentrations, and (b) PEC -, PTMC - and $\text{PEC}_x\text{PTMC}_y\text{-LiTFSI}$ 100 mol% blend electrolytes.

The electrolytes of polymers with LiFSI were also prepared and their ion-conductive properties were investigated as well. The reason for using LiFSI has already been mentioned above. The dependence on salt concentration of ionic conductivity for PEC- and PTMC-based electrolytes is shown in Figure 3-12. In the present study, the same behavior of the ionic conduction and glass transition of PEC-LiFSI electrolytes have obtained with our previous work,^[17] and the highest conductivity was displayed at 150 mol% salt loading (Figure 3-12a). Similarly, the conductivity of the PTMC-LiFSI electrolytes increases with increasing salt concentration (Figure 3-12b), but the change is smoother than for the PEC system. We have explained above that PEC- and PEMC-based electrolytes have a different glass transition behavior, which is the PEC systems show the continuously decreasing T_g values with increasing salt concentration (Figure 3-7a); but the PTMC systems increase T_g with increasing concentration at lower salt concentrations below 30 mol% (Figure 3-7b). This behavior of the PTMC system has been reported previously^[19], and this probably directly influences the slower increase in conductivity for the PTMC systems at the low concentration area (Figure 3-12b). In addition, the T_g of the PTMC system decreased with further increasing the salt concentration. This is a similar behavior to that observed in the concentrated PEC system (Figure 3-12a) in that the T_g decreases by the existence of many aggregated ions without stable solvation between polymer chains and Li ions, increasing the conductivity^[25].

Figure 3-13 shows the PEC content dependence of the conductivity for $\text{PEC}_x\text{PTMC}_y\text{-LiFSI}$ 150 mol% blend electrolytes at 50 °C and 25 °C. All of the polymer electrolytes show acceptable conductivities of the order of 10^{-5} S cm^{-1} at 50 °C and 10^{-6} S cm^{-1} at 25 °C. The conductivity of the blend electrolytes slightly increases with increasing PEC content and the $\text{PEC}_9\text{PTMC}_1$ electrolyte exhibits the highest conductivity of all blend electrolytes. This behavior is similar to the PEC/PEO blend electrolyte system reported previously.^[15] The PEC may play a role for a better ion-conductive phase in the blend electrolyte. However, the thermal properties of PEC-

rich electrolytes such as pure PEC and the $\text{PEC}_9\text{PTMC}_1$ blend electrolyte seem to be unsuitable for battery applications.^[18,26] Therefore, a $\text{PEC}_6\text{PTMC}_4$ blend electrolyte was chosen for further measurements.

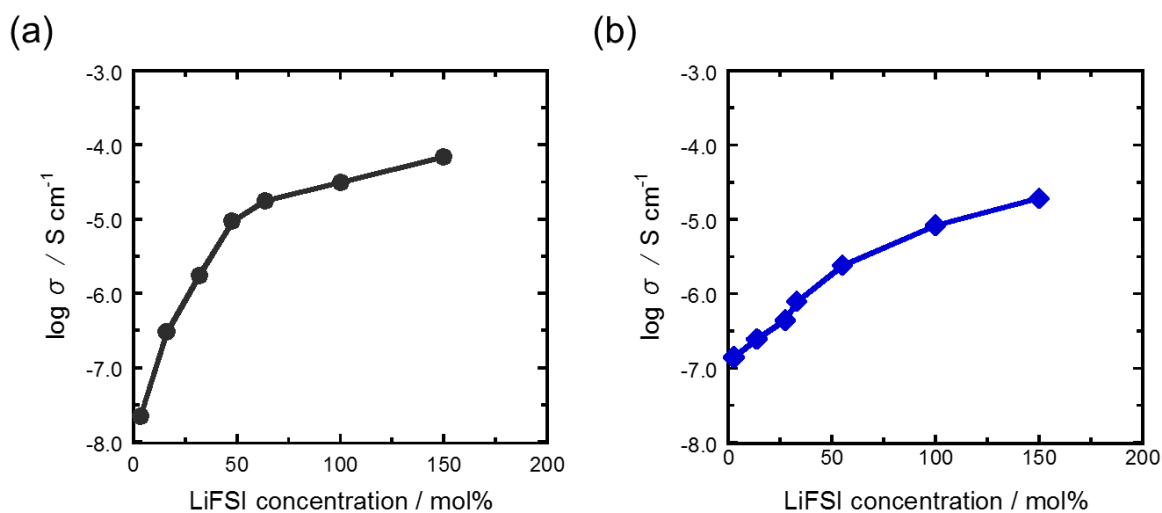


Figure 3-12. Dependence on salt concentration of ionic conductivity (σ) for (a) PEC-LiFSI and (b) PTMC-LiFSI electrolytes at 50 °C.

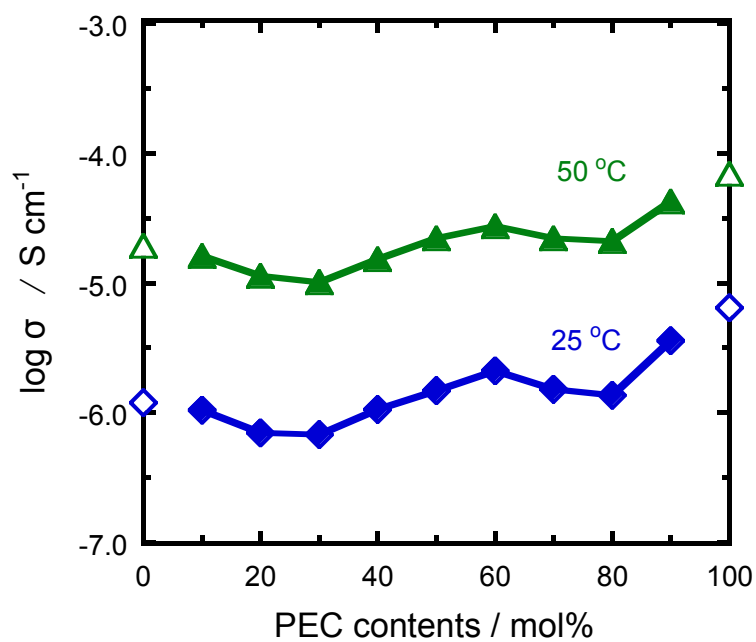


Figure 3-13. PEC content dependence of the ionic conductivity for $\text{PEC}_x\text{PTMC}_y\text{-LiFSI}$ 150 mol% electrolytes.

3-3-3 Electrochemical properties

It is known that polycarbonate-based electrolytes can exhibit excellent Li-ion transport properties such as high Li-ion transference number (t_+).^[27-29] In this study, the values of t_+ for PEC, PTMC, and their blend electrolytes were measured, and the t_+ value is also given by the Eq (2-2) which we have introduced in the chapter 2. Results of t_+ measurements are arranged in Table 3-1, and chronoamperometry profiles and the Nyquist plots of the impedance spectra for all samples are shown in Figure 3-14. All electrolytes exhibited a very high t_+ of more than 0.6, and the value was determined as 0.63 for PEC-LiFSI 150 mol%, 0.61 for PTMC-LiFSI 150 mol%, and 0.73 for PEC₆PTMC₄-LiFSI 150 mol%. The excellent t_+ for the concentrated PEC-based electrolytes have been revealed in our previous papers,^[17,18,30,31] and the PTMC system also has good Li-ion transport properties.^[32] Moreover, the blend electrolyte displayed slightly higher and stable values of current with the smallest impedance response (Figure 3-14c). This implies that there are many mobile Li-ions, and they can move faster and easier in the blend electrolyte than in the original polymer electrolytes. These observations suggest that the combination of carbonyl group-containing polymers, which separately have good t_+ , can result in an improvement in the Li-ion transport properties.

Table 3-3. Current (I_0 , I_{ss}), charge transfer resistance (R_0 , R_{ss}) and lithium transference numbers (t_+) data, as determined electrochemically ^[21] for (a) PEC-LiFSI 150 mol%, (b) PTMC-LiFSI 150 mol%, R_0 , R_{ss} and (c) PEC₆PTMC₄-LiFSI 150 mol% electrolytes at 50 °C.

Sample	$I_0 / \mu\text{A}$	$I_{ss} / \mu\text{A}$	R_0 / Ω	R_{ss} / Ω	t_+
(a) PEC-LiFSI 150 mol%	0.45	0.32	11254	13542	0.63
(b) PTMC-LiFSI 150 mol%	0.35	0.24	8546	8784	0.61
(c) PEC ₆ PTMC ₄ -LiFSI 150 mol%	0.50	0.38	8177	9881	0.73

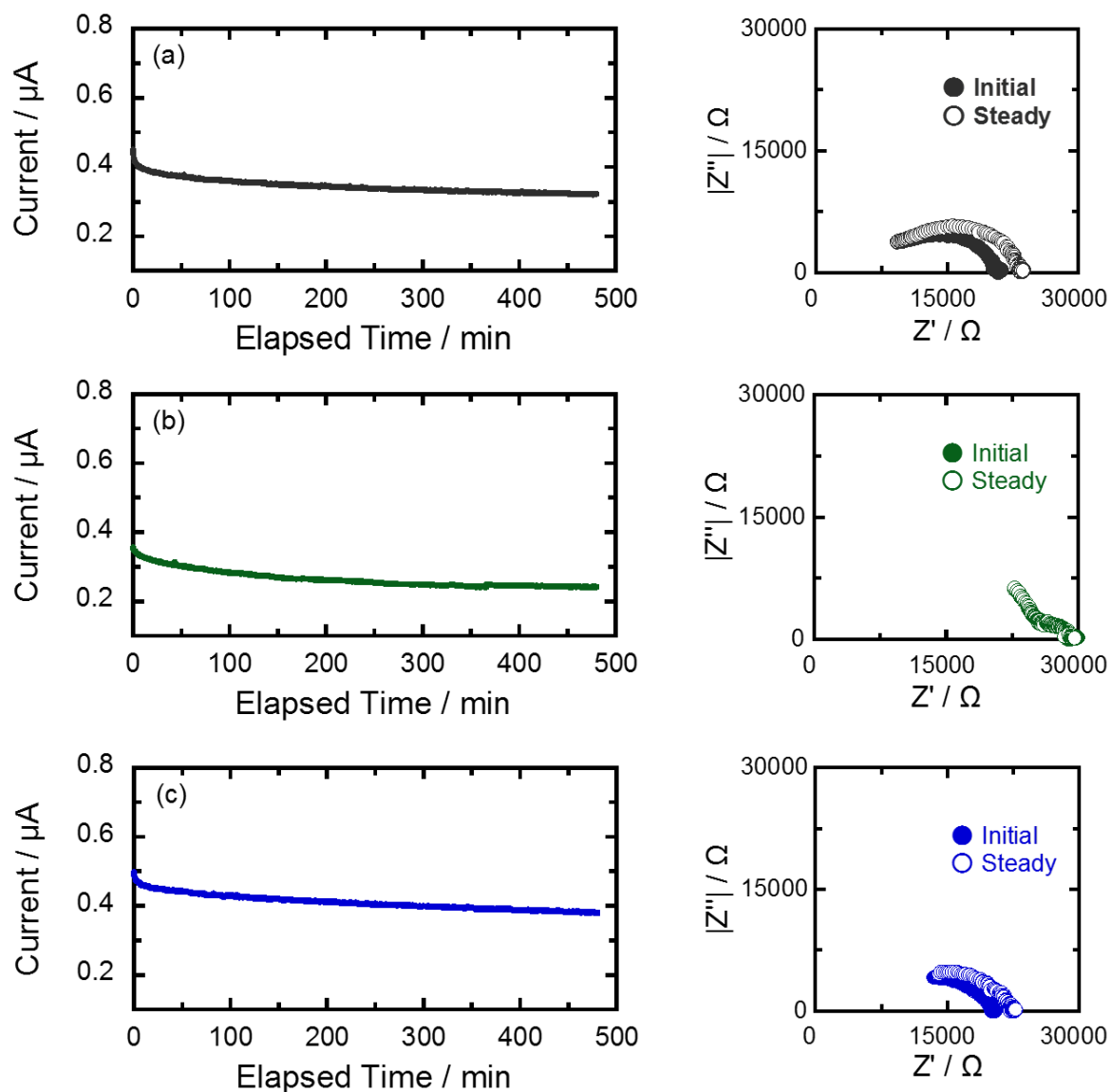


Figure 3-14. Chronoamperometry profiles and Nyquist plots of EIS measurements before and after polarization related to the calculation of the lithium transference number (t^+). Measurements performed on Li/Li symmetrical cells using (a) PEC-LiFSI 150 mol%, (b) PTMC-LiFSI 150 mol%, and (c) PEC₆PTMC₄-LiFSI 150 mol% electrolytes at 50 °C.

3-3-4 FT-IR spectroscopic study

The formation of complexes between polymer mixtures (PEC and PTMC) and LiTFSI can be studied by fourier transform infrared (FT-IR) spectroscopic measurement. For the polycarbonate-based electrolytes, interaction is clearly observed between C=O groups and Li⁺, useful information for the ion-conductive behavior. Figure 3-15 shows the FT-IR spectra of the C=O stretching vibration region for the pure polymer blend (PEC₆PTMC₄) and the electrolytes containing various concentrations of LiTFSI. It is known that the band of free C=O groups appears at around 1740 cm⁻¹, and the band corresponding to C=O groups interacting with Li ions (C=O···Li⁺) shifts to lower wavenumbers around 1720 cm⁻¹.^[20, 30-31] The PEC and PTMC mixture (0 mol%) clearly showed a strong free C=O band at around 1735 cm⁻¹, and the band shifted slightly to lower wavenumber with the addition of LiTFSI. For the blend with higher concentration (50 and 100 mol%) of LiTFSI, a new band appeared around 1716-1722 cm⁻¹. This new band may be due to interaction between C=O groups and Li⁺ in both PEC and PTMC phases. In fact, the interaction bands for both PEC- and PTMC-LiTFSI 100 mol% were observed at 1723 cm⁻¹ and 1717 cm⁻¹, respectively. If there is only one interaction between C=O of PEC and Li⁺, the band should appear only at 1723 cm⁻¹. The band between 1716-1722 cm⁻¹ of the interacting C=O in the blend electrolytes suggests that a compatible amorphous phase of PEC and PTMC was induced by dissolved ions such as Li⁺. Moreover, this phase may provide easier ion pathways.

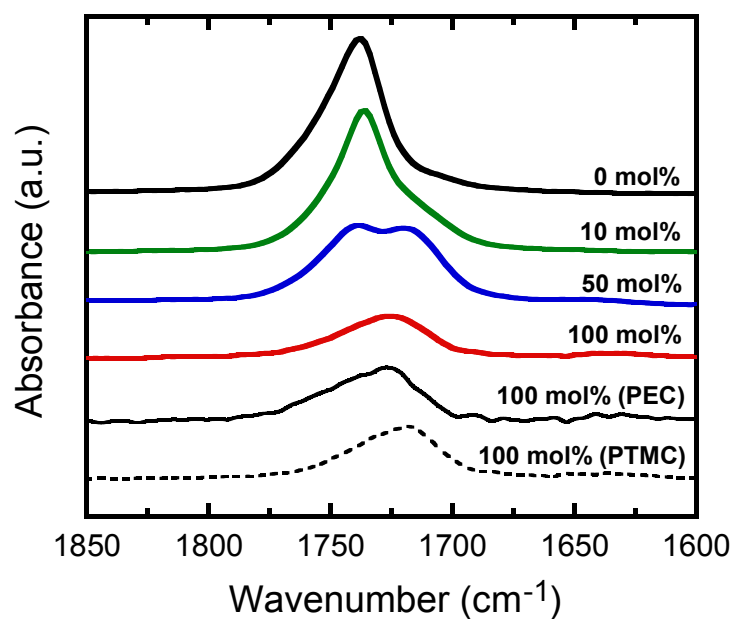


Figure 3-15. FT-IR spectra of polymer electrolytes (PEC-LiTFSI 100 mol%, PTMC-LiTFSI 100 mol% and PEC₆PTMC₄-LiTFSI *n* mol%) in the stretching vibration region of the free and interacting C=O groups.

3-4 Conclusions

In this study, a simple blend electrolyte consisting of amorphous PEC and PTMC with LiTFSI and LiFSI was prepared and their thermal and ion-conductive properties were analyzed. PEC and PTMC are immiscible with each other even though they have similar chemical structures. DSC measurements were carried out in order to observe the compatibility of PEC and PTMC mixtures, and two glass transition curves delivered from the original polymers were confirmed by all polymer mixture compositions. However, PEC and PTMC changed to a miscible system upon adding Li salts, the two glass transition curves became weaker, and merged into a single curve with further addition of Li salts. Moreover, the ionic conductivity of blend electrolytes increase with increasing salt concentration. In case of PEC₆PTMC₄-LiTFSI 100 mol%, the ionic conductivity shows a value as high as $10^{-6} \text{ S} \cdot \text{cm}^{-1}$ at 50 °C. Simultaneously, the value of T_{d5} for PEC₆PTMC₄-LiTFSI electrolyte increased slightly with increasing LiTFSI and PTMC contents. It is clear that the interaction between C=O groups and Li⁺ gives rise to a compatible amorphous phase of PEC and PTMC.

Additionally, PEC and PTMC with LiFSI electrolytes were also prepared and analyzed. Both PEC and PTMC single-polymer electrolytes reveal increasing ionic conductivity with increasing LiFSI salt concentration. Meanwhile, the glass transition temperature of PTMC-based electrolytes showed an increase with increasing salt concentration in the low-concentration regime, but a decrease in the concentrated regime. All of the PEC and PTMC blend electrolytes with LiFSI 150 mol%, show higher ionic conductivity than LiTFSI system which is the order of $10^{-5} \text{ S cm}^{-1}$ at 50 °C and the ionic conductivity increases slightly with increasing PEC content. The electrochemical investigation revealed t_+ values of more than 0.6 for both PEC and PTMC single-polymer electrolytes, but the PEC₆PTMC₄-LiFSI 150 mol% electrolyte has as high as 0.73 at 50 °C.

References

- [1] Z. Gadjourova, Y.G. Andreev, D.P. Tunstall, P.G. Bruce, Ionic conductivity in crystalline polymer electrolytes, *Nature*. **412** (2001) 520–523.
- [2] F. Croce, L. Settimi, B. Scrosati, Superacid ZrO₂-added, composite polymer electrolytes with improved transport properties, *Electrochem. Commun.* **8** (2006) 364–368.
- [3] B. Scrosati, F. Croce, S. Panero, Progress in lithium polymer battery R&D, *J. Power Sources*. **100** (2001) 93–100.
- [4] H.A. Every, F. Zhou, M. Forsyth, D.R. MacFarlane, Lithium ion mobility in poly(vinyl alcohol) based polymer electrolytes as determined by ⁷Li NMR spectroscopy, *Electrochim. Acta*. **43** (1998) 1465–1469.
- [5] M. Forsyth, S. Jiazeng, D.R. MacFarlane, Novel high salt content polymer electrolytes based on high, *Electrochim. Acta*. **45** (2000) 1249–1254.
- [6] S. Zhang, Z. Chang, K. Xu, C.A. Angell, Molecular and anionic polymer and oligomer systems with microdecoupled conductivities, *Electrochim. Acta*. **45** (2000) 1229–1236.
- [7] J. J.LaceyTimBowdenDanielBrandell, PPS(2017)_Beyond PEO—Alternative Host Materials for Li⁺-Conducting Solid Polymer Electrolytes.pdf, (2017).
- [8] S.N. M. Z. A. Munshi, B. B. Owens, Measurement of Li⁺ Ion Transport Number in Poly(ethylene oxide)-LiX complexes, *Polym. J.* **20** (1988) 597–602.
- [9] X. Zhang, P.S. Fedkiw, Ionic Transport and Interfacial Stability of Sulfonate-Modified Fumed Silicas as Nanocomposite Electrolytes, *J. Electrochem. Soc.* **152** (2005) A2413–A2420.
- [10] M.A. Ratner, D.F. Shriver, Ion Transport in Solvent-Free Polymers, *Chem. Rev.* **88** (1988) 109–124.
- [11] L.C. Rodrigues, M.M. Silva, M.J. Smith, Synthesis and characterization of amorphous

- poly(ethylene oxide)/poly(trimethylene carbonate) polymer blend electrolytes, *Electrochim. Acta.* **86** (2012) 339–345.
- [12] I. Nicotera, L. Coppola, C. Oliviero, M. Castriota, E. Cazzanelli, Investigation of ionic conduction and mechanical properties of PMMA-PVdF blend-based polymer electrolytes, *Solid State Ionics.* **177** (2006) 581–588.
- [13] L. Yu, K. Dean, L. Li, Polymer blends and composites from renewable resources, *Prog. Polym. Sci.* **31** (2006) 576–602.
- [14] D. Zhang, L. Zhang, K. Yang, H. Wang, C. Yu, D. Xu, B. Xu, L.M. Wang, Superior Blends Solid Polymer Electrolyte with Integrated Hierarchical Architectures for All-Solid-State Lithium-Ion Batteries, *ACS Appl. Mater. Interfaces.* **9** (2017) 36886–36896.
- [15] W.-T. Whang, C.-L. Lu, Effects of polymer matrix and salt concentration on the ionic conductivity of plasticized polymer electrolytes, *J. Appl. Polym. Sci.* **56** (1995) 1635–1643.
- [16] Y.-Z.M. Xiao-Yuan Yu, Min Xiao, Shuang-Jin Wang, Qi-Qiang Zhao, Fabrication and characterization of PEO/PPC polymer electrolyte for lithium-ion battery, *J. Appl. Polym. Sci.* **115** (2010) 2718–2722 456.
- [17] Y. Tominaga, K. Yamazaki, Fast Li-ion conduction in poly(ethylene carbonate)-based electrolytes and composites filled with TiO₂ nanoparticles, *Chem. Commun.* **50** (2014) 4448–4450.
- [18] Z. Li, H. Matsumoto, Y. Tominaga, Composite poly(ethylene carbonate) electrolytes with electrospun silica nanofibers, *Polym Adv Technol.* **29** (2018) 820–824.
- [19] B. Sun, J. Mindemark, K. Edström, D. Brandell, Polycarbonate-based solid polymer electrolytes for Li-ion batteries, *Solid State Ionics.* **262** (2014) 738–742.
- [20] B. Sun, J. Mindemark, K. Edström, D. Brandell, Realization of high performance polycarbonate-based Li polymer batteries, *Electrochem. Commun.* **52** (2015) 71–74.

- [21] J. Evans, C.A. Vincent, P.G. Bruce, Electrochemical measurement of transference numbers in polymer electrolytes, *Polymer (Guildf)*. **28** (1987) 2324–2328.
- [22] H. Kim, F. Wu, J.T. Lee, N. Nitta, H.T. Lin, M. Oschatz, W. Il Cho, S. Kaskel, O. Borodin, G. Yushin, In situ formation of protective coatings on sulfur cathodes in lithium batteries with LiFSI-based organic electrolytes, *Adv. Energy Mater.* **5** (2015) 1–8.
- [23] I.A. Shkrob, T.W. Marin, Y. Zhu, D.P. Abraham, Why bis(fluorosulfonyl)imide is a “magic anion” for electrochemistry, *J. Phys. Chem. C*. **118** (2014) 19661–19671.
- [24] J. Qian, W.A. Henderson, W. Xu, P. Bhattacharya, M. Engelhard, O. Borodin, J.-G. Zhang, High rate and stable cycling of lithium metal anode, *Nat. Commun.* **6** (2015) 6362.
- [25] K. Kimura, J. Motomatsu, Y. Tominaga, Correlation between Solvation Structure and Ion-Conductive Behavior of Concentrated Poly(ethylene carbonate)-Based Electrolytes, *J. Phys. Chem. C*. **120** (2016) 12385–12391.
- [26] Z. Li, R. Mogensen, J. Mindemark, T. Bowden, D. Brandell, Y. Tominaga, Ion-Conductive and Thermal Properties of a Synergistic Poly(ethylene carbonate)/Poly(trimethylene carbonate) Blend Electrolyte, *Macromol. Rapid Commun.* **39** (2018).
- [27] J. Li, C. Ma, M. Chi, C. Liang, N.J. Dudney, Solid electrolyte: The key for high-voltage lithium batteries, *Adv. Energy Mater.* **5** (2015) 1–6.
- [28] J.K. Kim, Y.J. Lim, H. Kim, G.B. Cho, Y. Kim, A hybrid solid electrolyte for flexible solid-state sodium batteries, *Energy Environ. Sci.* **8** (2015) 3589–3596.
- [29] D. Santhanagopalan, D. Qian, T. McGilvray, Z. Wang, F. Wang, F. Camino, J. Graetz, N. Dudney, Y.S. Meng, Interface Limited Lithium Transport in Solid-State Batteries, *J. Phys. Chem. Lett.* **5** (2014) 298–303.
- [30] T. Morioka, K. Nakano, Y. Tominaga, Ion-Conductive Properties of a Polymer

- Electrolyte Based on Ethylene Carbonate/Ethylene Oxide Random Copolymer, *Macromol. Rapid Commun.* **38** (2017) 1–5.
- [31] K. Kimura, H. Matsumoto, J. Hassoun, S. Panero, B. Scrosati, Y. Tominaga, A Quaternary Poly(ethylene carbonate)-Lithium Bis(trifluoromethanesulfonyl)imide-Ionic Liquid-Silica Fiber Composite Polymer Electrolyte for Lithium Batteries, *Electrochim. Acta.* **175** (2015) 134–140.
- [32] J. Mindemark, B. Sun, E. Törmä, D. Brandell, High-performance solid polymer electrolytes for lithium batteries operational at ambient temperature, *J. Power Sources.* **298** (2015) 166–170.
- [33] J. Wang, Y. Wu, X. Xuan, H. Wang, Ion-molecule interactions in solutions of lithium perchlorate in propylene carbonate + diethyl carbonate mixtures: An IR and molecular orbital study, *Spectrochim. Acta Part A Mol. Biomol. Spectrosc.* **58** (2002) 2097–2104.
- [34] J. Motomatsu, H. Kodama, T. Furukawa, Y. Tominaga, Dielectric relaxation behavior of a poly(ethylene carbonate)-lithium bis-(trifluoromethanesulfonyl) imide electrolyte, *Macromol. Chem. Phys.* **216** (2015) 1660–1665.

Chapter 4

Electrochemical characterization and battery performance of concentrated polycarbonate-based composite electrolytes

4-1 Introduction

As mentioned in the chapter 1, solid-state lithium batteries (SSLBs) have attracted a great deal of attention, since they are safer, better thermal and electrochemical stabilities than those of typical Li batteries using liquid electrolytes.^[1-5] Solid electrolyte is obviously a key for development of SSLBs, and it mainly can be classified into two types, which are inorganic ceramic and organic polymer electrolytes (solid polymer electrolytes (SPEs)). Inorganic electrolytes exhibit high ionic conductivity exceeding the order of $10^{-2} \text{ S}\cdot\text{cm}^{-1}$ at ambient temperature.^[3] However, problems on the interface between electrolyte and electrode and complex manufacturing process are big issues for battery application.^[6-8] In contrast, SPEs can solve these problems because of its flexible properties.^[9] Moreover, SPEs have been praised as safe electrolytes for application in SSLBs due to their advantages of nonvolatility, no leakage, and suppression of Li dendrites.^[10-12]

Recently, polycarbonates such as poly(ethylene carbonate) and poly(trimethylene carbonate), are attracting much attentions as new hosts for SPEs because their electrolytes exhibit completely different ion-conductive behavior and high cation-conductive properties compared with typical polyether-based electrolytes.^[13-15] Furthermore, polycarbonate-based electrolytes reveal good electrochemical stabilities, such as anodic oxidation stability up to 5 V and protecting cathode current collector.^[16,17] However, further improvement in the conductivity, thermal stability and mechanical properties are still needed for the application of long-term stable polymer batteries.

In the study of the chapter 2, the PEC-based electrolytes filled with silica nanofiber (SNF) have investigated for improving electrolyte properties. The ionic conductivity, thermal stability and mechanical properties were actually improved by addition of SNFs. Moreover, in the study of chapter 3, PEC and PTMC blend electrolyte have investigated and revealed better

electrochemical properties and stable thermal properties than their single polymer electrolytes. Therefore, the possibility to take advantage of the PEC-based electrolyte filled with SNF and PEC/PTMC blend electrolyte for SSLBs were thus considered in this chapter.

In addition, a suitable Li salt exploration for SPEs is one of important key point. Recently, lithium bis(fluorosulfonyl)imide (LiFSI) has been interested as appropriate conducting salt for Li^+ batteries due to its high ionic conductivity and capability of forming stable solid electrolyte interface (SEI) layers on various electrodes.^[18,19] The salt was also demonstrated a good electrochemical properties in the SPEs.^[14,19] This salt was therefore used and demonstrated good electrochemical properties in the SPEs.

For the cathode active material, LiFePO_4 (LFP) was used for the battery preparation in this chapter. The choice of LFP as active material comes from its excellent safety and structural stability. In addition, LFP is the most popular active material for lithium-ion batteries due to its cost effective, environmental benignity, well-defined performance, long-term stability, and accepted operating voltage platform.^[20,21] On the other hand, LFP delivers a low operating voltage (3.2 V) that the load on the electrolytes is relatively lower compared with those other active materials. Due to these reasons, LFP is one of the most used active materials for research on battery revolution of new electrolyte materials.

4-2 Experimental

4-2-1 Materials and electrolyte preparation

Poly(ethylene carbonate) (PEC; $M_w=238,000$, QPAC[®]25) was purchased from Empower Materials in USA. Poly(trimethylene carbonate) (PTMC; $M_w=300,000$) was synthesized by ring-opening polymerization by using $\text{Sn}(\text{Oct})_2$ as catalyst,^[16] was denoted by Prof. Daniel Brandell's group from Uppsala University, Sweden, and lithium bis(fluorosulfonyl)imide, (LiFSI; Kishida Chemical) battery grade was used. The chemical structures of PEC, PTMC, and LiFSI are presented in Figure 4-1. Anhydrous acetonitrile (electrochemical grade) was obtained from Kanto Chemical and used as received. The LiFSI concentration of electrolyte was set in 150 mol% and calculated by the monomer range of LiFSI and carbonyl group (C=O) units in the polymers ($([\text{Li}^+]/[\text{C}=\text{O}]) \times 100 = a \text{ mol}\%$). The silica nanofiber with an average diameter of 700 (SNF₇₀₀) was added in a mass ratio of the total electrolyte amount of 5 wt%. In the case of blend electrolytes, the ratio of PEC and PTMC blend was decided in their molar rate of C=O units and the PEC₆PTMC₄ mixture was carried out and analyzed in this chapter. Those materials of filler added and blend electrolytes were mixed in acetonitrile for around 8 hours at room temperature, electrolyte solutions were dried in a vacuum oven at 60 °C for 72 hours in order to eliminate all residual solvents. Then, highly homogeneous and free-standing electrolyte films obtained.

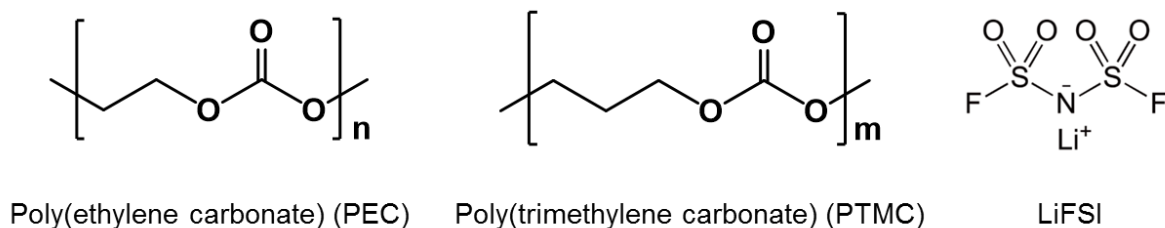
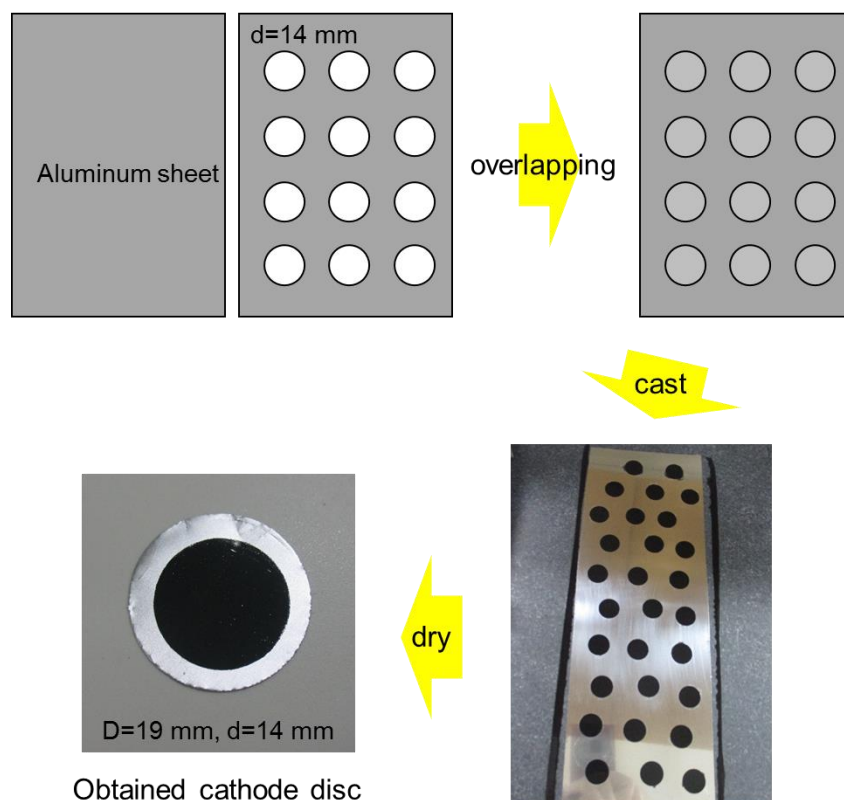


Figure 4-1. Chemical structures of PEC, PTMC, and LiFSI

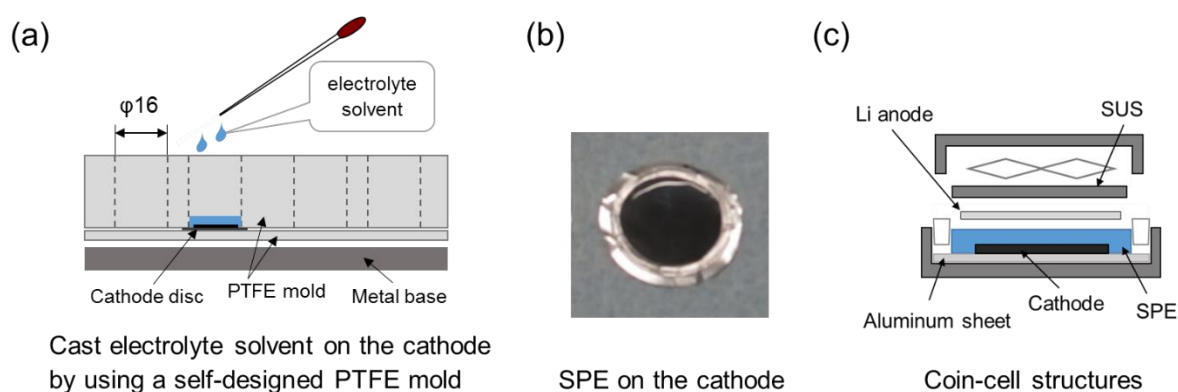
4-2-2 Coin-cell preparation

The commercial LiFePO_4 (LFP, Tatung Fine Chemicals Co., Taiwan) as active material, poly(vinylidene fluoride) (PVdF, KYNAR 741, ARKEMA Co., France) as binder and acetylene black (Denka Black[®], Denka Co., Japan) as conductive additive were used for preparing cathode. These materials were blended in the weight ratio of 90:6:4% in *N*-methyl-2-pyrrolidinone (NMP, > 99.5%, Kanto Chemical Co., Japan). The obtained slurry was casted on an overlapped Al current collector using doctor blade, and then dried for 8 hours at 85 °C for removing all residual solvents. Finally, the dried Al film cut out as 19 mm diameter Al with 14 mm circle-shape cathode materials in the center. The schematic image of the cathode electrode preparation is shown in Scheme 4-1. The obtained cathode disc was pressed at 3 MPa for several seconds before use.



Scheme 4-1. Schematic image of cathode electrode preparation procedure.

A self-designed PTFE mold was used for improving wettability of electrolyte/electrode interface, and preparing a homogeneous polymer electrolyte film on the cathode electrode. The LFP cathode disc which were mentioned above, was set into the PTFE mold and fixed with screws. Then, some amount of electrolyte solutions were casted into the mold (Scheme 4-2a) and dried under vacuum at 60 °C for 72 hours as same as the polymer electrolyte preparation process. A great homogeneous and easy handled SPE on the cathode with average electrolyte thickness of 110 μm was obtained as shown in Scheme 4-2b. A CR2032 coin-type half-cell using the electrolyte on the LFP cathode sample was prepared. As shown the structure images in the Scheme 4-1c, this coin-cell do not include any separators or spacers.



Scheme 4-2. Schematic image of coin-cell preparation procedure. (a) images of electrolyte solution casting process by using self-designed mold, (b) photograph of dried SPEs on the cathode disc, and (c) structure images of coin-cell used in this study.

4-2-3 Characterization

Galvanostatic cycling

Lithium stripping/deposition tests of Li/SPE/Li symmetric cells were performed by using coin-type cells (CR2032) to investigate the stability at the Li/SPE interface. A cut out polymer electrolyte membrane with 16 mm diameter, was simply sandwiched by two piece of circled Li foils ($d=15$ mm) without separator and sealed by coin-cell. The cell was kept in a thermostat which was set at 50 °C, and the measurement was carried out by a HJ1001SM8A battery test system (Hokuto Denko). The lithium stripping/deposition galvanostatic cycling measurement was performed by applying a constant current of 0.1 mA cm^{-2} with a step duration of 1 hour until 100 cycles. The voltage limit was set at +1 V and -1 V.

Electrochemical impedance spectroscopy (EIS)

The Li/electrolyte interface resistance of original polymer electrolytes upon cell storage were analyzed by performing EIS tests on symmetrical Li/SPE/Li coin-type cells. A cut out polymer electrolyte membrane was sandwiched by Li foil electrode without separator, and the EIS was performed by applying signal amplitude voltage of 30 mV in the frequency range 100 mHz to 7 MHz using a potentiostat/galvanostat SP-200 (Bio-Logic Instrument) at 50 °C. The stainless steel as electrode SS/SPE/SS coin cells were also carried out for the comparative analysis and their EIS were also performed in the same measurement condition.

Battery test

The CR2032 coin-type half-cell using LFP as cathode active material was assembled for the battery test. The galvanostatic charge-discharge cycling tests were performed using a

HJ1001SM8A battery test system at 50 °C. All cells were kept at 50 °C for 12 hours before battery tests and electrochemically activated by a galvanostatic cycle rate at C/20, C/10, and C/5 ($1C = 170 \text{ mA h g}^{-1}$) within a cutoff voltage of 2.5 to 4.0 V.

4-3 Results and discussion

4-3-1 Electrochemical stabilities

Lithium stripping/deposition stability

In Li metal batteries, electrolytes, solvents and salts react with exposed Li during battery cycling, resulting in consumption of electrolyte and formation of detrimental degradation layers and Li dendrites on the surface of the anode that degrade the batteries.^[22-24] The battery performance is therefore influenced directly by the interfacial stability between the Li metal anode and the electrolyte. A comparison of the electrochemical features for PEC, PTMC, and PEC₆PTMC₄-LiFSI 150 mol% in terms of the Li/electrolyte interface stability is shown in Figure 4-2. At early stages of cycling for cells with both PEC and PTMC electrolytes, very unstable voltage profiles appear with high overpotentials, which means poor interfacial stability between Li metal anode and electrolyte (Figure 4-2a and b). However, these voltage profiles became stable after cycling more than 10 hours. The polymer in concentrated electrolytes may decompose to cyclic carbonate and various other degradation products through the reaction with Li metal under continuously applied current during the electrochemical cycling.^[23,25] The concentrated polycarbonate-based electrolytes have many benefits such as excellent Li-ion transportation, wide electrochemical window and corrosion prevention of Al current collector,^[14,26,27] but the polymer decomposition is one of the issues that need to be resolved. In contrast to both original polymer electrolytes, the blend electrolyte shown in Figure 4-2c displayed a stable voltage profile, the PEC₆PTMC₄-LiFSI 150 mol% cell maintains a polarization as low as 5 mV. This result clearly demonstrates that the PEC₆PTMC₄ electrolyte has better interfacial stability against the Li anode and a more stable solid electrolyte interphase (SEI) than that of the original electrolyte system which can mitigate the degradation upon cycling.

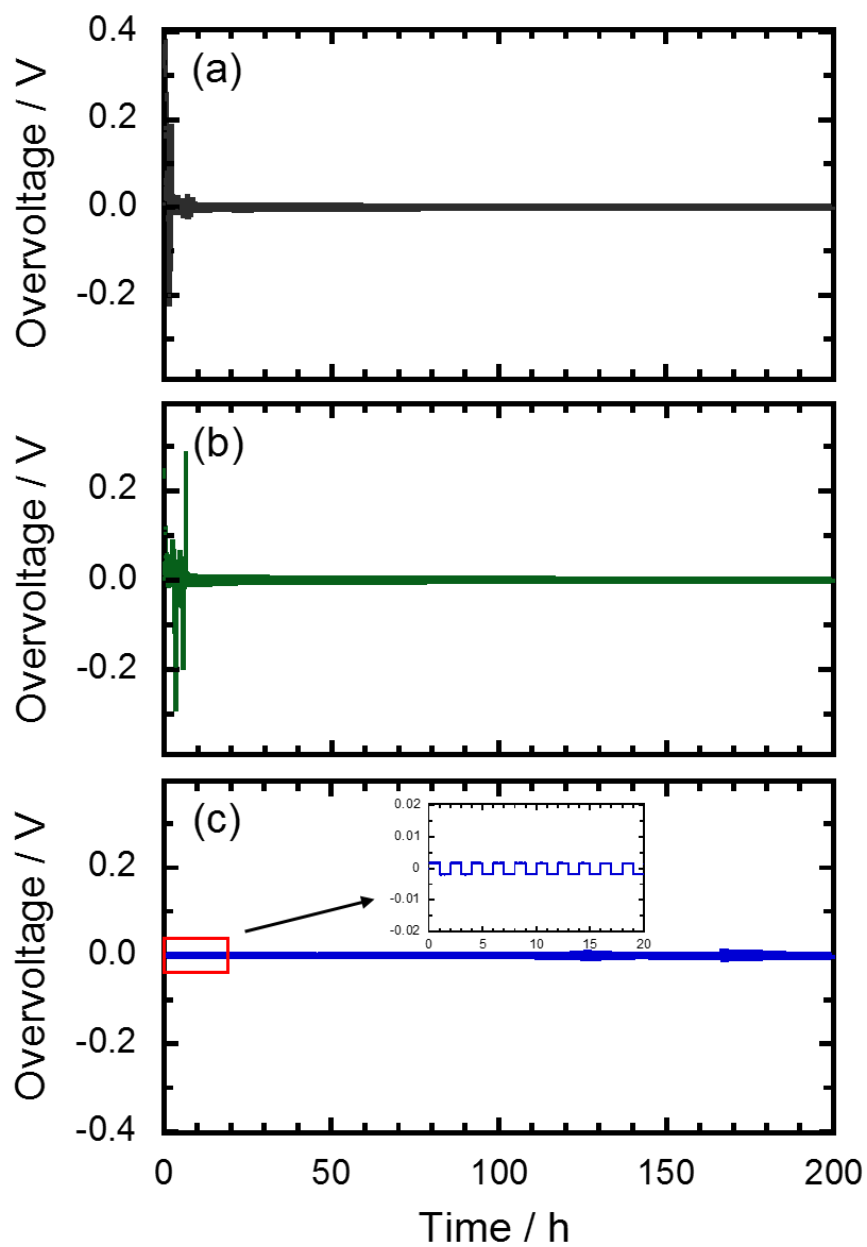


Figure 4-2. Lithium stripping/deposition tests for (a) PEC-LiFSI 150 mol%, (b) PTMC-LiFSI 150 mol%, and (c) PEC₆PTMC₄-LiFSI 150 mol% electrolytes in symmetrical Li/Li cells at a constant current of 0.1 mA cm⁻² (voltage limit: +1 V – -1 V; step time 1 hour each).

Li/electrolyte interfacial impedance stability

In order to investigate the stability between the Li anode and three kinds of electrolytes, impedance analysis was further carried out. Electrolytes aging storage stabilities were analyzed before investigate the Li/electrolyte interfacial impedance stabilities. Figure 4-3 shows the Nyquist plots related to EIS measurements of cells using PEC, PTMC, and PEC₆PTMC₄-LiFSI 150 mol% electrolytes, performed during storage of SS/SPE/SS coin cells at 50 °C. For the fresh cells at 0 h, there is only a single semicircle due to the bulk resistance was observed for all electrolytes. However, another semicircle at lower frequency due to the interfacial resistance between SS electrode and electrolyte is clearly appeared after more than 10 hours for PTMC (Figure 4-3b) and PEC₆PTMC₄ blend electrolytes (Figure 4-3c). In contrast, the interfacial resistance derived semicircle is scarcely seen in the PEC electrolyte (Figure 4-3a). It turns out that the interfacial semicircle appeared at the PEC₆PTMC₄ blend electrolyte was derived from that of the PTMC system. The reason is not known yet, but it is also can be considered that PTMC electrolyte system is easy to make interfacial resistance with SS electrode during the storages. In addition, no changes in the bulk resistance for any of the electrolytes have been observed with increasing time, which indicates no bulk degradation and reaction occur during measurement.

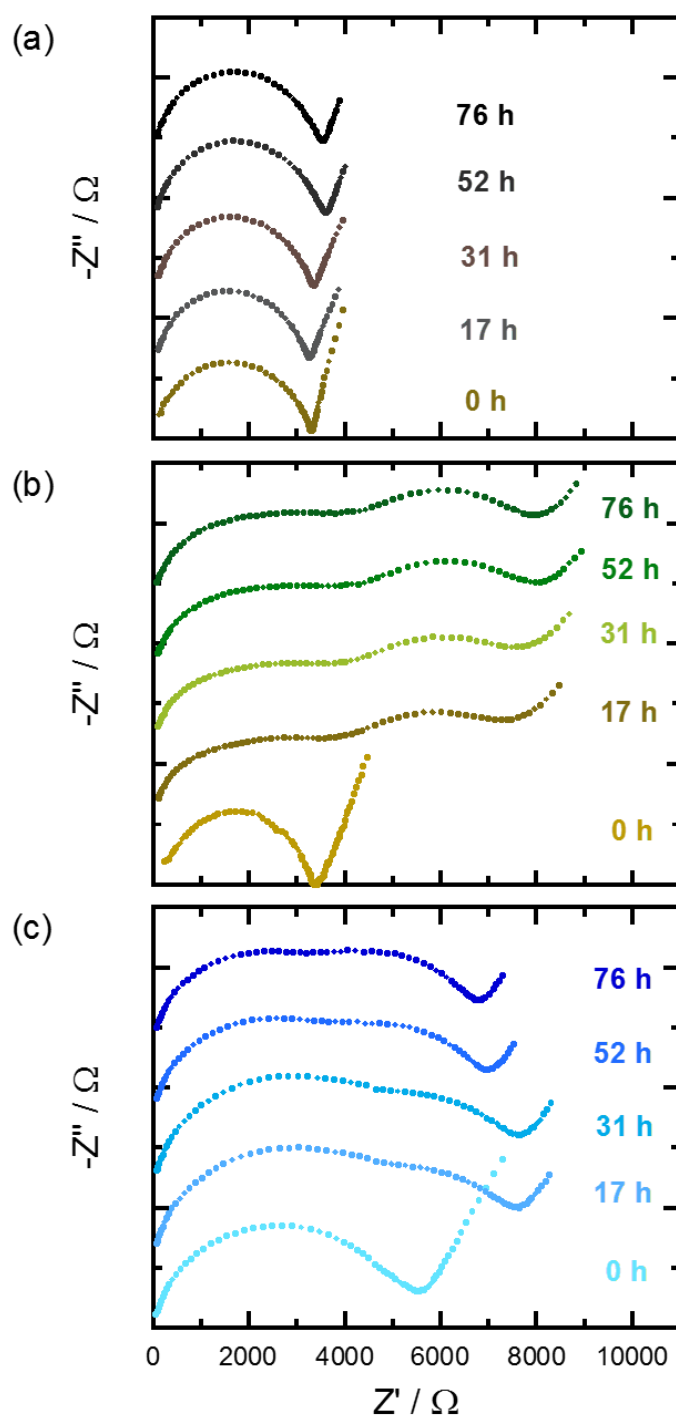


Figure 4-3. Nyquist plots related to EIS measurements performed during storage of SS|SPE|SS symmetrical cells using (a) PEC-LiFSI 150 mol%, (b) PTMC-LiFSI 150 mol%, and (c) PEC₆PTMC₄-LiFSI 150 mol% electrolytes at 50 °C.

The stability of the Li/electrolyte interface under static condition, that is, chemical stability, is also one of important electrolyte properties for using batteries. In case of the Li/SPE/Li cell, the bulk and interfacial resistances during storage of PEC, PTMC, and PEC₆PTMC₄-LiFSI 150 mol% electrolytes are also investigated without current flowing and the data are summarized in Figure 4-4, all corresponding Nyquist plots performed by EIS measurements are shown in Figure 4-5. Certain increases in both bulk and interfacial resistances have been observed in all electrolytes for first 17 hours. This may indicate that something have been led the electrolyte decomposition and increase the bulk resistance of the electrolyte by connecting Li electrode to the concentrated electrolytes,^[28,29] which mean the instability between Li electrode and concentrated electrolytes. As seen in Figure 4-4a, both original electrolytes exhibit a continuous increase in the bulk resistance, especially the PEC-based electrolyte reveals a significant increase. This may explain that PEC-based concentrated electrolytes have poor chemical stability with Li anode than PTMC-based systems. In contrast to both PEC and PTMC original electrolytes, the PEC₆PTMC₄ blend electrolyte has almost constant value after 17 hours. The change in the interfacial resistance for all electrolytes is similar with the bulk, and the PEC-based electrolyte exhibits significant increase in both resistances compared with the other systems (Figure 4-4b). This may be due to the poor chemical stability of electrolyte, give rise to further instability between electrolyte and Li electrode. On the other hand, the blend electrolyte has a relatively stable resistance changes exhibiting the lowest values. It can be considered that there may have advantageous interactions in between PEC, PTMC, and Li salt to improvement of the properties of polycarbonate blend electrolytes. Therefore, the combination of PEC and PTMC could improve the stability of the electrolyte on the Li electrode.

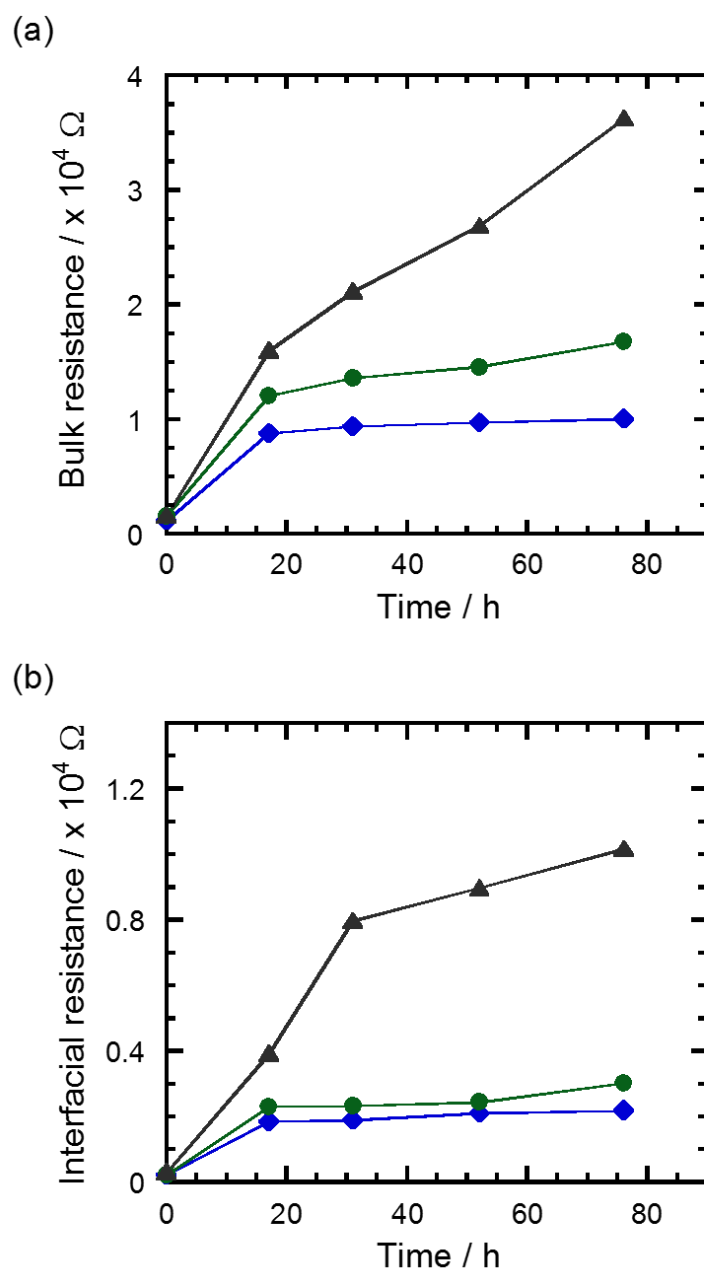


Figure 4-4. Changes of (a) bulk resistance and (b) interfacial resistance of Li|SPE|Li cells for PEC-LiFSI 150 mol% (▲), PTMC-LiFSI 150 mol% (●), and PEC₆PTMC₄-LiFSI 150 mol% (◆) electrolytes at 50 °C.

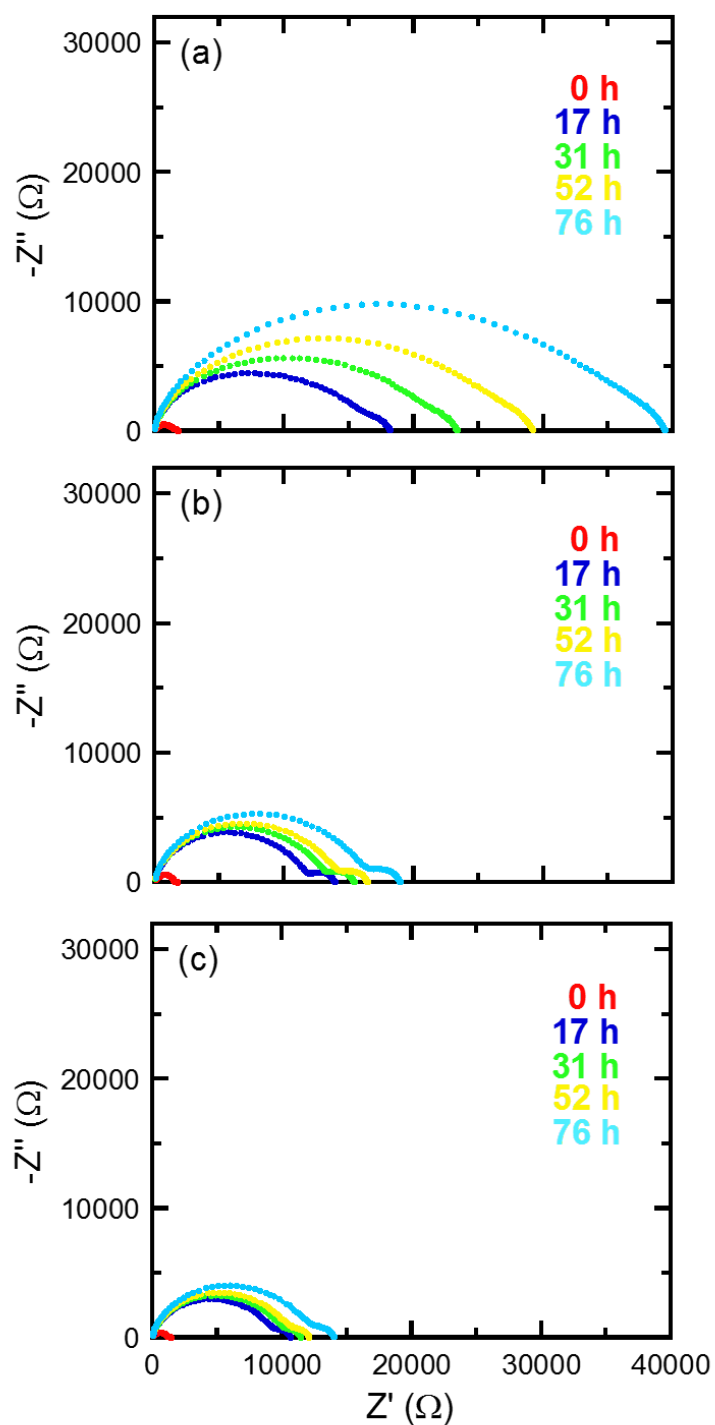


Figure 4-5. Nyquist plots of Li|SPE|Li symmetrical cells using (a) PEC-LiFSI 150 mol%, (b) PTMC-LiFSI 150 mol%, and (c) PEC₆PTMC₄-LiFSI 150 mol% electrolytes at 50 °C. EIS performed by applying an alternate voltage signal with amplitude of 30 mV within the frequency range from 100 mHz to 7 MHz.

4-3-2 Battery performance of Li/LiFePO₄ cells

Figure 4-6 shows galvanostatic charge-discharge properties of LFP/SPE/Li cells based on PEC, PTMC, and PEC₆PTMC₄-LiFSI 150 mol% electrolytes at 50 °C. The cell with the PEC-based electrolyte delivers a discharge capacity of approximately 160 mAh g⁻¹ in the first cycle (Figure 4-6a). However, a decrease in the capacity was observed, which is mainly due to the degradation in the concentrated electrolyte. A similar behavior was also confirmed from the Li/electrolyte impedance analysis as shown in Figure 4a. The cell with the PTMC-based electrolyte also exhibits a reversible capacity approaching to 140 mAh g⁻¹ at the first cycle and increased a while (Figure 4-6b), and the same tendency has observed in a previous work.^[30] It have been explained above that PTMC-based electrolytes are easier to make interface resistance with electrode (Figure 4-6b) and this behavior might be the reason of increasing capacities in the first few cycles. However, these data are comparable to those of PEC- and PTMC- based electrolytes reported previously.^[26,30] In contrast, the cell with the blend electrolyte reveals the most stable charge-discharge performance and the initial capacity approached 150 mAh g⁻¹, which is 88% of the theoretical value. Indeed, these data are probably due to a combination of the formation of a stable Li/electrolyte interface and a good interface with the LFP cathode, induced by the blend of PEC and PTMC, as confirmed by the galvanostatic tests in Figure 4-2 as well as by the EIS in Figure 4-3. Moreover, the extended cycle performance of PEC, PTMC, and blend electrolyte cells are shown in Figure 4-7. Both original electrolytes have large decreases in the capacity at around 10 cycles and the cells exhibit poor cycle stability. On the other hand, the cell with blend electrolyte exhibit better and stable cycle performance compared with the both original electrolytes more than 20 cycles. It has been confirmed that the combination of PEC and PTMC improved interface between Li electrode and electrolyte, as well as stripping/deposition of the original electrolytes. Therefore, the effects of the blend electrolyte are also demonstrated at the battery performance.

The different polymer composition and salt concentration have also prepared and tested for battery cells in this chapter. The galvanostatic charge-discharge curves of LFP/SPE/Li cells based on PEC, PTMC, and PEC₈PTMC₂-LiFSI 127 mol% electrolytes and cycle performance of the blend electrolyte cell at 50 °C were shown in Figure 4-8. A similar battery performance behaviors with above mentioned electrolytes were obtained. Those cells with the PEC- and PTMC-based electrolytes showed very poor charge-discharge curves just in 5 cycles. In the case of PEC-based electrolyte, the overcharge and deterioration of cell have happened at the 5th cycle. In the case of PTMC-based electrolyte, it unable to maintain the stability of charge-discharge properties. The cell with the PEC₈PTMC₂-LiFSI 127 mol% electrolyte delivers a discharge capacity of approximately 150 mAh g⁻¹ at the C/20 cycle rate and reveals the most stable charge-discharge curves. However, the charge and discharge capacity at C/5 displayed a poor behavior, but recovered again at the C/10 cycle rate (Figure 4-8d). This may the rapid ion transportation was suppressed due to the low conductivity of the blend electrolyte. These studies indicate that polycarbonate blend electrolytes can improvement of defects of single polymer electrolytes, whereas the ion-conductive properties still needed to further improve for practical realization.

In addition, the SNF filled in PEC-based composite electrolyte for battery cells have been done as well. Figure 4-9 and Figure 4-10 shown galvanostatic charge-discharge properties and cycle performance of LFP/SPE/Li cells with PEC-LiFSI 120 mol% and SNF 5 wt% electrolytes at 50 °C. As results, both original PEC-based electrolyte and SNF composite electrolyte exhibits poor charge and discharge properties. In the case of PEC-based electrolyte, the cell shows discharge capacity of roughly 140 mAh g⁻¹ at the C/10 cycle rate in the first cycle, and charging and discharging were ceased due to the deterioration and decomposition of PEC-based electrolyte for only 10 cycles (Figure 4-9a and Figure 4-10a). In the case of the electrolyte filled with SNF, the overcharge was appeared from the first charge, but the discharge capacity still shows at

around 120 mAh g⁻¹ in the first cycle and decreases for a while (Figure 4-9b). In general, if overcharging occurs, the battery could not work in a while due to the deterioration and decomposition of the electrolyte (Figure 4-10b and Figure 4-7a). Nevertheless, the battery cell with SNF filled electrolyte was able to go through charging and discharging up to 90 cycles, even the cell shows very unstable performance properties during all cycles (Figure 4-10b). In the chapter 2, it has been explained that filled with SNF can improve not only the ionic conductivity, but also electrochemical stability. These effects of SNF may protect or prevent the electrolyte from the complete deterioration and keep the cell working further. However, the composite electrolyte filled with SNF still has many problems need to be improved for using in all-solid- state batteries, such as dispersibility of SNF in the electrolyte, the best SNF content for batteries and so on.

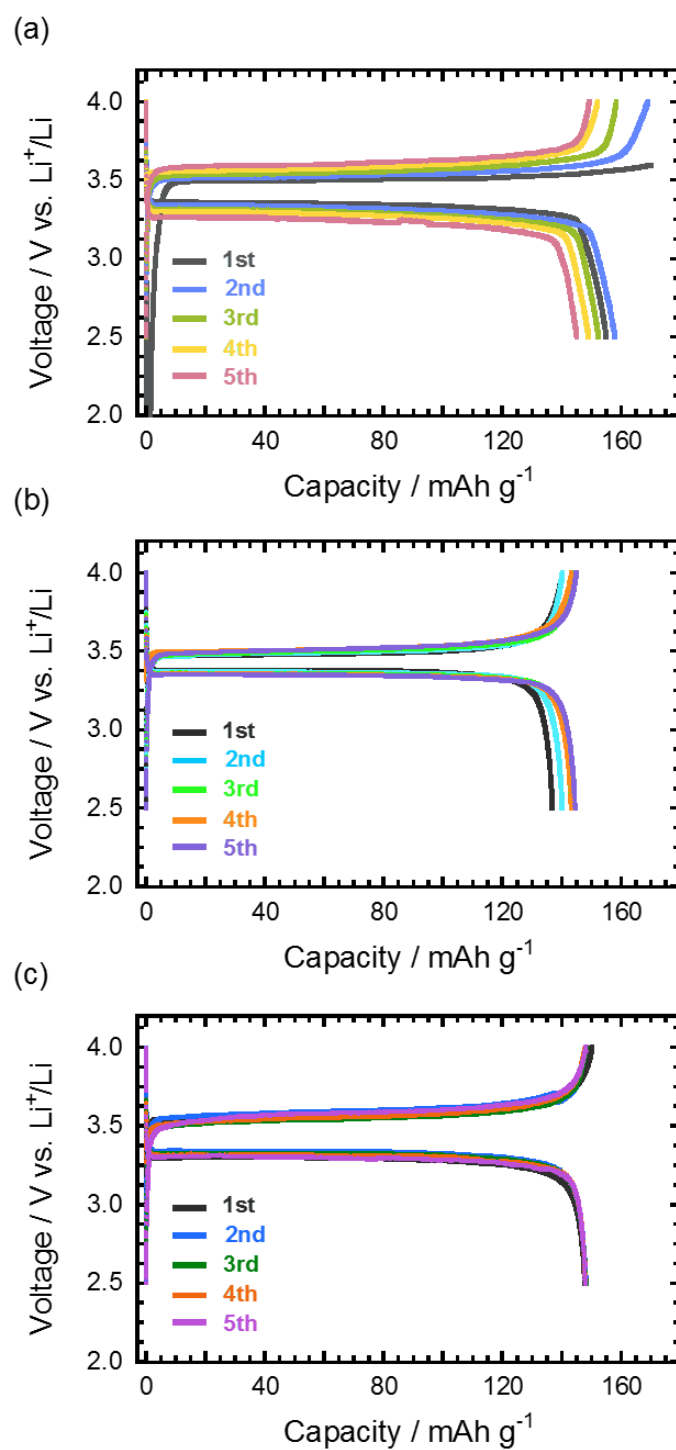


Figure 4-6. Galvanostatic charge-discharge curves of LFP|SPE|Li cells: (a) PEC-LiFSI 150 mol%, (b) PTMC-LiFSI 150 mol%, and (c) PEC₆PTMC₄-LiFSI 150 mol% cells at C/10 rate (1 C = 170 mA g⁻¹) and 50 °C.

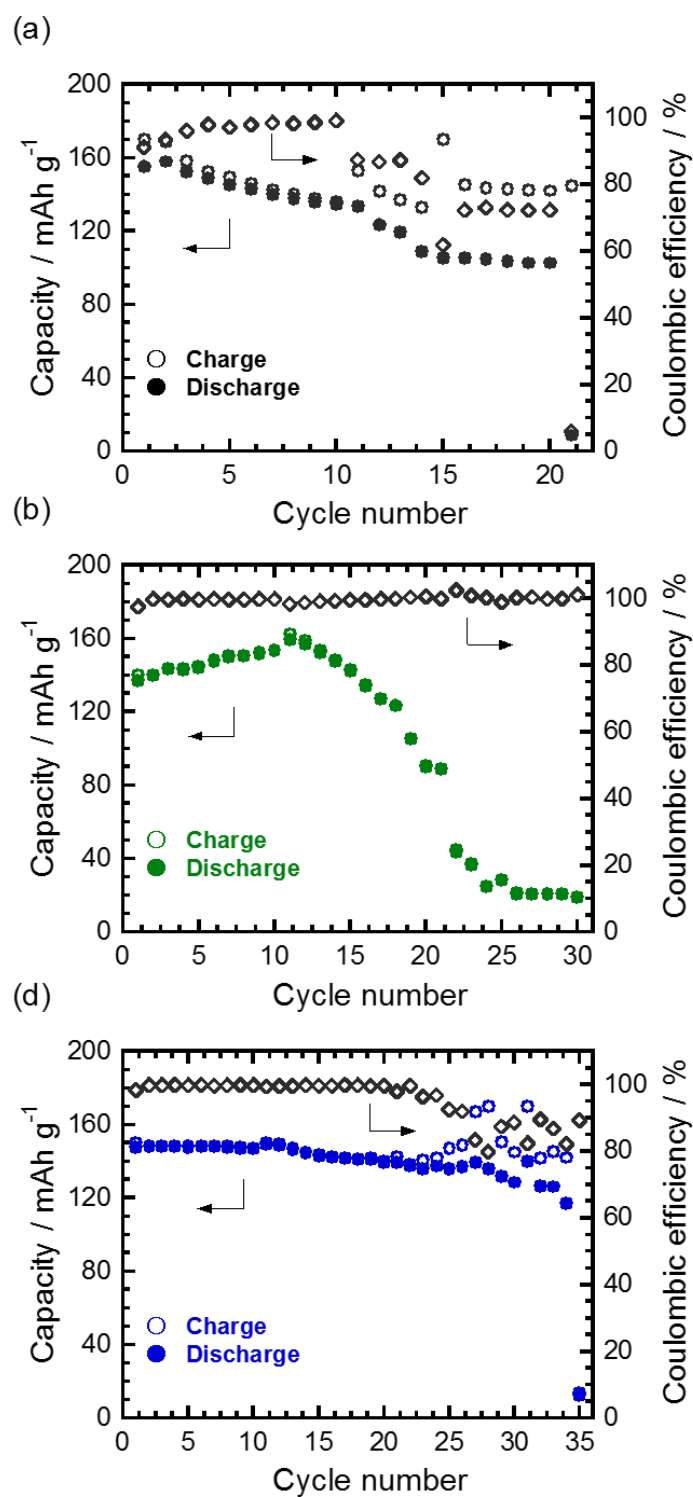


Figure 4-7. Galvanostatic charge-discharge cycle performance of LFP|SPE|Li cells: (a) PEC-LiFSI 150 mol%, (b) PTMC-LiFSI 150 mol%, and (c) PEC₆PTMC₄-LiFSI 150 mol% cells at C/10 rate (1 C = 170 mA g⁻¹) and 50 °C.

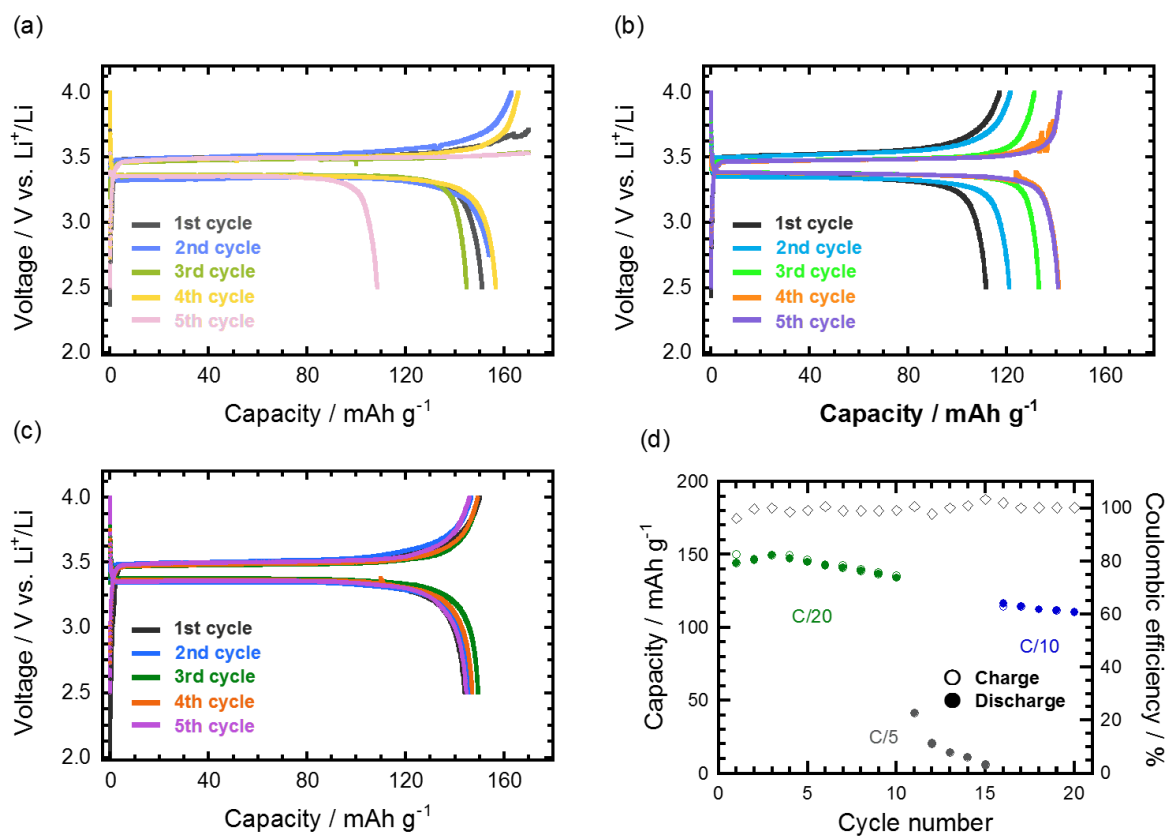


Figure 4-8. Galvanostatic charge-discharge curves of LFP|SPE|Li cells: (a) PEC-LiFSI 127 mol%, (b) PTMC-LiFSI 127 mol%, and (c) PEC₈PTMC₂-LiFSI 127 mol%, and (d) cycle performance of Li|PEC₈PTMC₂-LiFSI 127 mol%|LFP cells at C/20 rate (1 C = 170 mAh g⁻¹) and 50 °C.

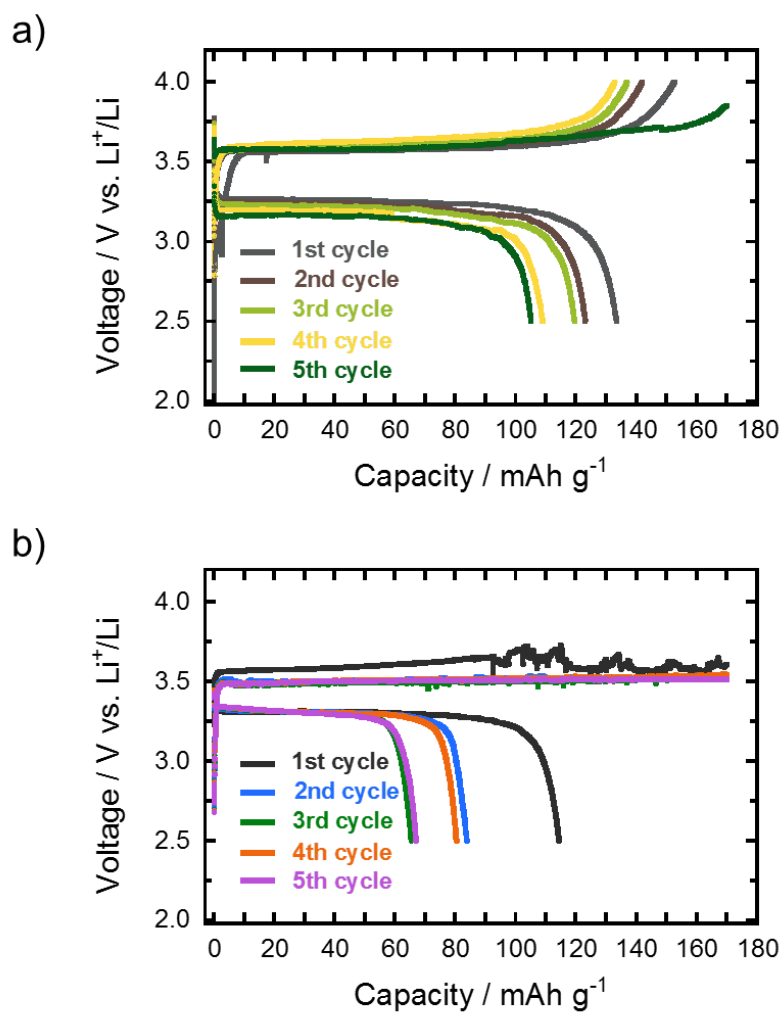


Figure 4-9. Galvanostatic charge-discharge curves of LFP|SPE|Li cells: (a) PEC-LiFSI 120 mol%, (b) PEC-LiFSI 120 mol%-SNF 5 wt% cells at C/10 rate ($1\text{ C} = 170\text{ mA g}^{-1}$) and $50\text{ }^{\circ}\text{C}$.

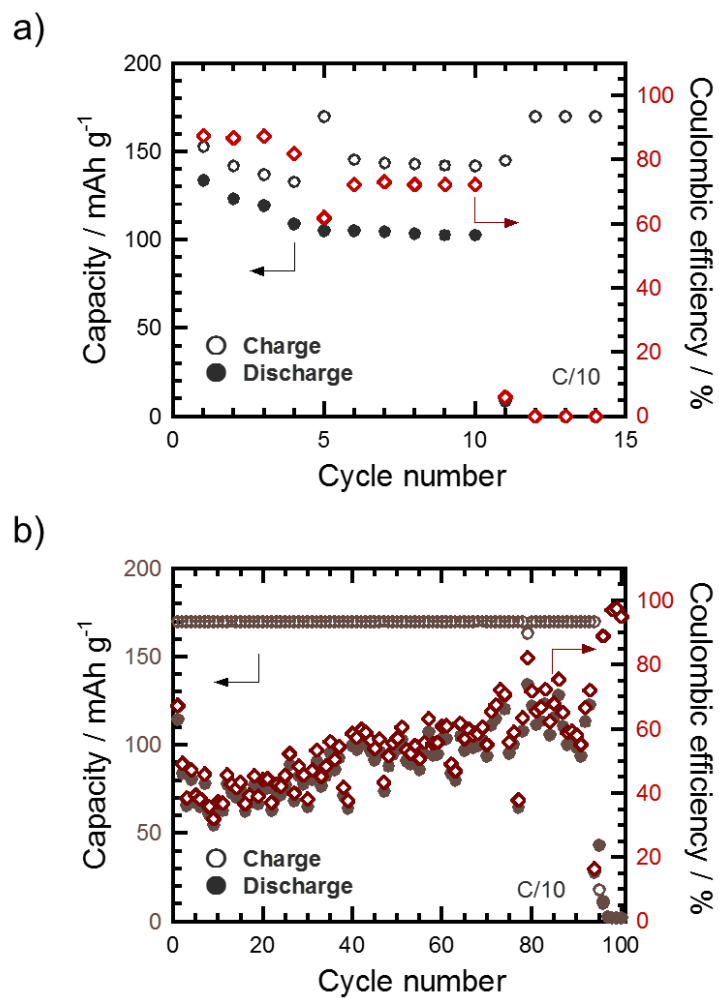


Figure 4-10. Galvanostatic charge-discharge cycle performance of LFP|SPE|Li cells: (a) PEC-LiFSI 120 mol%, (b) PEC-LiFSI 120 mol%-SNF 5 wt% cells at C/10 rate (1 C = 170 mA g⁻¹) and 50 °C.

4-4 Conclusions

In this chapter, high concentration PEC/PTMC blend electrolyte and PEC-based electrolytes filled with SNF were prepared and investigated for all-solid-state LFP/SPE/Li cells. Furthermore, highly concentrated polymer electrolytes of PEC, PTMC, and their mixture with LiFSI were investigated for Li/electrolyte interfacial and electrochemical stability. The PEC₆PTMC₄-LiFSI 150 mol% electrolyte demonstrated better the Li/electrolyte electrochemical and interfacial stability than that of PEC and PTMC single-polymer electrolytes. The LFP/SPE/Li cell with PEC and PTMC single-polymer electrolytes showed a very poor cycle performance, while the battery cell with PEC₆PTMC₄-LiFSI 150 mol% electrolyte exhibited better cycle stability than others and delivered a reversible charge-discharge capacity close to 150 mAh g⁻¹ at 50 °C and C/10 rate, which is 88% of the theoretical value (1 C = 170 mA h g⁻¹). On the other hand, the cell for PEC-based electrolyte filled with SNF revealed a better cycle life compare with original PEC-based electrolyte, but an extremely unstable and poor battery performances.

The present study also suggests that significant light on the potential of unexplored polycarbonate blend for SPE application. It has known that highly concentrated polycarbonate-based electrolytes exhibit better properties than that of typical electrolytes like higher conductivity, excellent t_+ , better electrochemical stability, and prevention of metal corrosion reaction simultaneously. However, there are also side effects due to the high concentration such as poor thermal and mechanical properties, deficiency of electrolyte stability and so on. This study of polycarbonate blend electrolyte demonstrate higher t_+ and better interfacial stabilities than that of both PEC- and PTMC-based concentrated electrolytes. Therefore, the PEC and PTMC blend electrolyte is more suitable for batteries than that of either original electrolytes. In addition, many recent reports have explained that SPEs are the optimal electrolyte for future of all-solid-state batteries, such as high capacity organic electrode batteries. The study of this

chapter suggests that the highly concentrated polycarbonate blend electrolytes may potentially be used for those future battery systems.

References

- [1] J.M. Tarascon, M. Armand, Issues and challenges facing rechargeable lithium batteries, *Nature*. **414** (2001) 359–367.
- [2] M. Armand, J.M. Tarascon, Building better batteries, *Nature*. **451** (2008) 2–7.
- [3] N. Kamaya, K. Homma, Y. Yamakawa, M. Hirayama, R. Kanno, M. Yonemura, T. Kamiyama, Y. Kato, S. Hama, K. Kawamoto, A. Mitsui, A lithium superionic conductor, *Nat. Mater.* **10** (2011) 682–686.
- [4] J. Li, C. Ma, M. Chi, C. Liang, N.J. Dudney, Solid electrolyte: The key for high-voltage lithium batteries, *Adv. Energy Mater.* **5** (2015) 1–6.
- [5] X. Fu, D. Yu, J. Zhou, S. Li, X. Gao, Y. Han, P. Qi, X. Feng, B. Wang, Inorganic and organic hybrid solid electrolytes for lithium-ion batteries, *CrystEngComm*. **18** (2016) 4236–4258.
- [6] H.W. Kim, P. Manikandan, Y.J. Lim, J.H. Kim, S.C. Nam, Y. Kim, Hybrid solid electrolyte with the combination of $\text{Li}_7\text{La}_3\text{Zr}_2\text{O}_{12}$ ceramic and ionic liquid for high voltage pseudo-solid-state Li-ion batteries, *J. Mater. Chem. A*. **4** (2016) 17025–17032.
- [7] J.K. Kim, Y.J. Lim, H. Kim, G.B. Cho, Y. Kim, A hybrid solid electrolyte for flexible solid-state sodium batteries, *Energy Environ. Sci.* **8** (2015) 3589–3596.
- [8] D. Santhanagopalan, D. Qian, T. McGilvray, Z. Wang, F. Wang, F. Camino, J. Graetz, N. Dudney, Y.S. Meng, Interface Limited Lithium Transport in Solid-State Batteries, *J. Phys. Chem. Lett.* **5** (2014) 298–303.
- [9] S. Muench, A. Wild, C. Friebe, B. Häupler, T. Janoschka, U.S. Schubert, Polymer-Based Organic Batteries, *Chem. Rev.* **116** (2016) 9438–9484.
- [10] V. Di Noto, S. Lavina, G.A. Giffin, E. Negro, B. Scrosati, Polymer electrolytes: Present, past and future, *Electrochim. Acta*. **57** (2011) 4–13.
- [11] D.T. Hallinan, N.P. Balsara, Polymer electrolytes, *Annu. Rev. Mater. Res.* **43** (2013)

- 503–525.
- [12] H. Zhang, C. Li, M. Piszcz, E. Coya, T. Rojo, L.M. Rodriguez-Martinez, M. Armand, Z. Zhou, Single lithium-ion conducting solid polymer electrolytes: Advances and perspectives, *Chem. Soc. Rev.* **46** (2017) 797–815.
- [13] Y. Tominaga, K. Yamazaki, V. Nanthana, Effect of anions on lithium ion conduction in poly(ethylene carbonate)-based polymer electrolytes, *J. Electrochem. Soc.* **162** (2015) 3133–3136.
- [14] Y. Tominaga, K. Yamazaki, Fast Li-ion conduction in poly(ethylene carbonate)-based electrolytes and composites filled with TiO₂ nanoparticles, *Chem. Commun.* **50** (2014) 4448–4450.
- [15] J. Mindemark, B. Sun, E. Törmä, D. Brandell, High-performance solid polymer electrolytes for lithium batteries operational at ambient temperature, *J. Power Sources.* **298** (2015) 166–170.
- [16] B. Sun, J. Mindemark, K. Edström, D. Brandell, Polycarbonate-based solid polymer electrolytes for Li-ion batteries, *Solid State Ionics.* **262** (2014) 738–742.
- [17] K. Kimura, J. Motomatsu, Y. Tominaga, Highly concentrated polycarbonate-based solid polymer electrolytes having extraordinary electrochemical stability, *J. Polym. Sci. Part B Polym. Phys.* **54** (2016) 2442–2447.
- [18] H. Kim, F. Wu, J.T. Lee, N. Nitta, H.T. Lin, M. Oschatz, W. Il Cho, S. Kaskel, O. Borodin, G. Yushin, In situ formation of protective coatings on sulfur cathodes in lithium batteries with LiFSI-based organic electrolytes, *Adv. Energy Mater.* **5** (2015) 1–8.
- [19] X. Judez, H. Zhang, C. Li, J.A. González-Marcos, Z. Zhou, M. Armand, L.M. Rodriguez-Martinez, Lithium Bis(fluorosulfonyl)imidePoly(ethylene oxide) Polymer Electrolyte for All Solid-State Li–S Cell - The Journal of Physical.pdf, *J. Phys. Chem. Lett.* **8** (2017) 1956–1960.

- [20] A.K. Padhi, K.S. Nanjundaswamy, J.B. Goodenough, Phospho - olivines as positive - electrode materials for rechargeable lithium batteries, *Jpurnal Electrochem. Soc.* **144** (1997) 1188–1194.
- [21] J.B. Goodenough, K. Park, The Li-Ion Rechargeable Battery: A Perspective, *J. Am. Chem. Soc.* **135** (2013) 1167–1176.
- [22] A.C. Kozen, C.F. Lin, O. Zhao, S.B. Lee, G.W. Rubloff, M. Noked, Stabilization of Lithium Metal Anodes by Hybrid Artificial Solid Electrolyte Interphase, *Chem. Mater.* **29** (2017) 6298–6307.
- [23] P. Verma, P. Maire, P. Novák, A review of the features and analyses of the solid electrolyte interphase in Li-ion batteries, *Electrochim. Acta.* **55** (2010) 6332–6341.
- [24] D. Aurbach, Review of selected electrode–solution interactions which determine the performance of Li and Li ion batteries, *J. Power Sources.* **89** (2000) 206–218.
- [25] B. Sun, C. Xu, J. Mindemark, T. Gustafsson, K. Edström, D. Brandell, At the polymer electrolyte interfaces: the role of the polymer host in interphase layer formation in Li-batteries, *J. Mater. Chem. A.* **3** (2015) 13994–14000.
- [26] K. Kimura, M. Yajima, Y. Tominaga, A highly-concentrated poly(ethylene carbonate)-based electrolyte for all-solid-state Li battery working at room temperature, *Electrochem. Commun.* **66** (2016) 46–48.
- [27] Z. Li, H. Matsumoto, Y. Tominaga, Composite poly(ethylene carbonate) electrolytes with electrospun silica nanofibers, *Polym Adv Technol.* **29** (2018) 820–824.
- [28] M.C. Smart, B.L. Lucht, B. V. Ratnakumar, Electrochemical Characteristics of MCMB and $\text{LiNi}_x\text{Co}_{1-x}\text{O}_2$ Electrodes in Electrolytes with Stabilizing Additives, *J. Electrochem. Soc.* **155** (2008) A577–A568.
- [29] W. Li, A. Xiao, B.L. Lucht, M.C. Smart, B. V. Ratnakumar, Surface Analysis of Electrodes from Cells Containing Electrolytes with Stabilizing Additives Exposed to High Temperature, *J. Electrochem. Soc.* **155** (2008) A648.

- [30] B. Sun, J. Mindemark, K. Edström, D. Brandell, Realization of high performance polycarbonate-based Li polymer batteries, *Electrochem. Commun.* **52** (2015) 71–74.

Chapter 5

Summary and future perspectives

In the present study, we focused on the ion-conductive behavior and physical properties of solid polymer electrolytes (SPEs), especially consisting of poly(ethylene carbonate) (PEC)-based composite polymer electrolytes. The CO₂/epoxide synthesized PEC electrolytes show unusual ion-conductive behaviors, such as an increase in ionic conductivity with increasing salt concentration, excellent Li⁺ transference properties and stable electrochemical properties. However, their poor thermal and mechanical properties are drawbacks for battery application and the ionic conductivity also needed to be further improved. The silica nanofiber (SNF) filled and poly(trimethylene carbonate) added PEC-based CPEs are developed. The study provided the results summarized below.

In Chapter 2 “*Effect of silica nanofiber addition on poly(ethylene carbonate)-based composite electrolytes*”, we showed an attempt to enhance the ion-conductive, thermal and mechanical properties of a PEC electrolyte by utilizing electrospun silica nanofibers (SNFs) as additives. There is a tradeoff relationship between ionic conductivity and mechanical strength, because the ionic conduction in polymer is typically based on the segmental motion of polymer chains. However, it has well known that the addition of inorganic filler to the SPEs, can improve ion-conductive and mechanical properties due to the Lewis acid-base interaction between polymer chain and functional groups on the surface of inorganic fillers. The resulting PEC-LiTFSI- SNF ternary composite is a self-standing membrane with a good handling capability. The results demonstrates that the addition of ceramic nanofiber can be an effective way to enhance both conductivity and mechanical property of SPEs. Additionally, the thinner SNFs the effective on the composite electrolytes.

In Chapter 3 “*Characterization and ion-conductive properties of carbonate-based polymer blend electrolytes*”, we developed a polycarbonate blend electrolyte by using PEC and PTMC. Previously, there is no report on CPE systems of combination of both linear polycarbonate. As

we showed in the previous chapter, both PEC and PTMC have very similar chemical structures. However, they are completely immiscible with each other, but the detail phase separations between both polycarbonates are not known yet. Interestingly, PEC and PTMC become miscible, even the ionic conductivity was increased with the further addition of Li salts. We consider that a compatible amorphous phase of PEC and PTMC is induced by dissolved ions such as Li^+ . Moreover, this phase may provide easier ion pathways. In addition, the Li^+ transference number (t_+) was improved by blending, and the thermal properties of blend electrolytes were improved by increasing PTMC contents.

Lastly in Chapter 4 “*Electrochemical characterization and battery performance of concentrated polycarbonate-based composite electrolytes*”, the studies confirmed that the highly concentrated blend electrolyte gives rise to favorable electrochemical properties, including Li stripping/deposition and Li/electrolyte interfacial stabilities. It has known that highly concentrated polycarbonate-based electrolytes exhibit better properties than that of typical electrolytes like higher conductivity, high t_+ , better electrochemical stability, and so on. However, there are also side effects due to the high concentration such as poor thermal and mechanical properties, deficiency of electrolyte stability and so on. The blending of two concentrated polycarbonates improved on Li/electrolyte interfacial compared with both PEC and PTMC original electrolytes. So far it also connects to better and stable battery performance by using blend electrolytes. The results demonstrate a better promising features suitable for lithium-metal battery application.

As conclusion, compounding of the electrolyte is an effective method for development of more excellent electrolytes for batteries. We also believe that the present study will contribute to realize application of all-solid-state lithium batteries with polymer electrolytes in the future. The current research direction of the SPE field, where vast majority is directed to only

polyether-type and its derivatives that cannot meet the future requirements of diversification and performance improvement of rechargeable battery systems. In contrast, the study of polycarbonate-based electrolytes suggested unknown potentials of unexplored polymer materials, by breaking the conventional notion about suitable polymer structures for SPE use. The polycarbonate-base electrolytes reveal a different ion-conductive and electrochemical behavior, such as ion-conductive behaviors dependence on salt concentration and excellent electrochemical properties, based on a specific solvation structure. Fortunately, composite electrolytes not only can further improve in electrochemical properties of polycarbonate-base electrolytes, but also their physical properties as well. Therefore, studies for the future perspectives should put more emphasis on take advantage of features and improve drawbacks of polycarbonate-based electrolytes. Moreover, it is also necessary to find out good combination structures or characters with polycarbonate structures.

List of publications

Papers included in this thesis

- 1) Z. Li, H. Matsumoto, Y. Tominaga, Composite poly(ethylene carbonate) electrolytes with electrospun silica nanofibers, *Polym. Adv. Technol.*, **29** (2018) 820-824.
(Chapter 2)
- 2) Z. Li, R. Mogensen, J. Mindemark, T. Bowden, D. Brandell, Y. Tominaga, Ion-conductive and thermal properties of a synergistic poly(ethylene carbonate)/poly(trimethylene carbonate) blend electrolyte, *Macromol. Rapid Commun.*, **39** (2018) 1800146.
(Chapter 3)
- 3) Z. Li, J. Mindemark, D. Brandell, Y. Tominaga, A concentrated poly(ethylene carbonate)/poly(trimethylene carbonate) blend electrolyte for all-solid-state Li battery, Accepted (*Polymer Journal*).
(Chapter 3, 4)

Papers not included in this thesis

- 1) S. Y. Wei, S. Inoue, Z. Li, K. Kimura, Y. Tominaga, L. Pandini, D. Di Lecce, J. Hassoun, Glyme-based electrolytes for lithium metal batteries using insertion electrodes: an electrochemical study, Under review (*Electrochimica. Acta*)

Acknowledgements

Firstly, I would like to express my sincere gratitude to my advisor Professor Yoichi Tominaga for the continuous support of my Ph.D study and related research, for his patience, motivation, and rich experience. His guidance helped me in all the time of research and writing of this thesis.

Besides my advisor, I would like to thank the rest of my thesis committee: Professor Kenji Ogino, Professor Eika W. Qian, Associate Professor Nobuyuki Akai, and Associate Professor Susumu Inasawa, for their insightful comments and encouragement, but also for the hard question which incited me to widen my research from various perspectives.

The study of Chapter 3 and Chapter 4 were conducted as a joint project with Uppsala University, Sweden. My sincere thanks also goes to Professor Daniel Brandell, Associate Professor Jonas Mindemark, and Mr. Ronnie Mogensen, who gave me a lot inspiration and without their precious support it would not be possible to conduct this research. I also would like to thank Dr. Hidetoshi Matsumoto from Tokyo Institute of Technology, Japan, for kindly donating electrospun silica nanofibers.

I thank my fellow lab mates in for the stimulating discussions, and also to Dr. Takashi Morioka, Dr. Kento Kimura, Dr. Azlini Binti Ab Aziz, and Ms. Nur Azrini Ramlee, who gave me a lot hints and advices. Because of your kind support I can enjoy more my Ph.D study.

Last but not the least, I would like to thank all of my friends, who always supporting me and in beside of me. Without your encouragement and friendship I was unable to overcome those many difficulties. The most importantly, I would like to thank my family: my father Li Zhongji, my mother Piao Jizi, and my brother Li Zhenxi for supporting me spiritually throughout writing this thesis and my life in general. Finally, many thanks to my wife Liang Yanbo for the endless love and support.

Zhenguang Li
February, 2019